J Mammal Evol (2009) 16:235–305
DOI 10.1007/s10914-009-9119-9

ORIGINAL PAPER

The Phylogeny of Living and Extinct Pangolins (Mammalia, Pholidota) and Associated Taxa: A Morphology Based Analysis

Timothy J. Gaudin · Robert J. Emry · John R. Wible

Published online: 28 August 2009

Abstract The present study was undertaken in order to effect a comprehensive phylogenetic analysis of the order Pholidota, examining seven of the eight currently recognized extant species (absent is *Manis culionensis*, formerly recognized as a subspecies of *Manis javanica*) and nearly all the well-known fossil taxa, and employing a wide range of osteological characters from the entire skeleton. In addition, the relationship of pangolins to several putative early Tertiary relatives, including palaeanodonts and the enigmatic "edentate" *Eurotamandua joresi*, were investigated. The goal of the study was to improve understanding of the systematics and the biogeographic and evolutionary history of the pangolins. A computer-based cladistic analysis of phylogenetic relationships among seven extant species of pangolins, five extinct pangolin species (including all but one of the well-preserved taxa), as well as *Eurotamandua* and two genera of metacheiromyid palaeanodonts, *Palaeanodon* and *Metacheiromys*, was performed based upon 395 osteological characteristics of the skull and postcranial skeleton. Characters were polarized via comparison to the following successive outgroups: the basal feliform carnivoran *Nandinia binotata* and the hedgehog *Erinaceus* sp., a eulipotyphlan laursiatherian placental. A revised classification is presented based on the results of the analysis. The results support the monophyly of Pholidota and Palaeanodonta by providing new anatomical characters that can serve to diagnose a pangolin/palaeanodont clade, termed here Pholidotamorpha. Pholidota is defined so as to include all living and fossil pangolins, including all three taxa of middle Eocene "edentates" from the Messel fauna of Germany, among them *Eurotamandua joresi.* The results do not support the monophyly of the remaining two Messel "edentates" originally placed in the same genus *Eomanis*, which is restricted to the type species *Eomanis waldi. Euromanis,* new genus, is named with *Eomanis krebsi* Storch and Martin, 1994, as the type species, to form a new combination *Euromanis krebsi* (Storch and Martin, 1994). The analysis strongly supports the monophyly of a crown clade of pangolins diagnosed by many anatomical synapomorphies, the family Manidae. This crown clade is sister

T. J. Gaudin (✉)
Department of Biological & Environmental Sciences,
University of Tennessee at Chattanooga,
615 McCallie Ave.,
Chattanooga, TN 37403-2598, USA
e-mail: Timothy-Gaudin@utc.edu

R. J. Emry
Department of Paleobiology, MRC 121,
National Museum of Natural History,
Smithsonian Institution,
P.O. Box 37012, Washington, DC 20013, USA
e-mail: emryr@si.edu

J. R. Wible
Section of Mammals, Carnegie Museum of Natural History,
5800 Baum Boulevard,
Pittsburgh, PA 15206-3706, USA
e-mail: WibleJ@CarnegieMNH.Org

to the family Patriomanidae, which includes two Tertiary taxa, *Patriomanis americana* and *Cryptomanis gobiensis,* within the superfamily Manoidea. The relationship of the Tertiary European pangolin *Necromanis* to these two families is unresolved. Within Manidae, the extant species are divided into three well-supported, monophyletic genera, *Manis* for the Asian pangolins, *Smutsia* for the African ground pangolins, and *Phataginus* for the African tree pangolins. The latter two form a monophyletic African assemblage, the subfamily Smutsiinae. The biogeographic implications of this phylogeny are examined. A European origin for Pholidota is strongly indicated. The fossil record of pangolins would seem to support a European origin for the modern forms, with subsequent dispersal into sub-Saharan African and then to southern Asia, and the phylogeny produced in this analysis is consistent with such a scenario.

Keywords Morphology · Pholidota · Palaeanodonta · Pangolins · Phylogeny · *Eurotamandua* · *Euromanis krebsi*

Introduction

The order Pholidota, including the eight living species of pangolins or scaly anteaters (Feiler 1998; Nowak 1999; Gaubert and Antunes 2005; Schlitter 2005), is one of the smallest of the extant placental mammal orders. Moreover, its modern representatives are restricted to the Old World tropics (Corbet and Hill 1991; Nowak 1999; Schlitter 2005), and the fossil record of the group is meager, likely due to the fact that these animals are toothless, may never have been speciose, and typically exist in low population densities, preferring forested environments with low preservation potential (Patterson 1978; Gaudin 1999b; Gaudin et al. 2006). Consequently, it is not surprising that the group remains poorly studied relative to other more diverse, abundant, and widespread placental orders, and therefore many aspects of its systematics, and biogeographic and evolutionary history are incompletely understood. Despite the low taxonomic diversity of Pholidota, its members display a large number of unusual anatomical and behavioral adaptations that are of interest to students of mammalian biodiversity and evolution—for example, their covering of external, overlapping epidermal scales and their highly modified feeding apparatus specialized for consuming ants and termites (Grassé 1955; Kingdon 1974, 1997; Nowak 1999). The small size of Pholidota renders it amenable to very detailed systematic study, making it practical to examine representative specimens of all extinct and extant species.

The species and generic-level taxonomy of extant pangolins has been a matter of unresolved controversy for nearly a century. As discussed in Gaudin and Wible (1999), the species from the Indian subcontinent and the species from southern China were assigned different specific epithets by different authors for much of the 20th century, although recent taxonomic treatments have appeared to settle on the name *Manis crassicaudata* for the former and *Manis pentadactyla* for the latter (Heath 1992a, 1995; Gaudin and Wible 1999; Nowak 1999; Schlitter 2005). The species from the East Indies also has been divided recently into two distinct species, *Manis javanica* for those animals that occupy the bulk of the formerly designated geographic range and *Manis culionensis* for a recognizably distinct former subspecies from the Palawan and Culion Islands in the western Philippines (Feiler 1998; Gaubert and Antunes 2005).

Through longstanding consensus the eight extant species are allocated to the single family Manidae. However, these species have been placed in as many as six genera (Pocock 1924), as few as a single genus (*Manis*; most recently by Nowak 1999; Schlitter 2005), with other authors suggesting: two genera, *Manis* for Asian pangolins and *Phataginus* for African pangolins (Patterson 1978; Corbet and Hill 1991); three genera, an Asian *Manis, Phataginus* for African tree pangolins, and *Smutsia* for African ground pangolins (Koenigswald 1999); or four genera, *Manis*, *Smutsia*, with the African tree pangolins placed in separate genera, *Phataginus* and *Uromanis* (McKenna and Bell 1997). Although the single genus arrangement is followed in recent Mammalogy textbooks (e.g., Vaughan et al. 2000; Martin et al. 2001; Feldhamer et al. 2007) and numerous recent publications on pangolins (e.g., Heath 1992b; Chan 1995; Swart et al. 1999; Gaubert and Antunes 2005; Gaudin et al. 2006; Botha and Gaudin 2007), both Emry (1970) and Gaudin and Wible (1999) expressed discomfort with the monogeneric arrangement, because it underrepresented the morphological diversity present among the extant taxa.

Nevertheless, Emry (1970) and Gaudin and Wible (1999) declined to suggest formal alternatives absent a more thorough taxonomic study of the issue. Indeed, Gaudin and Wible (1999) declined to do so despite the fact that their cladistic phylogenetic analysis of extant pangolins supported a three genus arrangement like that of Koenigswald (1999) described above. However, Gaudin and Wible's (1999) analysis was based on a rather restricted character base, considering only morphological characters drawn from the cranial skeleton. Their study provided strong support for the monophyly of the African tree pangolins and Asian pangolins, but the monophyly of the African ground pangolins collapsed with the addition of a single step to the most parsimonious tree, and the interrelationships among the three examined Asian species varied, depending on the character weighting and ordering schemes employed. As stated by Gaudin and Wible (1999), a more comprehensive analysis of the extant taxa, involving a broader base of morphological characters, would go far in resolving these taxonomic uncertainties.

As noted above, the fossil record of pangolins is relatively depauperate (Patterson 1978; Gaudin 1999b; Rose et al. 2005; Gaudin et al. 2006). There are, however, a number of well-known fossil taxa from Cenozoic deposits that are represented by reasonably complete skeletal material. They include: the genus *Eomanis*, the oldest pangolin, including two species (*E. waldi* and *E. krebsi*) from the middle Eocene Messel fauna of Germany (Storch 1978; Storch and Martin 1994; Horovitz et al. 2005); *Cryptomanis gobiensis*, a newly described genus and species from the late Eocene of the Inner Mongolia region of northern China (Gaudin et al. 2006); *Patriomanis americana,* the only pangolin known from the Western Hemisphere, deriving from the latest Eocene (Chadronian LMA) of western North America (Emry 1970, 1973, 2004); and *Necromanis,* a genus including several species of Oligocene-Miocene age from central Europe (Koenigswald 1969, 1999; Koenigswald and Martin 1990). There are more recent Plio-Pleistocene pangolin records from Europe, Africa, and southern Asia (Guth 1958; Emry 1970; Botha and Gaudin 2007). These are primarily based on fragmentary skeletons or isolated elements, with the exception of the nearly complete skeleton of the giant pangolin *Manis palaeojavanica* from the Pleistocene of Java (Dubois 1907, 1926; Hooijer 1947) and a partial skeleton of "*Manis*" *gigantea* from the Pliocene of South Africa (Botha and Gaudin 2007).

Gaudin and Wible (1999) noted that in previous treatments, fossil pangolins were typically allocated to the same family as the extant forms, the Manidae. Although these extinct taxa were recognized as being anatomically more primitive than the living taxa in various respects, neither their detailed relationships to modern pangolins nor the interrelationships among the fossil taxa themselves were formally addressed. In more recent literature (e.g., Szalay and Schrenk 1998; Storch 2003; Rose et al. 2005; Gaudin et al. 2006), the morphological diversity among extant and extinct pangolins was deemed sufficient to merit the recognition of additional families.

Gaudin and Wible (1999) tentatively suggested that several families may need to be recognized for extinct pangolins, although their study included only one extinct taxon, *Patriomanis*. Their study was restricted to characters of the skull and lower jaw, and *Patriomanis* was the only fossil pangolin represented by a significant amount of described and undescribed cranial material (Emry 1970, 2004). Gaudin and Wible's (1999) analysis was the first to explicitly support the monophyly of the extant pangolins exclusive of their extinct relatives. Modern pangolins were diagnosed by at least six unambiguous cranial synapomorphies not found in *Patriomanis,* and this node was one of the strongest in the study. These results strongly contradicted the taxonomic arrangement of McKenna and Bell (1997), who, without any explicit character support, linked the extinct Tertiary pangolin genera *Patriomanis, Necromanis,* and *Eomanis* to the extant Asian pangolins in a subfamily Maninae to the exclusion of the extant African pangolins, which were placed in a separate subfamily Smutsiinae.

Szalay and Schrenk (1998) erected a separate family Patriomanidae for *Patriomanis, Necromanis*, and *Eomanis*. However, Storch (2003) asserted that the oldest of these taxa, *Eomanis*, was distinctive, exhibiting a mix of plesiomorphic features and resemblances to the extinct group Palaeanodonta (see "Discussion" below) not found in other pangolins, and hence he designated a separate family Eomanidae to accommodate this genus. Storch (2003: 56) also claimed, based on "extremely rich and complete new material of *Necromanis*" that

"there is no justification for retaining *Necromanis* and *Patriomanis* together in the family Patriomanidae." Gaudin et al. (2006) contended that the Patriomanidae as defined by Szalay and Schrenk (1998) was paraphyletic, with *Eomanis* more primitive and *Necromanis* more derived than *Patriomanis*, largely in agreement with Storch (2003). However, Gaudin et al. (2006) also advocated the retention of Patriomanidae as a valid taxon if restricted to *Patriomanis* and their newly described genus *Cryptomanis*. Resolution of these family level taxonomic issues will require a detailed phylogenetic investigation that includes all these Tertiary fossil pangolin genera along with the extant species, such as that undertaken in the present study.

One final taxonomic concern involves the content of the order Pholidota. Traditionally, the group was restricted to extant pangolins and various extinct Tertiary forms that were clearly closely related (Simpson 1945). However, Emry (1970) suggested that Pholidota should also include Palaeanodonta as a suborder, an arrangement followed by McKenna and Bell (1997), although the latter considered Pholidota itself to be a suborder of a larger group, the order Cimolesta. Palaeanodonts are an uncommon, extinct group of specialized fossorial mammals with reduced dentitions that derive from lower Cenozoic deposits mainly in North America, although representatives are also known from Europe and Asia (Gaudin 1999a; Rose et al. 2005). In one of the first major treatments of palaeanodonts, Matthew (1918) hypothesized they were related to either Pholidota or the order Xenarthra. Simpson (1945) allied palaeanodonts only with xenarthrans, but the group's affinities have since been controversial (Rose et al. 2005). Although palaeanodonts share a number of derived cranial (Gaudin 2004) and particularly basicranial similarities (Patterson et al. 1992; Gaudin 1995) with Xenarthra, recent evidence documenting a variety of close resemblances to *Eomanis* suggests that palaeanodonts are probably more closely related to pangolins (Storch 2003; Rose et al. 2005). This relationship has yet to be confirmed by a comprehensive phylogenetic study of "edentate" relationships that examines an extensive set of representatives from Xenarthra, Palaeanodonta, pangolins, as well as a variety of other putatively related fossil taxa (e.g., *Eurotamandua*, *Ernanodon*). If confirmed, however, the relationship between palaeanodonts and pangolins would create certain nomenclatural problems. If palaeanodonts are included in Pholidota proper, following Emry (1970) and McKenna and Bell (1997), then there is no widely accepted name for the clade including living and extinct pangolins. Rose et al. (2005) and Gaudin et al. (2006) called the group of living and extinct pangolins "Pholidota *sensu stricto*," but this seems awkward as a permanent usage. Alternatively, the term Pholidota could be restricted to this pangolin clade, but that would leave the clade including pangolins and palaeanodonts unnamed.

In addition to the phylogenetic and taxonomic concerns discussed above, the biogeographic history of pangolins in not well understood (Gaudin et al. 2006). A long-standing hypothesis based on morphological studies of placental phylogeny (e.g., Novacek and Wyss 1986) is that Pholidota and Xenarthra are sister taxa. This would be consistent with a Gondwanan origin for Pholidota, more specifically an origin as an "Old African" order along with proboscideans, hyracoideans, and others. There is in fact a Paleogene record of Pholidota from Africa, a pair of isolated ungual phalanges from the early Oligocene of Egypt (Gebo and Rasmussen 1985). An African origin would also be consistent with the group's extant distribution. However, the oldest undisputed pangolins in the genus *Eomanis* come from central Europe, and all the well-known, well-preserved early Cenozoic fossil material, including *Cryptomanis*, *Patriomanis,* and *Necromanis,* obtains from Laurasian continents. This suggests a Laurasian origin for the group (Gaudin et al. 2006), and perhaps even more specifically, a European origin (Storch 2003). A northern origin would be consistent with recent molecular-based analyses of placental phylogeny (e.g., Springer et al. 2004) that place Pholidota within the Laurasian clade Laurasiatheria as sister to Carnivora. If the Laurasian palaeanodonts were confirmed as close relatives of Pholidota, this would further support a biogeographic genesis on the northern continents.

The biogeographic source for modern pangolins is also unclear. All the Paleogene pangolins occur in areas outside the biogeographic range of modern pangolins (Gaudin et al. 2006), which extends through sub-Saharan Africa, the Indian subcontinent, southeast Asia and the East Indies (Corbet and Hill 1991; Kingdon 1997; Nowak 1999; Schlitter 2005). Even the Asian *Cryptomanis* (Gaudin et al. 2006) and

the Oligocene pangolin record from Egypt (Gebo and Rasmussen 1985) lie well to the north of the extant range. Pangolins do not appear in their modern range until the Pliocene and Pleistocene. The sub-Saharan African records are slightly older than the Asian records (Guth 1958; Emry 1970; Botha and Gaudin 2007), and the phylogeny of Gaudin and Wible (1999) arranged the extant African species in a paraphyletic stem group below the monophyletic clade of Asian species. Both of these would suggest an African origin for modern pangolins, with subsequent dispersal into southern Asia. However, given the persistent phylogenetic uncertainty surrounding the relationships among the extant species and among the extant and extinct taxa, an Asian origin remains a plausible alternative. It is even possible that the origin of the modern forms lies neither in Africa nor Asia, but in Europe, with subsequent dispersal to Africa and Asia. There is a fragmentary Pliocene record of pangolins from eastern Europe (Kormos 1934). Moreover, records of the European genus *Necromanis* extend to the early Neogene. If this taxon could be shown to be a close relative of modern pangolins, a European origin for the modern forms would be further supported.

The goal of the present study is to conduct a comprehensive phylogenetic analysis of the order Pholidota, in order to improve understanding of the systematics and the biogeographic and evolutionary history of the group. Unlike the previous cladistic morphology-based study by Gaudin and Wible (1999), the present study incorporates a broader array of extinct taxa and a large number of characters drawn from the entire postcranial skeleton, in addition to cranial skeletal characters. The original intent of the project was to examine all extant and extinct pangolin taxa. The present study includes all extant pangolin species except *Manis culionensis,* which was not widely recognized as a distinct species at the time this study was being conducted (Gaubert and Antunes 2005), and is in any case quite similar in most aspects of its morphology to *Manis javanica* and would likely group as a sister taxon to this species. The present study also includes all well-known fossil pangolins (i.e., those known from more than isolated elements) except the giant Pleistocene *Manis palaeojavanica* (Dubois 1907, 1926; Hooijer 1947), which was not examined due to time and funding constraints, and the Pliocene remains of "*Manis*" *gigantea* described by one of us (Botha and Gaudin 2007) but unavailable at the time of the study. In addition, the enigmatic taxon *Eurotamandua joresi,* from the middle Eocene Messel deposits of Germany (Storch 1981), is included in order to evaluate its potential relationships to pangolins—there is substantial disagreement regarding its affinities, but at least some authors have suggested it might be allied with palaeanodonts or pangolins (Rose et al. 2005). Lastly, two of the best known and skeletally least derived palaeanodont genera, *Palaeanodon* and *Metacheiromys*, are included in the analysis.

Materials and methods

This project originated during a period of sabbatical study by one of us (TJG) in the Department of Paleobiology at the National Museum of Natural History, Smithsonian Institution, Washington, D.C. during the months of January–April 2002. At this time, a detailed, bone-by-bone comparison was made of the entire skeleton for seven of the eight currently recognized extant species of pangolin, as well as *Patriomanis americana* and *Cryptomanis gobiensis*. A total of 395 discrete skeletal characters were eventually obtained. The characters are described in Appendix 2, and include the 67 cranial skeletal characters used in the previous study of Gaudin and Wible (1999) (see Appendix 2: chars. 306–372). The characters were scored via direct observations of the specimens listed in Appendix 1. In the palaeanodonts *Palaeanodon* and *Metacheiromys*, these observations were supplemented by descriptions in the literature (Matthew 1918; Simpson 1931; Schoch 1984; Patterson et al. 1992; Szalay and Schrenk 1998; Gaudin and Wible 1999; Rose and Lucas 2000; Gaudin 2004; Wible and Gaudin 2004). Additional information used in scoring *Eurotamandua joresi* and *Eomanis waldi* was graciously provided by Dr. Gerhard Storch of the Senckenberg Museum in Frankfurt, Germany, based on his unpublished three-dimensional x-ray studies of these taxa. Dr. Storch also provided access to new, undescribed material of *Necromanis* to aid in the scoring of this taxon.

Of the 17 taxa listed in Appendix 1, 15 are ingroup taxa, including seven of the eight currently recognized extant pangolin species, five fossil pangolins, the "edentate" *Eurotamandua joresi,* and two meta-

cheiromyid palaeanodont genera, *Palaeanodon* and *Metacheiromys*. The data matrix of 395 characters and 17 taxa (Appendix 3) was analyzed using the computer program PAUP [Version 4.0b10 (Swofford 2002)]. This data matrix has been deposited in MorphoBank and can be obtained at http://www.morphobank.org. Analyses of the entire matrix were conducted using PAUP's branch and bound algorithm in order to ensure that a globally parsimonious solution would be obtained. Characters were optimized using PAUP's DELTRAN option in all analyses [see Gaudin (1995) for full justification—essentially this option is believed to be more conservative in that it only assigns synapomorphies to a clade if there is unambiguous evidence that the character evolves at the base of the clade], and all character state changes were weighted equally. In those instances in which intraspecific variation was noted for a given character in a given taxon, the taxon was coded for all relevant states and treated as polymorphic in the PAUP analyses. Of the 395 characters, 163 were multistate, and 87 of these were ordered along numerical, positional, or structural morphoclines (Appendix 2). Several characters proved to be parsimony uninformative in the final analyses, but all values reported for consistency index exclude uninformative characters.

Characters were polarized via comparison to two successive outgroups (following Maddison et al. 1984; Appendix 1). Most recent molecular phylogenetic analyses of supraordinal relationship among placental mammals have converged on the idea that modern pangolins are members of the supraordinal cluster Laurasiatheria, and more specifically, represent the sister taxon to the order Carnivora (Springer et al. 2004, 2005). Following the results of these studies, the basal feliform carnivoran *Nandinia binotata* (Flynn and Wesley-Hunt 2005) was employed as the most proximate outgroup to the pangolins and their putative relatives. The second outgroup was the skeletally rather generalized placental mammal *Erinaceus* sp., a member of the Eulipotyphla, a group that in turns occupies a basal position within Laurasiatheria in recent molecular phylogenies of placentals (Springer et al. 2004, 2005).

Robusticity of results was assessed using several different methods. The relative support for various groupings was assessed using a bootstrap analysis (Hillis and Bull 1993) and by determining branch support, i.e., the number of additional steps required to collapse each node (Bremer 1994). The bootstrap analysis employed PAUP's branch and bound algorithm, with 1000 bootstrap replicates. Other PAUP settings were identical to those described in the preceding paragraphs. Branch support was calculated by instructing PAUP to save trees progressively longer than the MPT, in increments of one step. At each incremental step, a strict consensus tree was generated. The PAUP settings were otherwise identical to those described in preceding paragraphs.

Because of the large amount of missing data for the fossil taxa, additional analyses were performed using only extant taxa, including seven living pangolin species and the two aforementioned outgroup taxa. In all other respects, these analyses were identical to those described above for the full data matrix. Bootstrap and Bremer support for this tree were calculated as described above. Results of this second set of analyses are compared to those using the entire data matrix below.

Finally, the results of the present study were compared to the previous phylogenetic hypotheses of Gaudin and Wible (1999). PAUP was constrained to produce the shortest tree(s) consistent with Gaudin and Wible's (1999) published cladogram. The results are compared below to the MPT resulting from the present study.

Institutional Abbreviations AMNH, American Museum of Natural History, New York, NY; CM, Carnegie Museum of Natural History, Pittsburgh, PA; FMNH, Field Museum of Natural History, Chicago, IL; GMH, Geiseltalmuseum, Martin-Luther-Universität, Halle-Wittenberg, Germany; HLMD, Hessisches Landesmuseum Darmstadt, Darmstadt, Germany; LNK, Landessammlungen für Naturkunde, Karlsruhe, Germany; SMF, Senckenberg Museum, Frankfurt am Main, Germany; USGS, United States Geological Survey collection now housed in USNM Department of Paleobiology, Washington, D.C.; USNM, National Museum of Natural History, Smithsonian Institution, Washington, D.C.; UTCM, University of Tennessee at Chattanooga Natural History Museum, Chattanooga, TN; YPM-PU, Princeton University collection housed at Peabody Museum, Yale University, New Haven, CT.

Other Abbreviations char(s)., character(s); CI, consistency index; GSL, greatest skull length; LMA, Land

Mammal Age; MPT, most parsimonious tree(s); RI, retention index; TL, tree length.

Results

The PAUP analyses performed using the entire data matrix yield two MPT (Fig. 1; TL=1452, CI=0.608, RI=0.648), differing only in the arrangement of the genus *Necromanis*. In one of the trees, *Necromanis* is the sister taxon to the living pangolins (Family Manidae, Node 8, Fig. 1), whereas in the other, *Necromanis* is the sister taxon to the clade including the extinct pangolins *Patriomanis americana* and *Cryptomanis gobiensis* (Family Patriomanidae, Node 7, Fig. 1). It is noteworthy that *Eurotamandua joresi* is interposed between *Eomanis waldi* and "*Eomanis" krebsi* at the base of the consensus tree (Fig. 1), the three forming successive sister taxa to all remaining pangolins. Based on these results, *Euromanis*, a new genus, is named to include "*Eomanis" krebsi* (see "Systematic Paleontology"). The results of these analyses are described in detail below. Characters will be referred to in these discussions according to the numeration provided in Appendix 2. A list of the apomorphies appearing at each of the nodes on the tree illustrated in Fig. 1 is provided in Appendix 4.

Node 1. Pholidotamorpha. Definition: Node-based, the least inclusive clade including the common ancestor of *Metacheiromys dasypus* and *Manis pentadactyla* and its descendents.

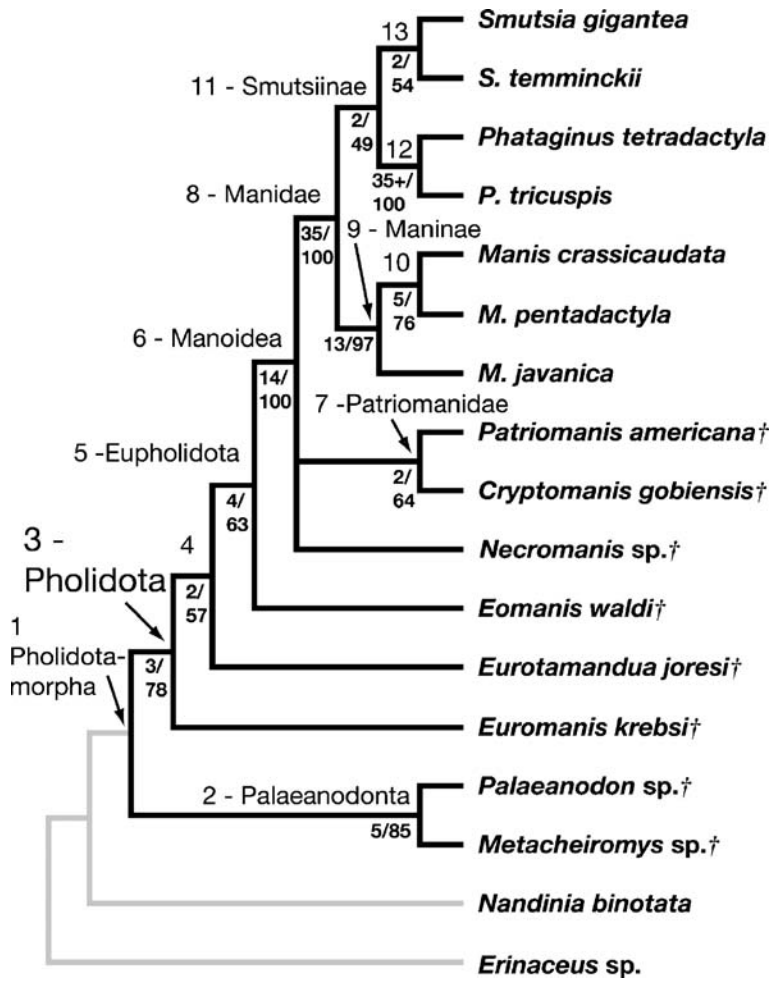

Fig. 1 Phylogeny of Pholidota based on PAUP analysis of 395 osteological characters in 15 ingroup taxa, including seven of the eight extant pangolin species, five fossil pangolins, *Eurotamandua joresi*, and two metacheiromyid palaeanodont genera. Characters are polarized via comparison to successive outgroups represented by the Laurasiatherian placental mammals *Nandinia binotata,* a basal feliform carnivoran, and the eulipotyphlan *Erinaceus* sp. This analysis yields two MPT (TL=1452, CI=0.608, RI=0.648). The numbers in bold type at each node represent Bremer support values (given first) and bootstrap values, calculated as described in Materials and Methods. As noted in the text, *Euromanis*, new genus, is named based on these results, with *Eomanis krebsi* Storch and Martin, 1994, as the type species, to form a new combination *Euromanis krebsi.*

Although some relationship between palaeanodonts and pangolins is presumed in the analysis (following Storch 2003; Rose et al. 2005), the specific nature of the relationship among *Palaeanodon, Metacheiromys*, and pangolins is not specified *a priori*. The phylogenetic results identify a Palaeanodonta clade (Node 2, Fig. 1) comprised of the two palaeanodont genera *Palaeanodon* and *Metacheiromys*. This clade is in turn the sister taxon to the pangolins. The more inclusive clade, composed of palaeanodonts and pangolins, is termed here the Pholidotamorpha. This node is supported by 41 unambiguous and two ambiguous synapomorphies, the former including one feature that is identified as unique to this node in the present analysis. Unique character states are herein defined as derived states of binary characters having a CI=1.0, or states of multistate characters that occur as synapomorphies of a given clade, appear in all members of that clade, and are not found in taxa outside that clade (following the definition of Gaudin and Wible 2006). The unique character that optimizes to this node is 340[1], squamosal forming much of the roof of the epitympanic recess (Fig. 2e).

Unambiguous synapomorphies of palaeanodonts and pangolins derive from a wide variety of skeletal elements, including the phalanges, tarsals, metatarsals, scapula, carpus, vertebrae, and the snout and ear region of the skull (Appendix 4, Fig. 2). These synapomorphies include several of the derived resemblances between palaeanodonts and pangolins noted by previous authors (Emry 1970; Rose and Emry 1993; Storch 2003; Rose et al. 2005) including: width of metatarsals III and IV >15%, <20% of length (19[1]), all metatarsals but the first wide and flat (20[1]), and width of metacarpal IV≥30%, <45% of its length (274[2]), all three characters roughly equivalent to "short and broad metapodials" of Rose et al. (2005); deltopectoral crest of humerus canted medially at its distal end (206[0]); supinator crest greatly enlarged, with free standing proximal extension reaching to humeral mid-shaft (216[0]); olecranon process of ulna moderately elongated (227[1]); radial shaft moderately deep (240[1]); dorsal (facial) process of premaxilla C-shaped, broad anteroposteriorly (309 [0]); and presence of an epitympanic sinus between squamosal and petrosal (391[1]). At least two of the pholidotamorph synapomorphies proposed by Storch (2003) and Rose et al. (2005) optimize to different nodes on the tree in the present study. The first, a medial buttress on the posterior portion of the mandibular ramus (395[1]), is optimized as an ambiguous convergence between Palaeanodonta (Node 2) and *Eomanis waldi*, because its condition is unknown in *"Eomanis" krebsi*, which lacks any cranial remains, and in *Eurotamandua joresi*, in which this part of the mandible is not visible. The second putative pangolin/palaeanodont synapomorphy, an elongate humeral entepicondyle (213[1]) is optimized as a convergence among *Nandinia binotata, Metacheiromys*, and Manoidea (Node 6), because *Palaeanodon, Eomanis waldi,* and *"Eomanis" krebsi* more closely resemble the condition in the second outgroup, *Erinaceus* sp.

Fig. 2 Synapomorphies of Pholidotamorpha. Characters numbered as in Appendix 2. **a** Close-up of the right scapula, humerus, radius and ulna of *Eomanis waldi* (SMF MEA 263 cast) in lateral view, illustrating the following characters: 216 [0], supinator crest greatly enlarged, with free standing proximal extension reaching to humeral mid-shaft; 227[1], olecranon process of ulna moderately elongated; 240[1], radial shaft moderately deep. **b** Right humerus of *Metacheiromys dasypus* (AMNH 11718 type) in anterior view, illustrating: 206 [0], deltopectoral crest of humerus canted medially at its distal end; 216[0], supinator crest greatly enlarged, with free standing proximal extension reaching to humeral mid-shaft. **c** Right manus of *Metacheiromys dasypus* (AMNH 11718 type) in dorsal view, illustrating: 7[1], distal condyles of manual and pedal proximal phalanges divided into medial and lateral pulleys; 274[2], width of metacarpal IV≥30, <45% of its length. **d** Skull of *Eomanis waldi* (Pohl specimen) in left ventrolateral view, illustrating: 309[0], premaxilla C-shaped, broad anteroposteriorly. **e** Left basicranial region of *Smutsia gigantea* (AMNH 53858) in ventral view, illustrating: 340[1], squamosal forming much of the roof of the epitympanic recess; 391[1], presence of an epitympanic sinus between squamosal and petrosal. Abbreviations: **as,** alisphenoid; **bo,** basioccipital; **bs,** basisphenoid; **cap,** capitate; **cpt,** capitulum; **dpc,** deltopectoral crest; **eec,** entepicondyle; **en,** entotympanic; **eo,** exoccipital; **er,** epitympanic recess; **gt,** greater tubercle; **h,** head; **hm,** hamate; **hu,** humerus; **iof,** infraorbital foramen; **ip,** intermediate phalanx; **jf/hf,** jugular and hypoglossal foramina (merged); **lt,** lesser tubercle; **lu,** lunate; **mand,** mandible; **mc,** metacarpal; **mf,** mental foramen; **mx,** maxilla; **pe,** petrosal; **pis,** pisiform; **pm,** premaxilla; **pp,** proximal phalanx; **pr,** promontorium of petrosal; **pt,** pterygoid hamulus; **r,** radius; **s,** scapula; **sc,** scaphoid; **scr,** supinator crest; **sq,** squamosal; **tpd,** trapezoid; **tr,** trochlea; **trq,** triquetrum; **tym,** tympanic (=ectotympanic); **ul,** ulna; **up,** ungual phalanx. **b** and **c** modified from Simpson (1931); **d** modified from Rose et al. (2005); **e** modified from Gaudin and Wible (1999). Scale bars=1 cm.

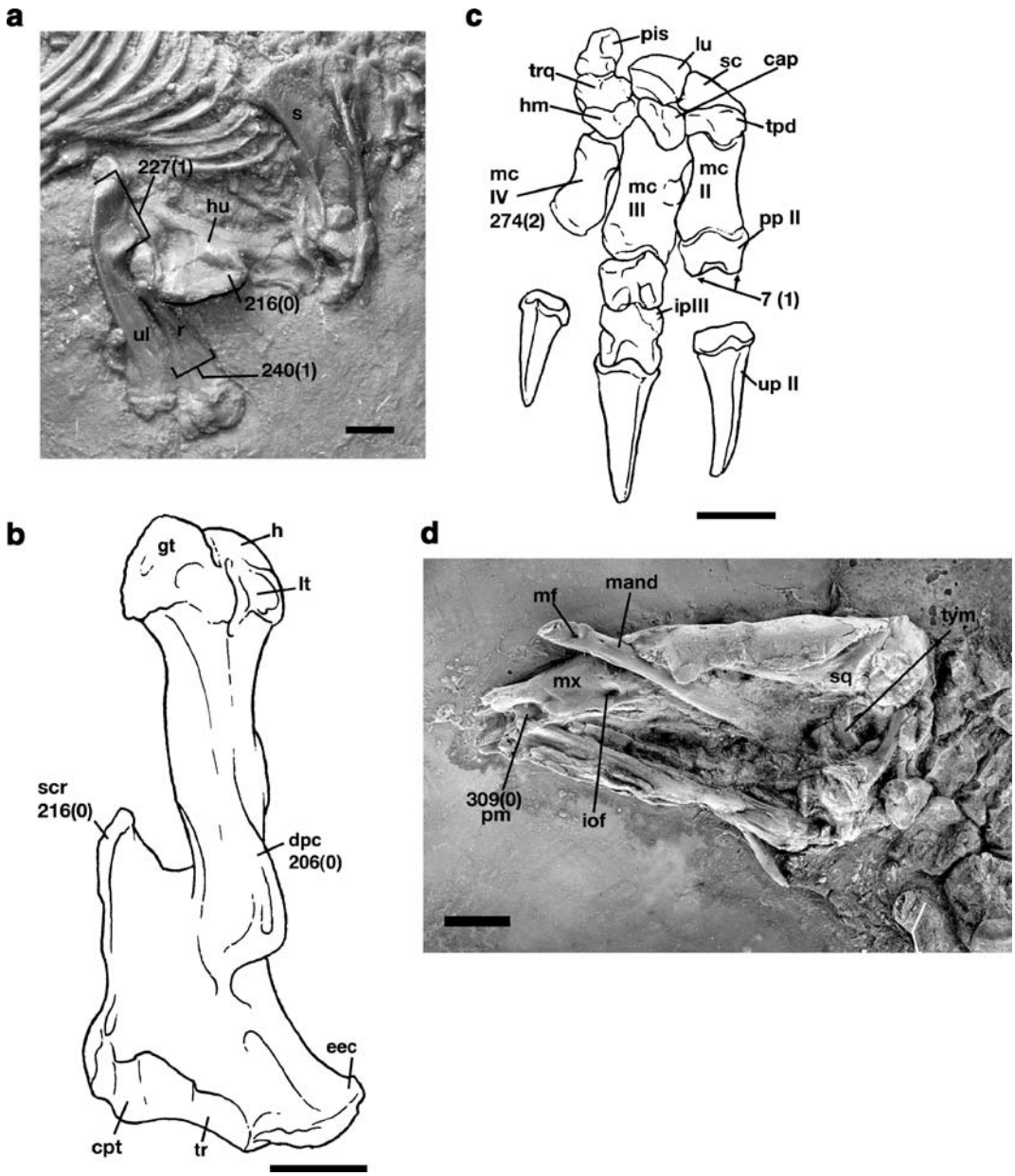

Node 2. Palaeanodonta.

The sister group relationship between *Metacheiromys* and *Palaeanodon* is diagnosed in the present study by 13 unambiguous and 15 ambiguous synapomorphies. Five of the unambiguous characters are unique features. These include: lateral tibial condyle elongated anteroposteriorly (115[2]); entepicondylar notch of humerus weakly developed (215[1]); dorsal tuberosity of radius prominent, much larger than styloid process, pseudostyloid process weakly developed (246[3]); extensor tubercles present on dorsal surface of metacarpals II and III (288[1]); and proximal articular surface of metacarpal IV concave transversely, convex anteroposteriorly (290[2]). There are also two unique character states that are ambiguously optimized to this node: pubis elongate, rod-like, attached to ilium beneath midpoint of acetabulum (155[0]); and teeth

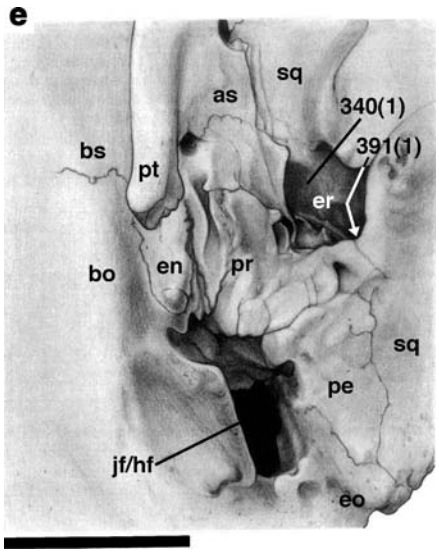

Fig. 2 (continued)

present but reduced with large triangular canine but only a few peg-like postcanine teeth (393[0]).

Node 3. Pholidota. Definition: Stem-based, the most inclusive clade including the common ancestor of *"Eomanis" krebsi* (assigned to new genus *Euromanis*—see "Systematic Paleontology") and *Manis pentadactyla* and its descendents, plus all taxa more closely related to this common ancestor than to *Metacheiromys dasypus.*

This node incorporates all the taxa whose pangolin affinities are unquestioned, plus the controversial *Eurotamandua joresi.* However, because *Eurotamandua* is nested within the clade, this node represents the most recent common ancestor of all undoubted extinct and extant pangolins, and hence seems the most reasonable place on the tree to receive the ordinal epithet Pholidota. The basal pholidotan node receives modest branch and bootstrap support (Fig. 1), but is diagnosed by a relatively small number of synapomorphies—only four unambiguous synapomorphies, two of which are unique, and eight ambiguous synapomorphies, none of which are unique (Appendix 4, Fig. 3). The two unique synapomorphies of Pholidota are the following: fibular facet of astragalus crescentic or boomerang-shaped, with concavity facing proximoplantarly or plantarly, or horseshoe-shaped, with concavity facing proximally (81[1]); and a prominent ischial spine (152[1]). The two additional unambiguous synapomorphies are: manual and pedal subungual processes form triangular platform in ventral view, with grooves along either side of subungual process leading to subungual foramina (4[1]); and distinct lateral process on lateral malleolus of fibula absent (95[0]), a character reversed in more derived pangolins (see Node 6, Appendix 4). Some of the characters ambiguously assigned to Node 4 could conceivably represent additional pholidotan synapomorphies, but their condition is unknown in *"Eomanis" krebsi*. These include the five unique characters optimized to Node 4, along with 12 other features (18[0], 34[0], 45 [2], 56[0], 236[0], 239[0], 257[0], 305[2], 308[1], 314 [1], 366[1], 384[1]; Appendix 4). The five unique features are (Fig. 3): obturator foramen small, maximum diameter of acetabulum ≥75% that of obturator foramen (150[1]); temporal lines absent (358[1]); basicranial/basifacial axis reflexed (392 [1]); teeth absent (393[2]); and horizontal ramus of mandible shallow, ≤10% of maximum mandibular length (394[1]). Character 393[2] was listed as a pholidotan synapomorphy in many previous works (e.g., Rose et al. 2005), character 358[1] was listed as pholidotan synapomorphy by Gaudin and Wible (1999), and character 150[1] was listed as a pholidotan synapomorphy by Rose et al. (2005).

Node 4.

Neither Storch's (2003) family Eomanidae nor the genus *Eomanis* itself is monophyletic in the trees resulting from the present study. In the cladogram illustrated in Fig. 1, *Eomanis waldi*, *Eurotamandua joresi*, and *"Eomanis" krebsi* form successive sister taxa to all remaining pangolins. The node uniting *Eurotamandua joresi* to other pangolins exclusive of *"Eomanis" krebsi* (Node 4, Fig. 1) is weakly supported, both in terms of branch support and bootstrap values. It is diagnosed by 23 ambiguous synapomorphies, including five unique features (Appendix 4), but, as discussed above, many of these features could not be scored in the only known specimen of *"Eomanis" krebsi*, including all the unique traits. Hence these features may represent synapomorphies of the entire Pholidota. There are three unambiguous synapomorphies assigned to Node

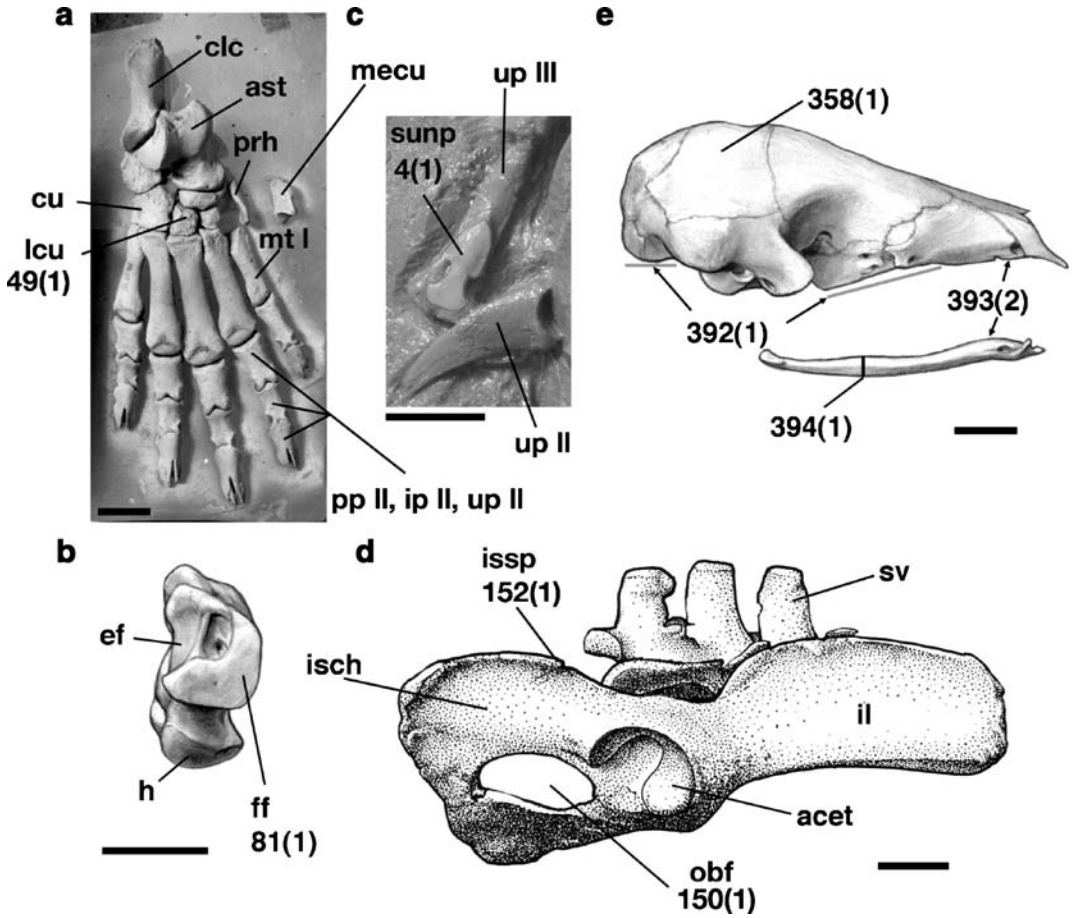

Fig. 3 Synapomorphies of Pholidota. Characters numbered as in Appendix 2. **a** Right pes of *Patriomanis americana* (USNM P299960) in dorsal view (the medial cuneiform illustrated is from the left side, as the right one is missing), illustrating the following character: 49[1], transverse width of dorsal surface of lateral cuneiform roughly equal to proximodistal height. **b** Right astragalus of *Patriomanis americana* (USNM P299960) in lateral view, illustrating: 81[1], fibular facet of astragalus crescent-shaped, with concavity facing proximoplantarly. **c** Right second and third ungual phalanges of *Euromanis krebsi* (SMF 94/1 cast), the latter shown in ventral view, the former in lateral view, illustrating: 4[1], manual and pedal subungual processes form triangular platform in ventral view, with grooves along either side of subungual processes leading to subungual foramina. **d** Right pelvis and sacral vertebrae of *Patriomanis americana* (USNM P299960) in lateral view, illustrating: 150[1], obturator foramen small, maximum diameter of acetabulum ≥75 % that of obturator foramen; 152[1], prominent ischial spine. **e** Skull of *Phataginus tricuspis* (CM 86715) in right lateral view, illustrating: 358[1], temporal lines absent; 392[1], basicranial/basifacial axis reflexed (gray lines indicate plane of basicranial and basifacial axes, respectively); 393[2], teeth absent; 394[1], horizontal ramus of mandible shallow, ≤10% of maximum mandibular length. Abbreviations: **acet,** acetabulum; **ast,** astragalus; **clc,** calcaneus; **cu,** cuboid; **ef,** ectal facet; **ff,** fibular facet; **h,** head; **il,** ilium; **ip,** intermediate phalanx; **isch,** ischium; **issp,** ischial spine; **lcu,** lateral cuneiform; **mecu,** medial cuneiform; **mt,** metatarsal; **obf,** obturator foramen; **pp,** proximal phalanx; **prh,** prehallux; **sunp,** subungual process; **sv,** sacral vertebrae; **up,** ungual phalanx. Scale bars=1 cm.

4 (Appendix 4, Fig. 3): transverse width of dorsal surface of lateral cuneiform roughly equal to proximodistal height (49[1]); astragalar head slightly displaced laterally, the distance from the lateral edge of the head to the lateral edge of the body 35–40% of the overall width of body (70[1]); and diaphragmatic vertebra situated at T10 (160[1]).

Node 5. Eupholidota. Definition: Stem-based, the most inclusive clade including the common ancestor of *Eomanis waldi* and *Manis pentadactyla* and its descendents, plus all taxa more closely related to this common ancestor than to *Eurotamandua joresi.*

In comparison to Nodes 3 and 4, Node 5 received stronger branch support, and is supported by many more unambiguous synapomorphies, though it has relatively weak bootstrap values. *Eomanis waldi* shares 13 unambiguous synapomorphies (Appendix 4, Fig. 4) with other pangolins exclusive of *"Eomanis" krebsi* and *Eurotamandua joresi*, four of which are unique features: lesser trochanter displaced distally, distance between femoral head and tip of lesser trochanter ≥25% maximum femoral length (129[1]); pubis short, flat, attached to ilium under posterior edge of acetabulum (155[2]); mandibular condyle at the level of the mandibular symphysis (370[1]); and temporal fossa on braincase strongly reduced (384 [2]). Node 5 also has 13 ambiguous synapomorphies, one of which is unique (Fig. 4b): long axis of humeral head oriented distomedially in posterior view (205 [1]). The condition for the latter character is unknown

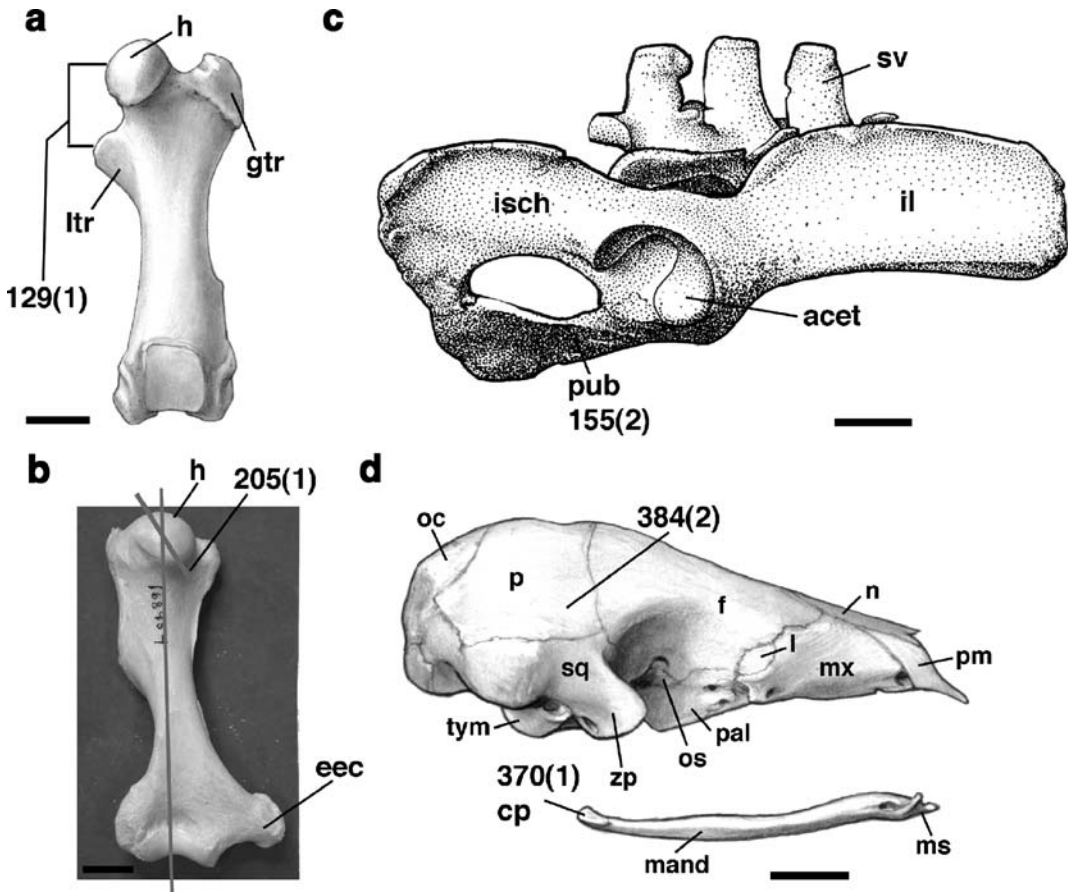

Fig. 4 Synapomorphies of Eupholidota. Characters numbered as in Appendix 2. **a** Right femur of *Phataginus tricuspis* (CM 16206) in anterior view, illustrating the following character: 129[1], lesser trochanter displaced distally, distance between femoral head and tip of lesser trochanter ≥25% maximum femoral length. **b** Left humerus of *Smutsia temminckii* (AMNH 168954) in posterior view, illustrating: 205[1], long axis of humeral head oriented distomedially in posterior view (gray lines indicate long axes of humeral head and humeral shaft, respectively). **c** Right pelvis and sacral vertebrae of *Patriomanis americana* (USNM P299960) in lateral view, illustrating: 155[2], pubis short, flat, attached to ilium under posterior edge of acetabulum. **d** Skull of *Phataginus tricuspis* (CM 86715) in right lateral view, illustrating: 370[1], mandibular condyle at the level of the mandibular symphysis; 384[2], temporal fossa on braincase strongly reduced. Abbreviations: **acet,** acetabulum; **cp,** condylar process; **eec,** entepicondyle; **f,** frontal; **gtr,** greater trochanter; **h,** head; **il,** ilium; **isch,** ischium; **l,** lacrimal; **ltr,** lesser trochanter; **mand,** mandible; **ms,** mandibular symphysis; **mx,** maxilla; **n,** nasal; **oc,** occipital; **os,** orbitosphenoid; **p,** parietal; **pal,** palatine; **pm,** premaxilla; **pub,** pubis; **sq,** squamosal; **sv,** sacral vertebrae; **tym,** tympanic (=ectotympanic); **zp,** zygomatic process. **a** modified from Gaudin et al. (2006). Scale bars=1 cm.

in both *"Eomanis" krebsi* and *Eurotamandua joresi*. As noted in Appendix 4, there is only one character that is convergent between *"Eomanis" krebsi* and *Eomanis waldi* on the tree in Fig. 1, and only one convergence between *"Eomanis" krebsi* and Node 5. Therefore, this analysis provides almost no support for the monophyly of *Eomanis*.

Node 6. Manoidea. Definition: Stem-based, the most inclusive clade including the common ancestor of *Patriomanis americana* and *Manis pentadactyla* and its descendents, plus all taxa more closely related to this common ancestor than to *Eomanis waldi.*

The clade including all extant pangolins plus the non-Messel fossil pangolins is one of the most robust on the tree. It has the third highest branch support, and a bootstrap value of 100. Because this node includes two apparently monophyletic families of pangolins, one extinct (Patriomanidae, Node 7) and one including all the extant taxa (Manidae, Node 8), the superfamilial name "Manoidea" is applied to this clade. Manoidea is diagnosed by a large number of synapomorphies (Appendix 4, Fig. 5), including many of the features used in prior works to diagnose the order Pholidota as a whole. There are 27 unambiguous synapomorphies assigned to this node, six of them unique: fissured ungual phalanges (1[1]); embracing lumbar zygapophyses (166[1]); neural spines of anterior thoracic vertebrae not dramatically elongated relative to those of more posterior thoracics (167[1]); acromion process of scapula rudimentary (198[1]); anterodorsolaterally directed prongs on outer surface of mandibular symphyseal region well developed into tooth-like, conical prongs (366 [2]); and alisphenoid/parietal contact absent (383 [1]). There are an additional 23 ambiguous synapomorphies assigned to this node, and six of these represent unique features (Fig. 5): prehallux present (36[1]); extension of astragalar trochlea onto ventral surface of astragalus absent (65[1]); astragalus/cuboid contact present (80[1]); presence of a pit for the attachment of the meniscal ligament anterior to the medial condyle of tibia (117[1]); foramen rotundum and sphenorbital fissure confluent, opening into same fossa (324[1]); and presence of tympanic process of pterygoid (347[1]). Of these latter six features, only one could be coded for either species of *Eomanis* (117[0] in *"Eomanis" krebsi*; Appendix 3), leaving open the possibility that some are derived at a more inclusive level. Additional unambiguous and ambiguous synapomorphies assigned to this node have appeared as pholidotan synapomorphies in the works of previous authors (Emry 1970; Gaudin and Wible 1999; Rose et al. 2005; Fig. 5), including: distance between proximal end of femur and third trochanter ≥50, <60% of maximum length of femur (128[1], unambiguous); coracoid process of scapula absent (200[2], ambiguous); presence of a sesamoid facet on the radial head (244[1], unambiguous); fusion of scaphoid and lunate bones (249[1], unambiguous); anterior border of nasal with a deep notch forming elongated medial and lateral processes (306[1], unambiguous); dorsal (facial) process of premaxilla inclined posterodorsally (309[1], unambiguous); zygomatic process of squamosal ventrally directed, elongated (355[1], unambiguous); tentorial ossification present but weak, developed only inferiorly on petrosal (361[1], ambiguous); and coronoid process of mandible present but strongly reduced in size (371[1], unambiguous).

Node 7. Patriomanidae. Definition: Stem-based, the most inclusive clade including the common ancestor of *Patriomanis americana* and *Cryptomanis gobiensis* and its descendents, plus all taxa more closely related to this common ancestor than to *Manis pentadactyla.*

Two fossil pangolins from the late Eocene together form a monophyletic clade in the present study, including the type genus for the family Patriomanidae erected by Szalay and Schrenk (1998), *Patriomanis*. The contents of this clade conform to Gaudin et al.'s (2006) redefined Patriomanidae, including their new taxon *Cryptomanis gobiensis* (Gaudin et al. 2006), but excluding *Eomanis* and *Necromanis*, taxa originally placed in the family by Szalay and Schrenk (1998). Patriomanidae receives only weak branch support and bootstrap values (Fig. 1). It is diagnosed by 16 unambiguous synapomorphies, three of them unique (Appendix 4, Fig. 6): posterior process of proximal fibula immediately distal to proximal tibial facet, process marked by elongated posterior groove(s)

bounded by lateral ridges (100[1]); distal tibial articulation for fibula not visible in distal view (112 [0]); and gluteal fossa on ilium large, with prominent lateral iliac crest, medial dorsal flange of ilium and caudal dorsal iliac spine (146[0]). Of the characters employed by Szalay and Schrenk (1998) to diagnose this group, one appears at this node as an ambiguous synapomorphy (Fig. 6a): astragalus with distinct ventral facet for the tendon of the m. flexor digitorum fibularis (66[0]). Other diagnostic features of Patriomanidae recognized by Szalay and Schrenk (1998—characters 76, 77, 88, 128, 166, 328, 381, 384) and Gaudin et al. (2006—character 241) are not found to support this node in the present analysis.

The results from the present study do not unambiguously resolve the phylogenetic affinities of the mid-Tertiary (Oligocene–Miocene) European pangolin *Necromanis.* In one of the MPT, *Necromanis* is placed as a sister taxon to Patriomanidae. In the other MPT, *Necromanis* is allied with modern pangolins as the sister-taxon to Manidae. The former relationship is supported by 12 ambiguous and ten unambiguous synapomorphies, including two unique features (Appendix 4, Fig. 7): ectal facet of astragalus very narrow, maximum length more than twice width measured perpendicular to long axis (74[0]); and deltopectoral crest elongated, extending >75% of the length of humerus (207[0]). Character 66(0) described above, the flexor digitorum fibularis facet on the astragalus, also serves as an unambiguous synapomorphy of *Necromanis* and Patriomanidae. An alliance of *Necromanis* within the Manidae is supported by a virtually identical numbers of synapomorphies—13 ambiguous and ten unambiguous synapomorphies, with three unique features (Appendix 4, Fig. 7): presence of medial depression on ventromedial surface of proximal metatarsal II (23[1]); lunate surface of acetabulum C-shaped, nearly a closed loop (148[1]); and loss of angular process of mandible (372[1]). In addition, two of the resemblances cited by Gaudin et al. (2006) between *Necromanis* and Manidae appear as unambiguous synapomorphies at this node: distal keel on metatarsals and metacarpals takes the form of an elongated ventral ridge on ventral half of articulation (8[1]—intermediate between the primitive condition and the condition in modern manids); and, distance between proximal end of femur and third trochanter ≥60%, <70% of maximum femoral length (128[2]).

Fig. 5 Synapomorphies of Manoidea. Characters numbered as in Appendix 2. **a** Right manus of *Phataginus tricuspis* (CM 16206) in dorsal view, illustrating the following characters: 1 [1], fissured ungual phalanges; 249[1], fusion of scaphoid and lunate bones. **b** Dorsal vertebrae, ribcage, sternum, sacrum and pelvis of *Phataginus tricuspis* (CM 16206) in left lateral view, illustrating: 167[1], neural spines of anterior thoracic vertebrae not dramatically elongated relative to those of more posterior thoracics. **c** Lumbar vertebra of *Patriomanis americana* (USNM P299960) in anterior view, illustrating: 166[1], embracing lumbar zygapophyses. **d** Left scapula of *Smutsia temminckii* (AMNH 168955) in lateral view, illustrating: 198 [1], acromion process of scapula rudimentary. **e** Skull of *Phataginus tricuspis* (CM 86715) in right lateral view, illustrating: 309[1], dorsal process of the premaxilla inclined posterodorsally; 324[1], foramen rotundum and sphenorbital fissure confluent, opening into same fossa; 355[1], zygomatic process of squamosal ventrally directed, elongated; 366[2], anterodorsolaterally directed prongs on outer surface of mandibular symphyseal region well developed into tooth-like, conical prongs; 383[1], alisphenoid/parietal contact absent. **f** Right pes of *Patriomanis americana* (USNM P299960) in dorsal view (the medial cuneiform illustrated is from the left side, as the right one is missing), illustrating: 1[1], fissured ungual phalanges; 36[1], prehallux present; 65[1], extension of astragalar trochlea onto ventral surface of astragalus absent; 80 [1], astragalus/cuboid contact present. **g** Right tibia of *Patriomanis americana* (USNM P299960) in proximal view, illustrating: 117[1], presence of a pit for the attachment of the meniscal ligament anterior to the medial condyle of the tibia. **h** Basicranium of *Smutsia gigantea* (CM 5764) in ventrolateral view, illustrating: 347[1], presence of tympanic process of pterygoid. Abbreviations: **ap,** acromion process; **ast,** astragalus; **bo,** basioccipital; **bs,** basisphenoid; **cap,** capitate; **cent,** vertebral centrum; **clc,** calcaneus; **cp,** condylar process; **cu,** cuboid; **cyf,** cyamelle facet; **f,** frontal; **hf,** hypoglossal foramen; **hm,** hamate; **il,** ilium; **ip,** intermediate phalanx; **isf,** infraspinous fossa; **jf,** jugular foramen; **l,** lacrimal; **lco,** lateral condyle; **lv,** lumbar vertebra; **mand,** mandible; **mc,** metacarpal; **mco,** medial condyle; **mecu,** medial cuneiform; **mnp,** mandibular prong; **mp,** metapophysis; **mt,** metatarsal; **mx,** maxilla; **ns,** neural spine; **occ,** occipital condyle; **os,** orbitosphenoid; **p,** parietal; **pal,** palatine; **pgf,** postglenoid foramen; **pis,** pisiform; **pm,** premaxilla; **pp,** proximal phalanx; **pr,** promontorium of petrosal; **prh,** prehallux; **pt,** pterygoid; **s,** scapula; **sclu,** scapholunate; **sq,** squamosal; **ssf,** supraspinous fossa; **tp,** transverse process; **tpd,** trapezoid; **tpm,** trapezium; **trq,** triquetrum; **up,** ungual phalanx; **vc,** vertebral canal; **xs,** xiphisternum; **zp,** zygomatic process. **b** based in part on Kingdon (1974). **c** modified from Rose et al. (2005). Scale bars=1 cm.

Node 8. Manidae. Definition: Stem-based, the most inclusive clade including the common ancestor of *Phataginus tricuspis* and *Manis pentadactyla* and its descendents, plus all taxa more closely related to this common ancestor than to *Patriomanis americana.*

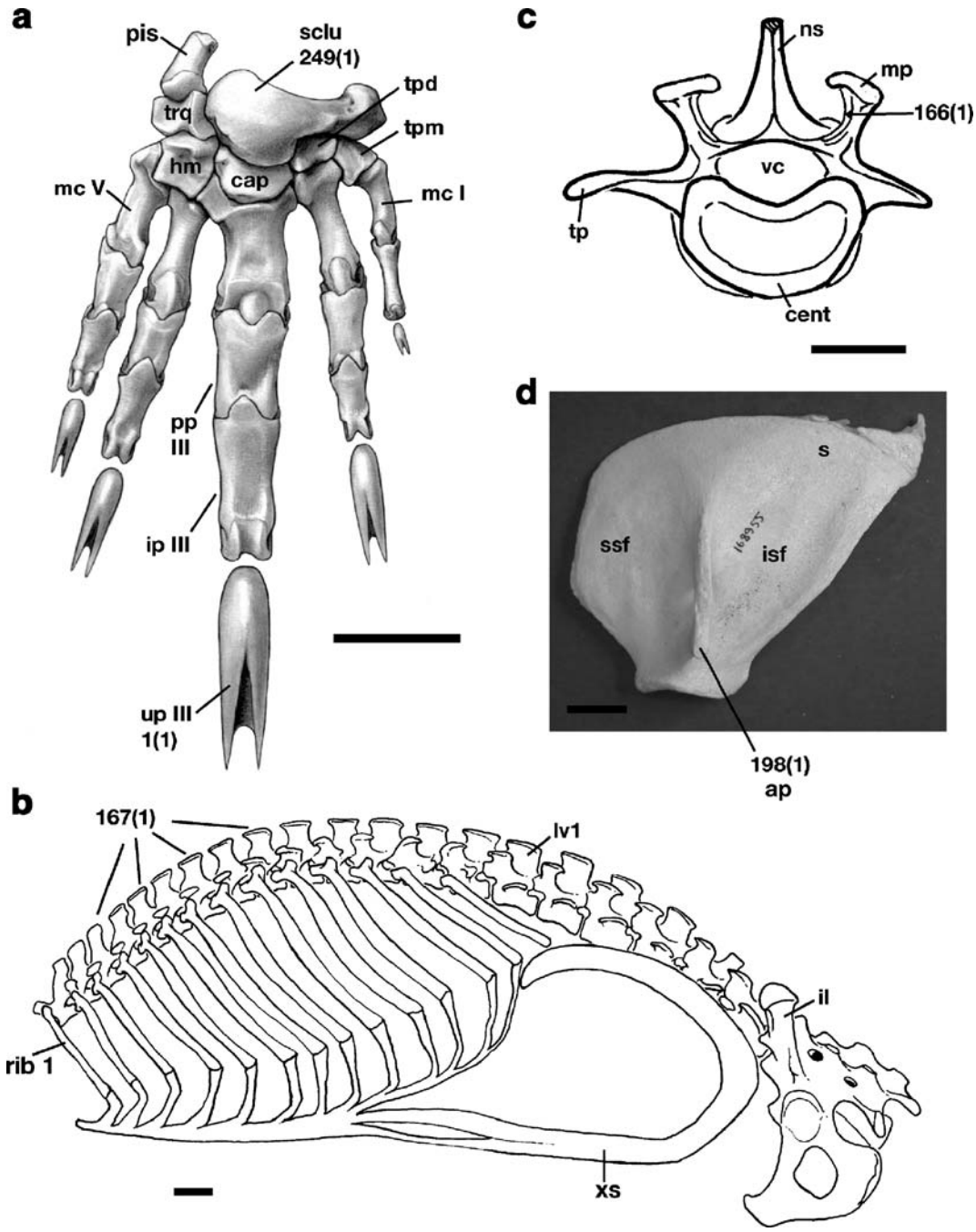

As in the previous phylogenetic analysis by Gaudin and Wible (1999), in the present study the extant pangolins are united in a monophyletic clade to the exclusion of the fossil forms. This clade is designated as the family Manidae, following the usage of Szalay and Schrenk (1998), Gaudin et al. (2006), and others. The living pangolins share a host of derived anatomical features not found in the known fossil pangolins, and the node is the second strongest on the tree, behind only the node uniting the African tree pangolins. It has a bootstrap value of 100 and a Bremer support of 35 (Fig. 1). The node is supported by the longest list of synapomorphies of any node in the analysis—77 unambiguous synapomorphies, 30 of which are unique,

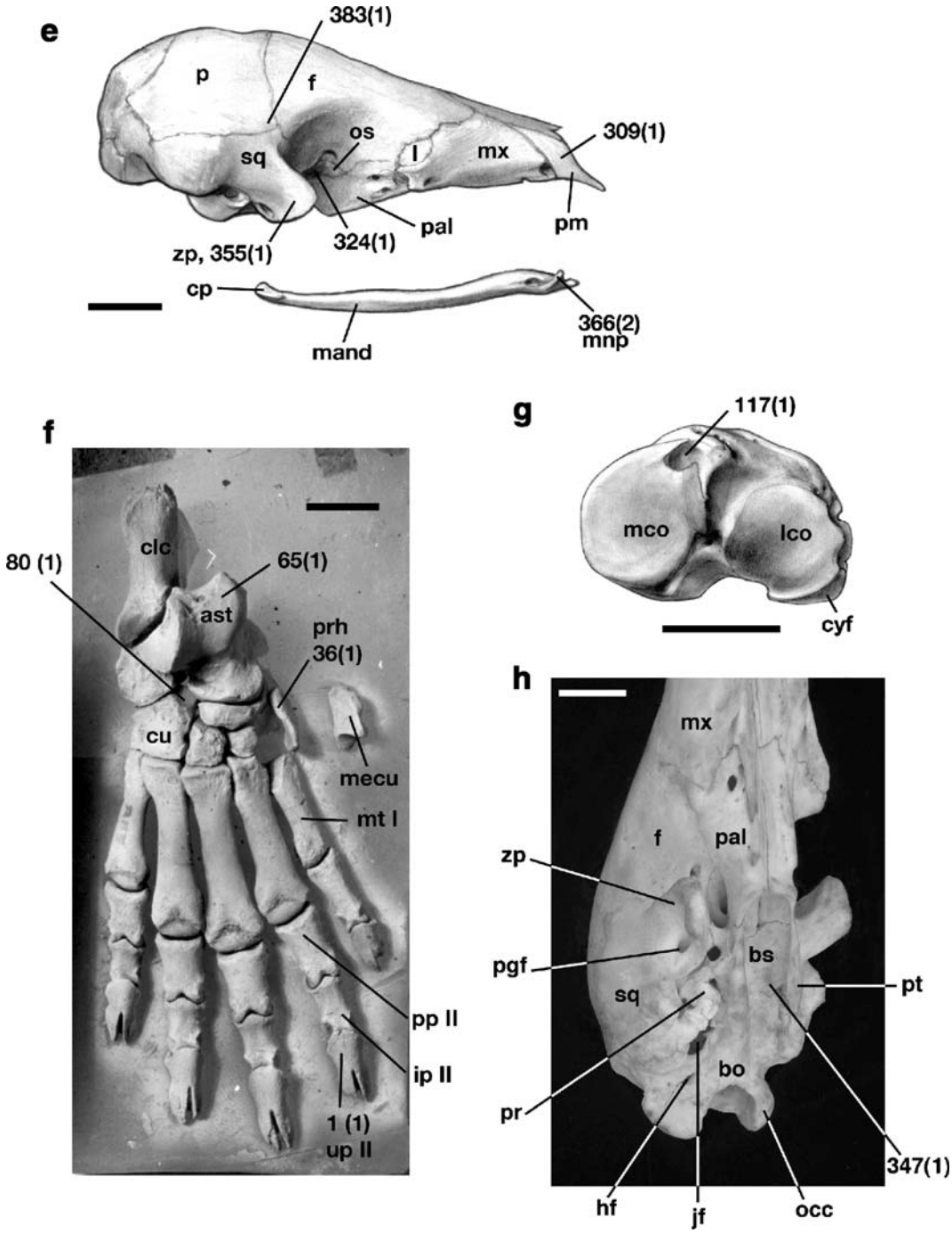

Fig. 5 (continued)

and 24 ambiguous synapomorphies, five of which are unique (Appendix 4, Fig. 8).

The following is a list of the unique, unambiguous synapomorphies of extant pangolins: proximal articulations of manual and pedal intermediate phalanges with deep paired fossae, elongated dorsoventrally with poorly marked lateral ridges (5[2]); distal keel on metatarsals and metacarpals extends along entire

dorsoventral length of condyle, dorsal fossa above condyle absent (8[2]); proximal end of metatarsal II expanded transversely (24[1]); dorsal surface of lateral cuneiform widened transversely, ratio of width to height ≥1.4 (49[2]); astragalar facet of navicular concave ventromedially, convex dorsolaterally, astragalar head with large corresponding concavity (59[1]); sustentacular facet on calcaneus situated well distal to ectal and fibular facets, contacting distal margin of calcaneus (89[2]); anterolateral eminence on proximal fibula present opposite tibial facet (102[2]); greater trochanter of femur compressed anteroposteriorly, anteroposterior depth ≤ transverse width (125[2]); fovea capitis of femur absent (131[1]); femoral trochanteric fossa and intertrochanteric ridge rudimentary or absent (132 [1]); sacroiliac attachment fused (136[1]); metapophyses of sacral vertebrae: elongated, >2/3 neural spine height (144[1]); ischial spine situated close to ischial tuberosities, dorsal to posterior portion of obturator foramen (153[1]); scapular spine reduced in height, <85% of mediolateral width of glenoid (204[1]); sesamoid facet on radial head large, visible in proximal view (244[2]); styloid process and dorsal tuberosity of distal radius prominent, pseudostyloid process rudimentary or absent (246[2]); trapezoid and capitular articular facets on scapholunar continuous (254[1]); scapholunar facet on trapezoid tilted to face proximally and medially in dorsal view (260 [2]); capitular facet of metacarpal III extended to form dorsal shelf, creating sigmoid-shaped surface in medial view (284[1]), dorsal surface of metacarpal IV T-shaped at proximal end, extended laterally and medially for articulations with metacarpals III and V (289[1]); proximal articulation of metacarpal IV mostly convex but with strong concave pit (290 [1]); shafts of proximal and intermediate manual phalanges compressed mediolaterally, width < depth (296[1]); proximal articulations of manual intermediate phalanges not visible in dorsal view due to presence of proximally elongated dorsal midline process (301[1]); fenestra cochleae situated immediately next to fenestra vestibuli, facing laterally and slightly posteriorly (337[1]); fossa incudis situated in medial wall of epitympanic recess, facing laterally (339 [2]); nuchal crest rudimentary to absent (352[1]); endocranial venous grooves absent (362[1]); floor of middle cranial fossa formed by squamosal (363[1]); lateral exposure of mastoid and posttympanic process of squamosal absent (387[1]); and superior petrosal sinus perforates ventral portion of tentorium (389[1]).

The above list includes four of the six unambiguous cranial synapomorphies of extant pangolins identified by Gaudin and Wible (1999), the only exceptions being the loss of the coronoid process of the mandible (371[2]), and a flat, weakly-developed promontorium of the petrosal (334[1]), both of which are unambiguous but not unique synapomorphies of manids in the present study. However, the present study recognizes an additional eight unambiguous cranial synapomorphies of Manidae (311[1], 317[2], 319[1], 336[1], 339[2], 353[1], 387[1], 389[1]) not identified in the Gaudin and Wible (1999) study, three of which are unique (339[2], 387[1], 389[1]).

Node 9. Maninae. Definition: Stem-based, the most inclusive clade including the common ancestor of *Manis javanica* and *Manis pentadactyla* and its descendents, plus all taxa more closely related to this common ancestor than to *Phataginus tricuspis.*

Manis Definition: Node-based, the least inclusive clade including the common ancestor of *Manis pentadactyla* and *Manis javanica* and its descendents.

The Manidae is split into two primary clades that reflect the main biogeographic divisions within the group. One clade includes the four African pangolin species—it will be discussed below. The other clade includes three species of Asian pangolins. These three species are placed in the genus *Manis*, because one of them, *M. pentadactyla,* is the type species for the genus (Pocock 1924; Schlitter 2005). This is also consistent with the usage of most authors who have split modern pangolins into multiple genera (Patterson 1978; Corbet and Hill 1991; McKenna and Bell 1997; Koenigswald 1999), the exception being Pocock (1924), who placed the three Asian species in three separate genera. This Asian clade receives strong support from the bootstrap analysis (bootstrap value of 97; Fig. 1) and has a high level of Bremer support (13; Fig. 1). The monophyly of *Manis* is supported by 24 unambiguous and 29 ambiguous synapomorphies (Appendix 4, Fig. 9). Seven of the unambiguous synapomorphies are unique to this clade: presence of

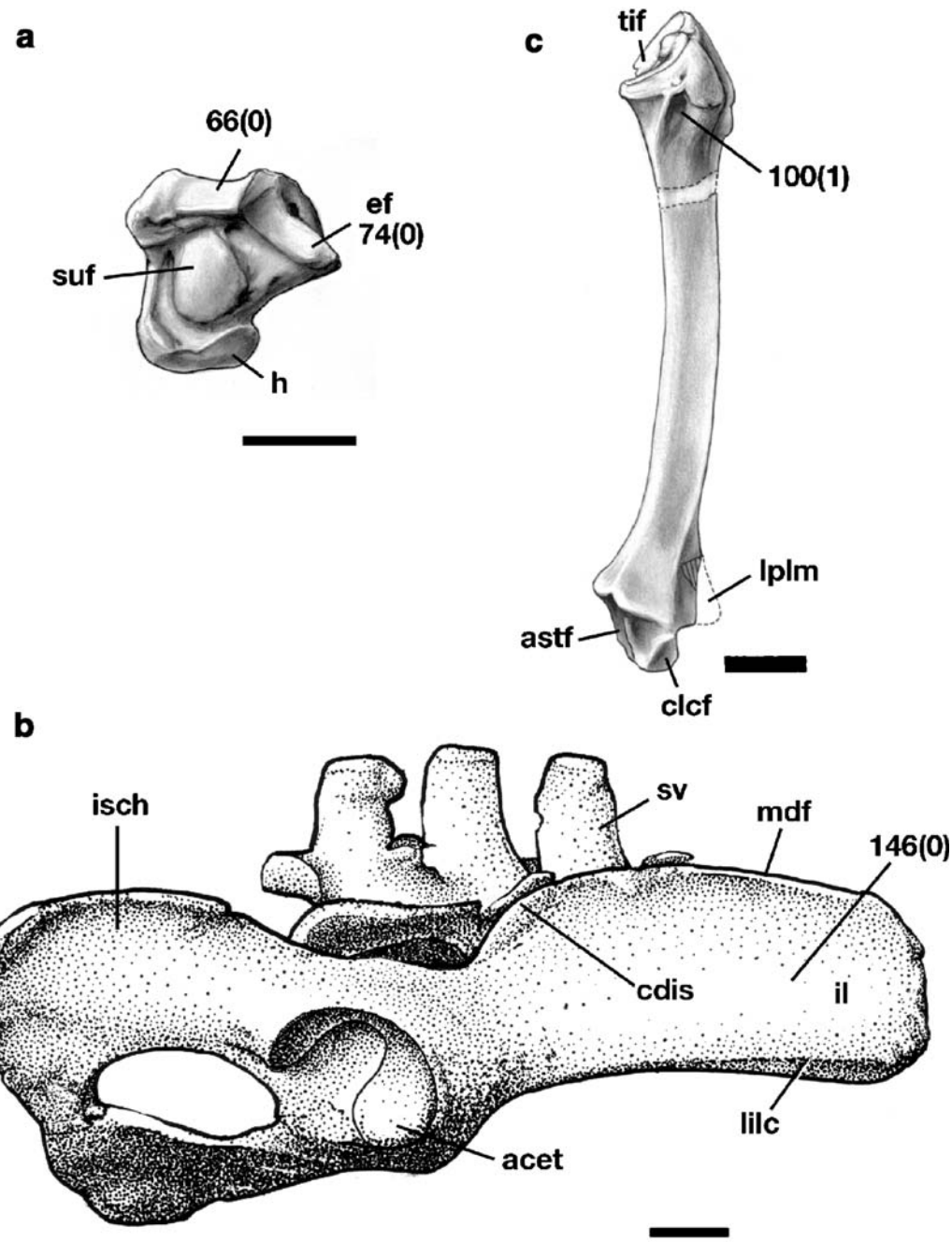

deep groove for calcaneal-navicular "spring" ligament on ventral margin of astragalar head (72[1]); groove for tendon of m. tibialis posterior on posterior distal surface of tibia deep, closed over by soft tissue to form a tunnel (108[1]); transverse foramen of axis visible in anterior view (185[1]); proximal articulation on capitate very wide, ≥85% of maximum dorsoventral depth of capitate (262[4]); broad orbitosphenoid/squamosal contact (322[2]); facial nerve travels within closed canal formed by promontorium and crista parotica (335[2]); and body of incus stout and rectangular, crura short (343[1]). There is also one unique ambiguous synapomorphy of this clade (Fig. 9d): cartilaginous extension of xiphisternum

◀ **Fig. 6** Synapomorphies of the Patriomanidae. Characters numbered as in Appendix 2. **a** Right astragalus of *Patriomanis americana* (USNM P299960) in ventral view, illustrating the following characters: 66[0], astragalus with distinct ventral facet for the tendon of the m. flexor digitorum fibularis; 74[0], ectal facet of astragalus very narrow, maximum length more than twice width measured perpendicular to long axis. **b** Right pelvis and sacral vertebrae of *Patriomanis americana* (USNM P299960) in lateral view, illustrating: 146[0], gluteal fossa on ilium large, with prominent lateral iliac crest, medial dorsal flange of ilium and caudal dorsal iliac spine. **c** Right fibula of *Cryptomanis gobiensis* (AMNH 26140) in posterior view, illustrating: 100[1], posterior process of proximal fibula immediately distal to proximal tibial facet, process marked by elongated posterior groove(s) bounded by lateral ridges. Abbreviations: **acet,** acetabulum; **astf,** fibular astragalar facet; **cdis,** caudal dorsal iliac spine**; clcf,** fibular calcaneal facet; **ef,** ectal facet; **h,** head; **il,** ilium; **isch,** ischium; **lilc,** lateral iliac crest**; lplm,** lateral process of lateral malleolus of fibula; **mdf,** medial dorsal flange of ilium; **suf,** sustentacular facet; **sv,** sacral vertebra; **tif,** proximal tibial facet of fibula. **c** modified from Gaudin et al. (2006). Scale bars=1 cm.

elongated, length much greater than ossified portion of xiphisternum, shovel shaped at distal end with central perforation (194[1]). Because it is a soft tissue character, it could not be coded for the fossil pangolin taxa.

Within the Asian clade, *M. crassicaudata* from the Indian subcontinent (Heath 1995) and *M. pentadactyla* from southern China and northern Indochina (Heath 1992a) are united to the exclusion of *M. javanica* from southern Indochina and the East Indies (Corbet and Hill 1991). The Bremer and bootstrap support for this node is moderately strong (5/76, Node 10, Fig. 1). The relationship is diagnosed by 23 unambiguous synapomorphies, including the following five unique features: anterior lateral distal process of tibia well developed, anterior distal process strongly reduced (104[2]); metacarpal I expanded distally in medial view, with shaft narrowing towards proximal end (277[2]); dorsal surface of metacarpal III with sharp midline crest terminating in prominent tubercle proximally (285[1]); proximal articulation of metacarpal IV semicircular in shape, with flat edge facing dorsally (291[2]); and maxilla lacking narrow posterior palatal process extending lateral to palatine (315[0]). Among the 20 ambiguous synapomorphies at this node, one is unique: distal joint surfaces flat or concavoconvex on metacarpals I-IV, joints between distal metacarpals and proximal phalanges immobile (276[2]).

Node 11. Smutsiinae. Definition: Stem-based, the most inclusive clade including the common ancestor of *Phataginus tricuspis* and *Smutsia temminckii* and its descendents, plus all taxa more closely related to this common ancestor than to *Manis pentadactyla*.

As noted above, the four species of African manids are united into a monophyletic clade in the present study. This clade is the equivalent of the subfamily Smutsiinae of McKenna and Bell (1997). With a bootstrap value of 49 and a branch support of 2 (Fig. 1), it is the most weakly supported node on the tree. Nevertheless, it is diagnosed by 21 unambiguous synapomorphies, five of which are unique, and 20 ambiguous synapomorphies, one of which is unique (Appendix 4, Fig. 10). The five unambiguous unique traits are as follows: fibular facet of calcaneus extends further proximally than astragalar facet (90[2]); posterior extension of neural spine of axis absent, posterior surface of neural spine with two oval concavities for attachment of nuchal ligament (177[0]); metacarpal V forms peg-and-socket articulation with hamate, lateral tubercle of metacarpal V lies proximal to articular surface on metacarpal IV (295[1]); mallear head rotated dorsad 90°, incudal facet facing dorsally, caudally, and medially (342[2]); and stapedial columella short, height much less than greatest width of footplate (344[1]). The only unique feature among the ambiguous synapomorphies (Fig. 10e) is the posterior elongation of the cartilaginous xiphisternum such that it reaches the pelvis and then curls dorsally toward vertebral column at its distal end (194[2]).

Node 12. *Phataginus*. Definition: Node-based, the least inclusive clade including the common ancestor of *Phataginus tricuspis* and *Phataginus tetradactyla* and its descendents.

This node is the strongest on the entire tree as measured by bootstrap and branch support. It has a bootstrap value of 100, and failed to collapse even with the addition of 35 steps to the shortest tree (Fig. 1). The union of the African tree pangolins into a single clade is consistent with the

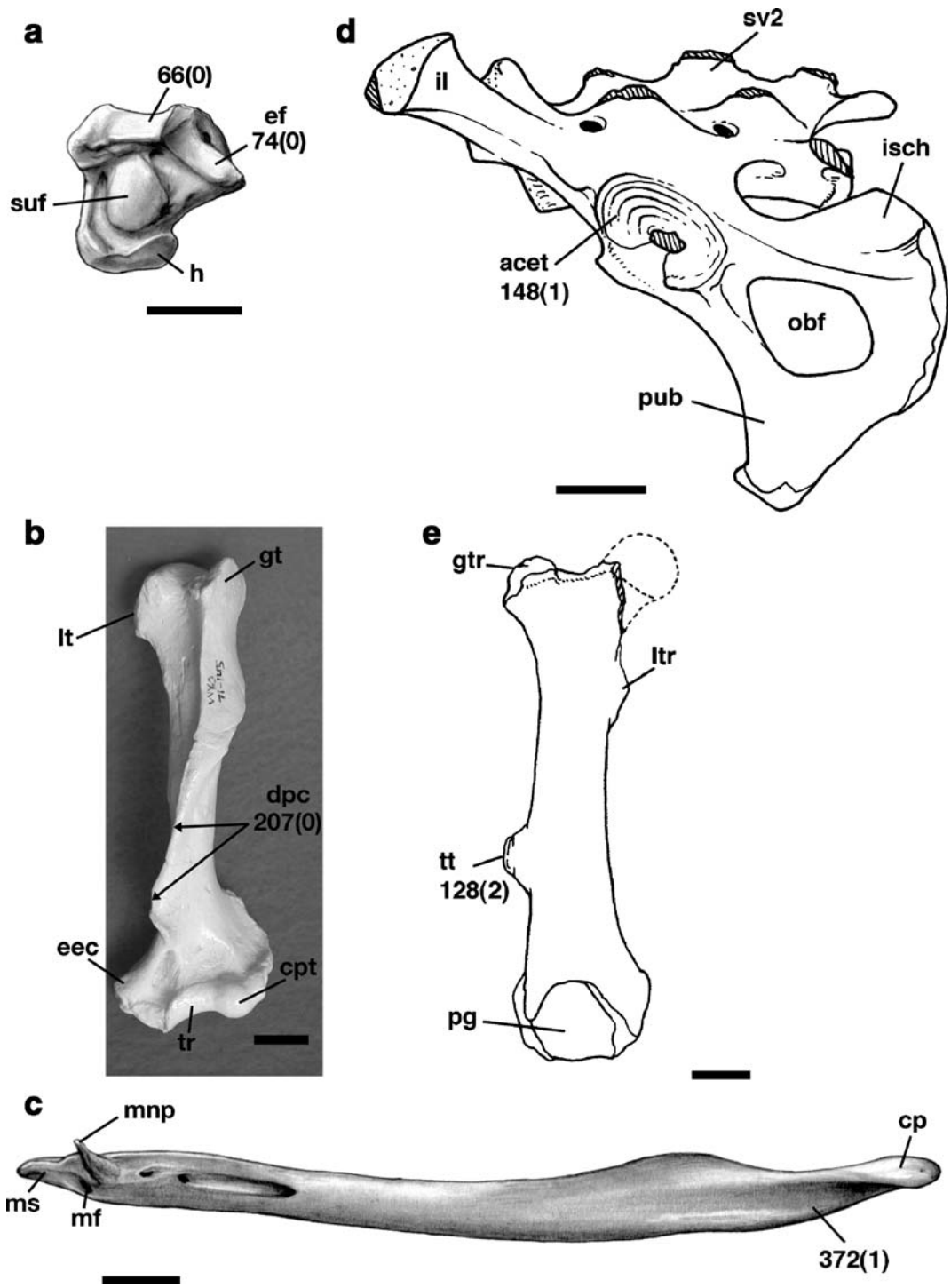

taxonomy of Koenigswald (1999), who placed these two taxa in a common genus *Phataginus*. Patterson (1978) used *Phataginus* for all four African pangolin species, but the type species of *Phataginus* is *P. tricuspis*, one of the arboreal forms (Pocock 1924). Therefore, it is appropriate to apply the generic epithet to this node. The genus *Phataginus* is diagnosed by a large number of synapomorphies in

◀ **Fig. 7** Synapomorphies of *Necromanis* with Patriomanidae and Manidae. Characters numbered as in Appendix 2. **a** Right astragalus of *Patriomanis americana* (USNM P299960) in ventral view, illustrating the following characters: 66[0], astragalus with distinct ventral facet for the tendon of the m. flexor digitorum fibularis; 74[0], ectal facet of astragalus very narrow, maximum length more than twice width measured perpendicular to long axis. **b** Right humerus of *Patriomanis americana* (USNM P531556) in anterior view, illustrating: 207 [0], deltopectoral crest elongated, extending >75% of the length of humerus. **c** Mandible of *Smutsia gigantea* (AMNH 53858) in left lateral view, illustrating: 372[1], absence of angular process. **d** Sacrum and pelvis of *Phataginus tricuspis* (CM 16206) in left lateral view, illustrating: 148[1], lunate surface of acetabulum C-shaped, nearly a closed loop. **e** Right femur of *Necromanis* in anterior view, illustrating: 128[2], distance between proximal end of femur and third trochanter ≥60%, <70% of maximum femoral length. Abbreviations: **acet,** acetabulum; **cp,** condylar process; **cpt,** capitulum; **dpc,** deltopectoral crest; **eec,** entepicondyle; **ef,** ectal facet; **gt,** greater tubercle; **gtr,** greater trochanter; **h,** astragalar head; **il,** ilium; **isch,** ischium; **lt,** lesser tubercle; **ltr,** lesser trochanter; **mf,** mental foramen; **mnp,** mandibular prong; **ms,** mandibular spout/symphysis; **obf,** obturator foramen; **pg,** patellar groove; **pub,** pubis; **suf,** sustentacular facet; **sv,** sacral vertebra; **tr,** trochlea; **tt,** third trochanter. **e** modified from Emry (1970). Scale bars=1 cm.

the present study—49 unambiguous synapomorphies, ten of which are unique, and 20 ambiguous synapomorphies, none of them unique (Appendix 4, Fig. 11). The ten unique synapomorphies of the arboreal African pangolins are as follows: lateral flange of metatarsal V elongate dorsoventrally, separated from cuboid facet by pit enclosed by dorsal and ventral ridges (31[2]); cuboid facet of metatarsal V transversely compressed with width < depth, but expanded ventrally (33[1]); navicular facet of lateral cuneiform butterfly-shaped, expanded transversely on dorsal and ventral ends with concave medial and lateral margins (50[1]); concavity on astragalar facet of navicular restricted to ventral side of convexity (60[1]); proximal edge (=posterior edge) of astragalar trochlea straight or convex in dorsal view (64[1]); distal tibia compressed, ratio of maximum width to anteroposterior depth ≥2 (113 [2]); lesser trochanter directed medially, largely obscured by head but visible medially in proximal view (130[2]); acetabular fossa opens ventrally (149 [0]); distal edge of trochlea of humerus convex in anterior view (219[1]); and manual ungual phalanx on digit I greatly reduced, <1/2 the length of ungual phalanx V (302[2]).

Node 13. *Smutsia.* Definition: Node-based, the least inclusive clade including the common ancestor of *Smutsia temminckii* and *Smutsia gigantea* and its descendents.

In contrast to the previous node, the clade including both African ground pangolins is substantially weaker, with a branch support of only 2 and a bootstrap value of 54 (Fig. 1). Moreover, it is supported by fewer synapomorphies than either of the other two modern genera—21 unambiguous synapomorphies, only three of which are unique, and 20 ambiguous synapomorphies, none of which are unique (Appendix 4). Nevertheless, this grouping is consistent with the taxonomies of Pocock (1924); McKenna and Bell (1997), and Koenigswald (1999) among others, and we follow these authors in assigning the two species to the genus *Smutsia*. The three unique synapomorphies of *Smutsia* are (Fig. 12): an enlarged attachment surface for the Achilles' tendon extending forward along plantar surface of calcaneus for more than half its length (87[1]); a wide anconeal process of ulna with a maximum width >15% of maximum ulnar length (231[2]); and presence of an elongated lateral perforation in mandibular canal (368[1]).

As noted in the Materials and Methods section above, a separate analysis has been conducted using only extant taxa, in order to understand the effect in the present study of fossils and the large amount of missing data that characterizes fossil taxa. The analysis of extant taxa yields a single MPT (TL=998, CI= 0.763, RI=0.661; Fig. 13). This tree differs from the tree in Fig. 1 in that the genus *Smutsia* is allied as the sister group to the Asian pangolins in the genus *Manis*, rather than as the sister group to the other African genus *Phataginus*. This alliance between *Smutsia* and *Manis* is diagnosed by 28 unambiguous and 20 ambiguous synapomorphies, of which nine unambiguous and three ambiguous features are unique, in the analysis of only living forms. However, of the 28 unambiguous synapomorphies of this clade, 19 are known to occur either in patriomanids, *Necromanis, Eomanis waldi*, *"Eomanis" krebsi,* or *Eurotamandua joresi*, suggesting that the support these characters provide for such a clade should be viewed with skepticism. If these 19 characters are discounted, there are only nine characters that unambiguously support joining the African ground pangolins to the Asian

Fig. 8 Synapomorphies of the Manidae. Characters numbered as in Appendix 2. **a** Left pes of *Phataginus tricuspis* (CM 16206) in dorsal view, illustrating the following characters: 8[2], distal keel on metatarsals and metacarpals extends along entire dorsoventral length of condyle, dorsal fossa above condyle absent; 21[1], metatarsal III short, <28% tibial length; 24[1], proximal end of metatarsal II expanded transversely; 26[1], proximal articular facet of metatarsal III overlaps dorsal surface of shaft; 49[2], dorsal surface of lateral cuneiform widened transversely, ratio of width to height ≥1.4; 56[1], maximum length of calcaneal facet of cuboid ≤80%, >70% maximum height of cuboid; 63[2], astragalar trochlea strongly asymmetrical, ratio of lateral to medial depth ≥1.4; 69[1], width of astragalar neck ≥60% maximum width of astragalus. **b** Right astragalus of *Phataginus tricuspis* (CM 16206, on left) and *Patriomanis americana* (USNM P299960, on right) in distal view, illustrating: 59[1], astragalar head of navicular concave dorsolaterally, convex ventromedially; 59[0], astragalar head evenly convex. **c** Left femur of *Phataginus tricuspis* (CM 16206, on left) and *Patriomanis americana* (USNM P299960, on right) in proximal view, illustrating: 125[0], anteroposterior depth of greater trochanter of femur > transverse width; 125[2], greater trochanter of femur compressed anteroposteriorly, anteroposterior depth ≤ transverse width; 131[0], fovea capitis present; 131[1], fovea capitis absent. **d** Left calcaneus of *Phataginus tricuspis* (CM 16206) in dorsal view, illustrating: 89[2], sustentacular facet on calcaneus situated well distal to astragalar and fibular facets, contacting distal margin of calcaneus. **e** Left femur of *Phataginus tricuspis* (CM 16206) in posterior view, illustrating: 132[1], femoral trochanteric fossa and intertrochanteric ridge rudimentary or absent. **f** Pelvis and sacrum of *Manis javanica* (USNM 198852) in dorsal view, illustrating: 136[1], sacroiliac attachment fused; 140[1], dorsal spinal nerve foramina of sacral vertebrae face dorsolaterally, situated immediately underneath metapophyses. **g** Right scapula of *Phataginus tricuspis* (CM 16206) in distal view, illustrating: 204[1], scapular spine reduced in height, height <85% mediolateral width of glenoid (gray lines indicate height of scapular spine and width of glenoid); **h** Left tibia and fibula of *Phataginus tricuspis* (CM 16206) in anterior view, illustrating: 102[2], anterolateral eminence on proximal fibula present opposite tibial facet; 103[2], cnemial crest of tibia weak, rounded, lacking lateral excavation. **i** Pelvis and sacrum of *Smutsia gigantea* (AMNH 53858) in right lateral view, illustrating: 142[1], transverse process of last sacral vertebra unexpanded, rod-like; 144[1], metapophyses of sacral vertebrae elongated, >2/3 neural spine height; 146[2], gluteal fossa poorly demarcated, iliac crest rounded, weak, dorsal flange absent, caudal dorsal iliac spine incorporated in sacroiliac junction; 153[1], ischial spine situated close to ischial tuberosity, dorsal to posterior portion of obturator foramen; 154[1], dorsal edge of ischium ventral to transverse processes of sacral vertebrae. **j** Left radius of *Phataginus tricuspis* (CM 16206, on left) and *Patriomanis americana* (USNM P299960, on right) in proximal view, illustrating: 244[2], sesamoid facet on radial head large, visible in proximal view. **k** Left radius of *Phataginus tricuspis* (CM 16206, on left) and *Patriomanis americana* (USNM P299960, on right) in anterior view, illustrating: 246[0], styloid process rudimentary, pseudostyloid process prominent, dorsal tuberosity weak; 246[2], styloid process and dorsal tuberosity of distal radius prominent, pseudostyloid process rudimentary or absent. **l** Right manus of *Phataginus tricuspis* (CM 16206) in dorsal view, illustrating: 6[2], distal condyles of manual and pedal intermediate phalanges nearly uniform in width, lateral fossae for tendinous insertion obscured in dorsal view by lateral ridges of distal condyles; 8[2], distal keel on metatarsals and metacarpals extends along entire dorsoventral length of condyle, dorsal fossa above condyle absent; 260[2], scapholunar facet on trapezoid tilted to face proximally and medially in dorsal view; 289[1], dorsal surface of metacarpal IV T-shaped at proximal end, extended laterally and medially for articulations with metacarpals III and V; 301[1], proximal articulations of manual intermediate phalanges not visible in dorsal view due to presence of proximally elongated dorsal midline process. **m** Left basicranial region of *Smutsia gigantea* (AMNH 53858) in ventral view, illustrating: 334[1], promontorium of petrosal weakly developed, flat; 336[1], distal tip of tympanohyal fused to lateral surface of promontorium; 337[1], fenestra cochleae situated immediately next to fenestra vestibuli, facing laterally and slightly posteriorly; 339[2], fossa incudis situated in medial wall of epitympanic recess, facing laterally. Abbreviations: **acet,** acetabulum; **ast,** astragalus; **bo,** basioccipital; **cav,** caudal vertebra; **clc,** calcaneus; **cpf,** capitular facet; **cu,** cuboid; **cuf,** cuboid facet; **dt,** dorsal tuberosity; **ef,** ectal facet; **en,** entotympanic; **fc,** fenestra cochleae; **ff,** fibular facet; **fi,** fossa incudis; **fib,** fibula; **fv,** fenestra vestibuli; **fvc,** fovea capitis; **gtr,** greater trochanter; **h,** head; **il,** ilium; **ip,** intermediate phalanx; **isch,** ischium; **issp,** ischial spine; **istb,** ischial tuberosity; **jf/hf,** jugular and hypoglossal foramina (merged); **lco,** lateral condyle; **lcu,** lateral cuneiform; **ltr,** lesser trochanter; **ltro,** lateral trochlea; **lv,** lumbar vertebra; **mc,** metacarpal; **mco,** medial condyle; **mecu,** medial cuneiform; **mma,** medial malleolus; **mp,** metapophysis; **mt,** metatarsal; **mtro,** medial trochlea; **nav,** navicular; **ns,** neural spine; **obb,** oblique border; **obf,** obturator foramen; **pe,** petrosal; **perp,** peroneal process; **pp,** proximal phalanx; **pr,** promontorium of petrosal; **prh,** prehallux; **pstp,** pseudostyloid process; **pt,** pterygoid hamulus; **pub,** pubis; **rtu,** radial tuberosity; **sef,** radial sesamoid facet; **sq,** squamosal; **stp,** styloid process; **suf,** sustentacular facet; **sv,** sacral vertebra; **th,** tympanohyal; **tib,** tibia; **tpd,** trapezoid; **trf,** trochanteric fossa; **trof,** trochlear facet; **ttb,** tibial tuberosity; **up,** ungual phalanx. **f** modified from Rose and Emry (1993). **h** modified from Gaudin et al. (2006). **m** modified from Gaudin and Wible (1999). Scale bars=1 cm.

pangolins. Of these, three are unique to the clade: sacroiliac junction extends past midpoint of acetabulum, sacral vertebrae contact anterior ischium (137[2]); acetabular fossa opens posteriorly (149[2]); and lacrimal bone and lacrimal foramen both absent (319[2]). One additional unique feature is found among the ambiguous synapomorphies that is not known to be present in the fossil taxa: proximal articular surface of metatarsal III roughly triangular in proximal view, narrowing ventrally (27[1]).

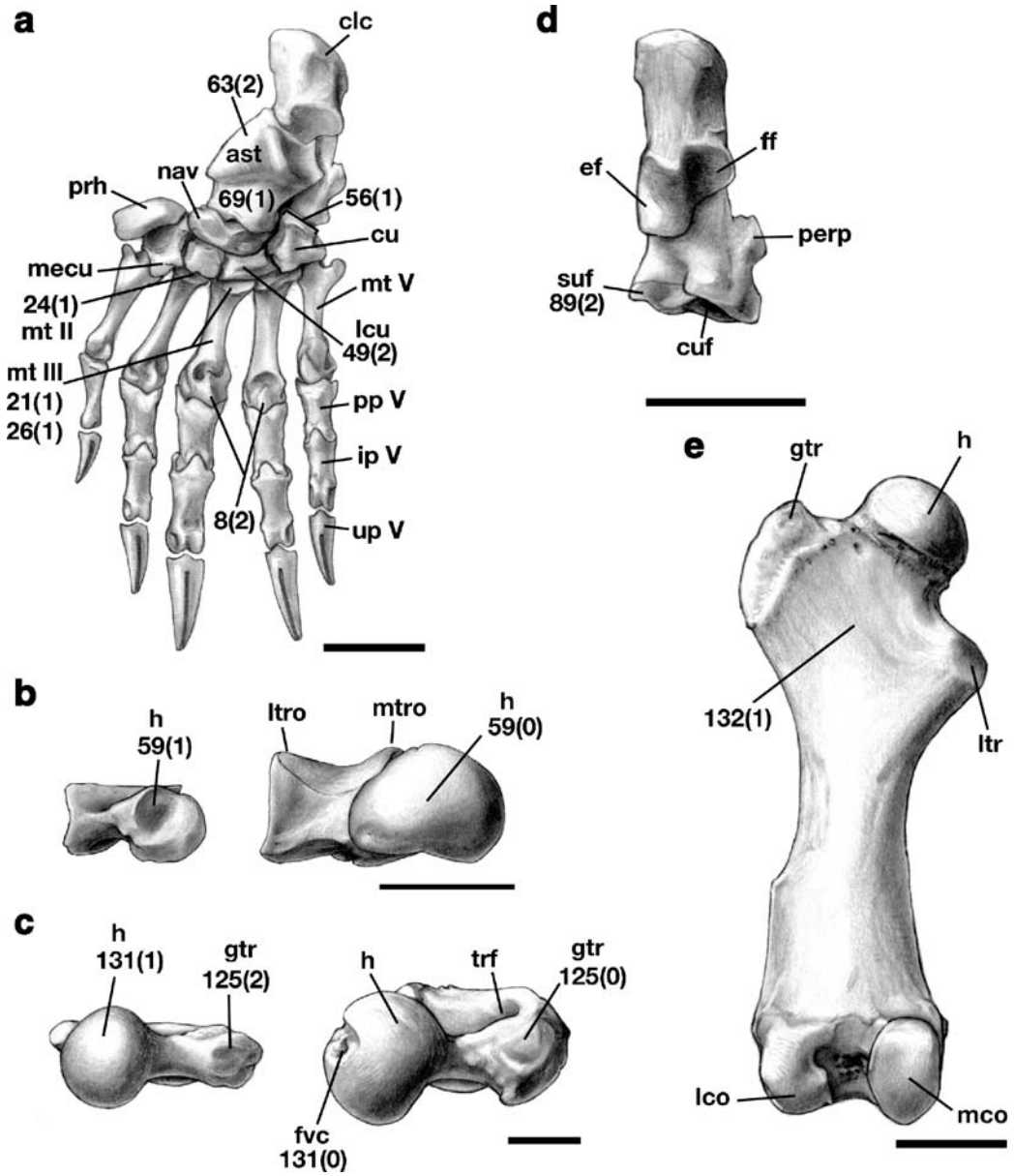

A final analysis has been performed in which PAUP was constrained to produce the shortest tree(s) consistent with Gaudin and Wible's (1999) previously published phylogenetic hypotheses. Gaudin and Wible's (1999) cladogram differs from that illustrated in Fig. 1 in the manner in which the three extant genera recognized here are related to one another, and in the manner in which the three Asian pangolin species are arranged. In Gaudin and Wible's study (1999), the African tree pangolins (placed here in *Phataginus*) formed the sister group to the Asian pangolins (*Manis*), whereas in the present study they are allied with the African ground pangolins (*Smutsia*). Furthermore, in Gaudin and Wible's (1999) study *M. crassicaudata* was the sister species to *M. javanica*, whereas in the present study it is more closely related to *M. pentadactyla*. The constrained analysis yields a single MPT (TL=1475) that is 23

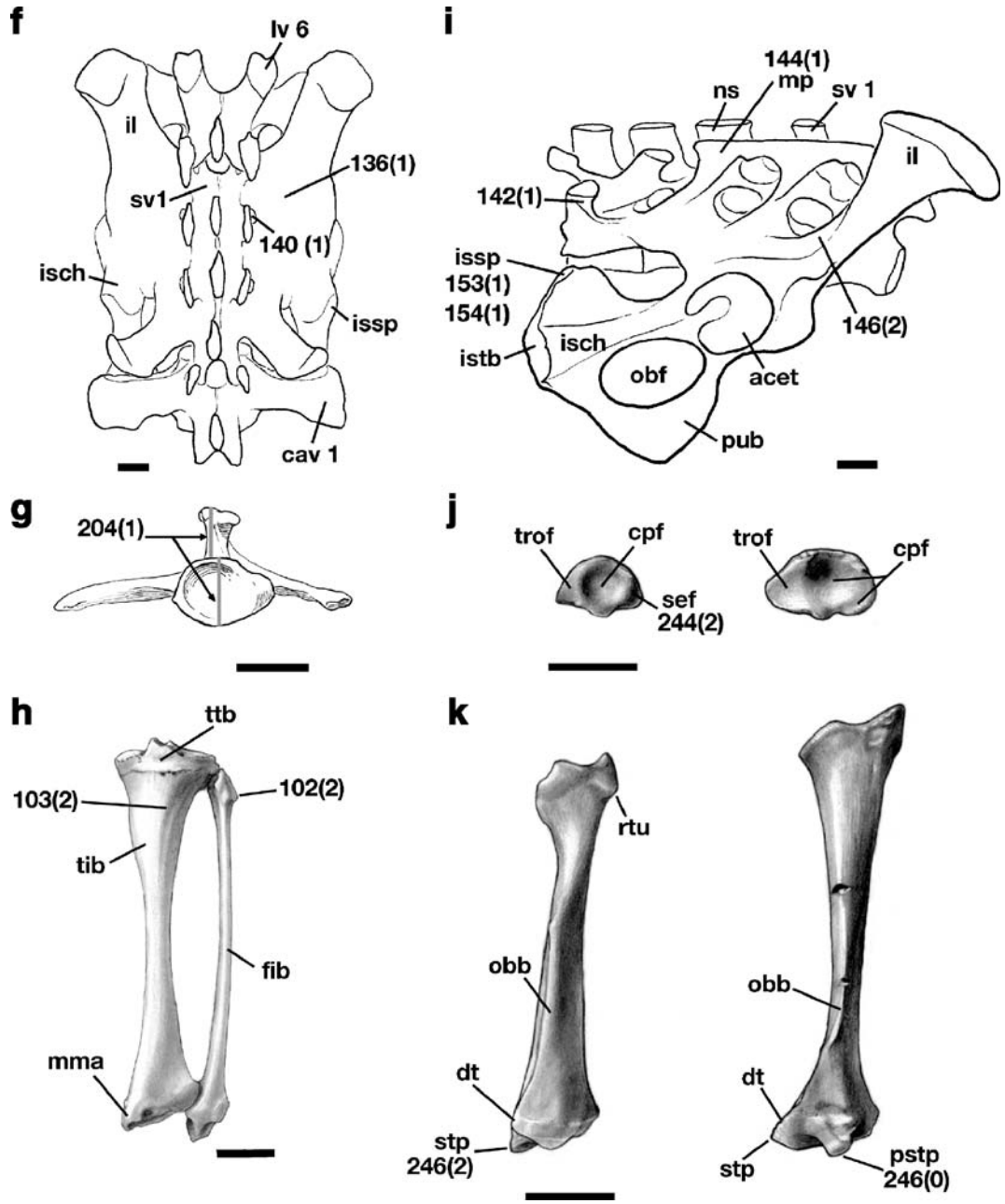

Fig. 8 (continued)

steps longer than the tree illustrated in Fig. 1. The constrained MPT places all the fossil taxa in nearly the same arrangement as that shown in Fig. 1, although it allies *Necromanis* with the Patriomanidae and it arranges the extant taxa according to the pattern illustrated by Gaudin and Wible (1999: fig. 5).

Discussion

Because the present study encompasses virtually all the known living and fossil diversity of pangolins, and is based upon an extensive data set of morphological characters, it provides an unusually detailed

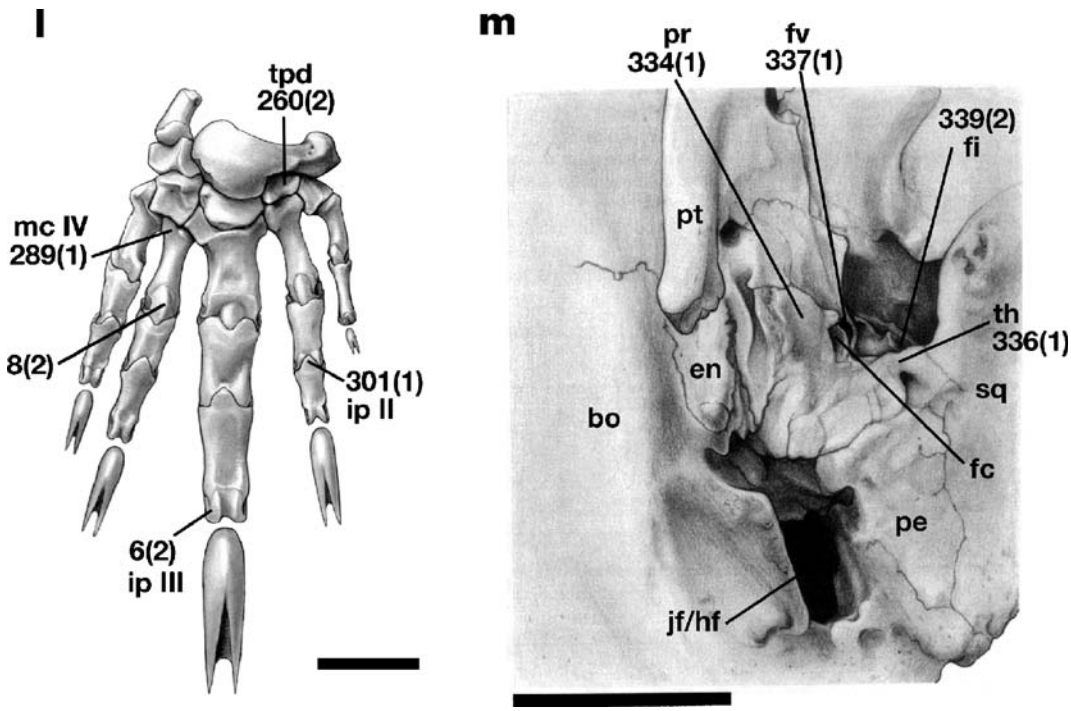

Fig. 8 (continued)

picture of the phylogenetic relationships within a mammalian order. The phylogenetic patterns that are produced by these analyses are well resolved, and the internal nodes on the cladogram are by and large well supported. Therefore, this analysis should provide a firm foundation for addressing some of the persistent questions that surround the phylogeny, taxonomy, and biogeographic history of the order Pholidota.

The nature of the relationship between the extinct Palaeanodonta and the extant orders Xenarthra and Pholidota has been a longstanding conundrum in the field of placental mammal paleontology and systematics. From their earliest descriptions, the palaeanodonts have been linked to xenarthrans and pangolins because of their fossorial adaptations and reduced dentitions (Matthew 1918). Although palaeanodonts display remarkable similarities in their basicranial anatomy to the Xenarthra (Patterson et al. 1992; Gaudin 1995, 2004), several recent studies have identified a series of detailed cranial and postcranial resemblances between metacheiromyid palaeanodonts and the oldest pangolins in the genus *Eomanis* (Storch 2003; Rose et al. 2005; Fig. 3). We have accepted the results of these studies, as well as the earlier hypotheses of Emry (1970; Rose and Emry 1993), and assumed at the outset that palaeanodonts and pangolins form some sort of clade, although we did not specify the nature of the relationships within that clade. The results of the present study are novel, in that they provide a large number of synapomorphies that can be used to diagnose a palaeanodont and pangolin clade, and they further confirm that within that clade, Palaeanodonta and Pholidota are monophyletic sister taxa. We have labeled this palaeanodont/pangolin clade the Pholidotamorpha, and we thus restrict the use of the term "Pholidota" to the clade including all those animals more closely related to modern pangolins than to palaeanodonts, in contrast to the usage by Emry (1970) and McKenna and Bell (1997). We believe, however, that our usage is a reasonable solution to the problem outlined in the Introduction of the present study, namely, that Pholidota has been used to refer both to the clade including palaeanodonts and pangolins and to the clade containing only the extinct and extant pango-

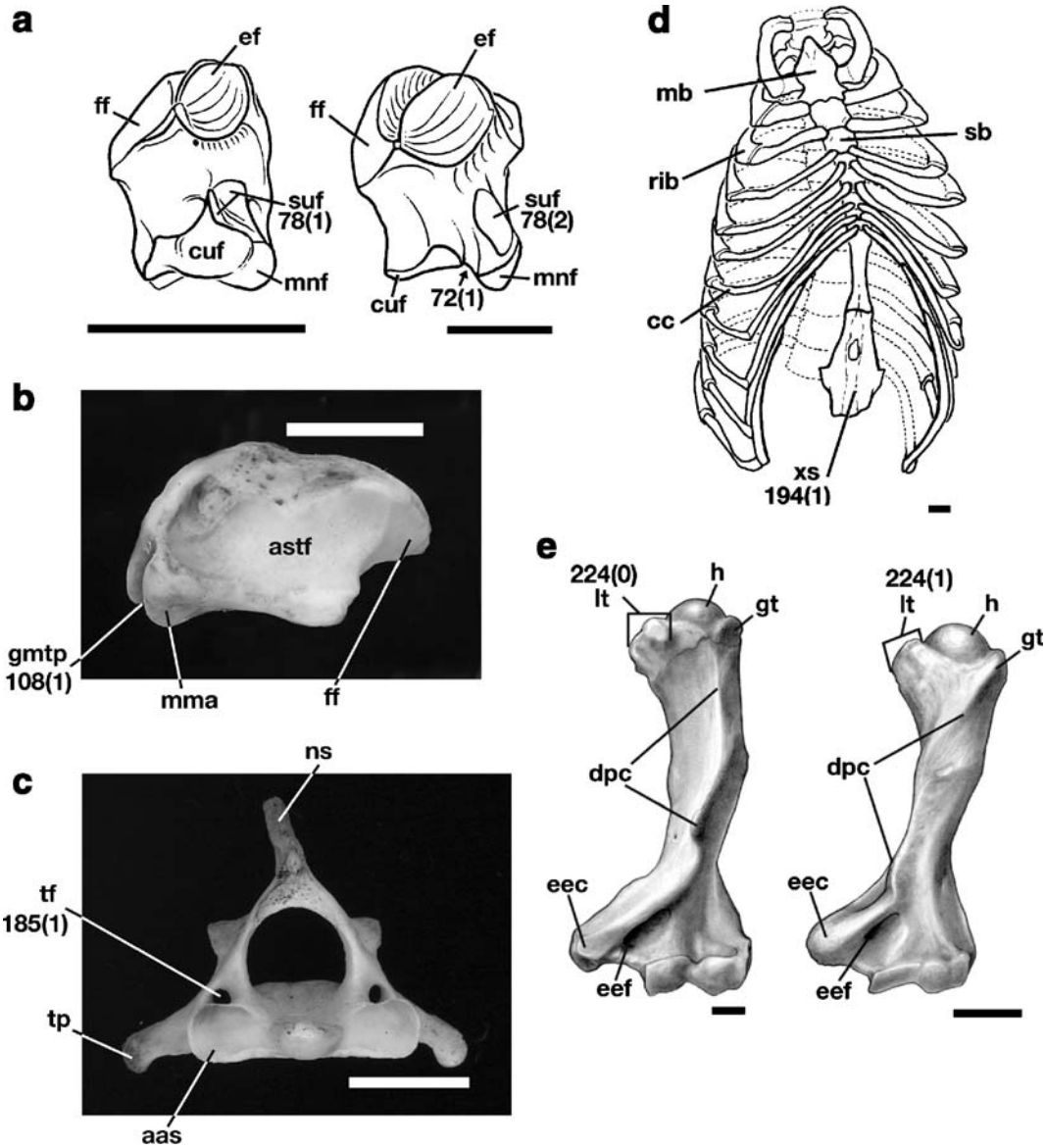

lins. Furthermore, it is consistent with the most common usage of the term Pholidota, as exemplified by Mammalogy textbooks (e.g., Vaughan et al. 2000; Feldhamer et al. 2007) and other general reference works (e.g., Nowak 1999), to refer to living and fossil pangolins only.

Although the present study identifies a number of synapomorphies for a pholidotamorph clade that includes palaeanodonts (Appendix 4, Fig. 3), it cannot completely settle the issue of palaeanodont affinities. Our sample of palaeanodonts was far from exhaustive, including neither a representative from the epoicotheriid palaeanodonts nor the oldest and most primitive known palaeanodont, *Escavadodon zygus* (Rose and Lucas 2000). Members of the Epoicotheriidae, the most diverse of the three palaeanodont families, possess a highly derived morphology due to extreme fossorial adaptations (e.g., Rose and Emry 1983), and hence are likely too specialized to shed much light on the broader relationships of palaeanodonts. However, it would be intriguing to include *Escavadodon zygus* in subsequent phylogenetic stud-

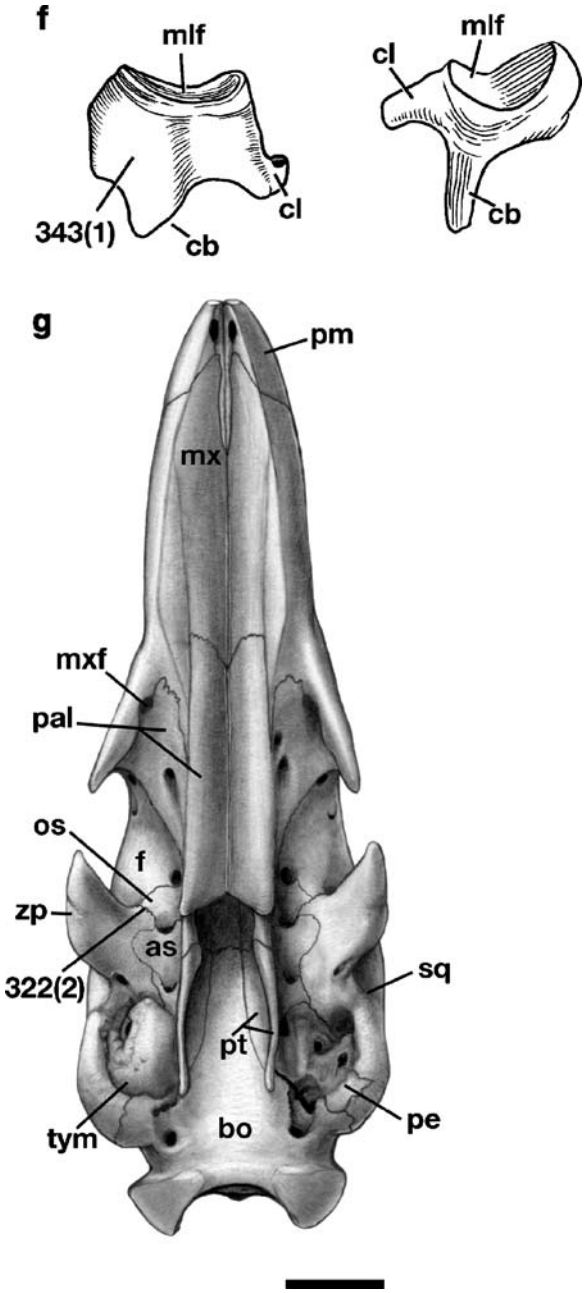

Fig. 9 (continued)

◀ **Fig. 9** Synapomorphies of *Manis*. Characters numbered as in Appendix 2. **a** Left astragalus of *Phataginus tricuspis* (CM 16206, on left) and *Manis javanica* (USNM 198852, on right) in ventral view, illustrating the following characters: 72[1], presence of deep groove for calcaneal-navicular "spring" ligament on ventral margin of astragalar head; 78[1], sustentacular facet of astragalus in midline of astragalar neck; 78[2], sustentacular facet near medial edge of astragalar neck. **b** Left tibia of *Manis javanica* (CM 40597) in distal view, illustrating: 108[1], groove for m. tibialis posterior tendon deep, closed over by soft tissue to form tunnel. **c** Axis of *Manis javanica* (CM 40597) in anterior view, illustrating: 185[1], transverse foramen of axis visible in anterior view. **d** Ribs, costal cartilages and sternum of *Manis javanica* (USNM 198852) in ventral view, illustrating: 194[1], cartilaginous extension of xiphisternum elongated, length much greater than ossified portion of xiphisternum, shovel shaped at distal end with central perforation. **e** Left humerus of *Phataginus tricuspis* (CM 16206, on left) and *Manis javanica* (USNM 198852, on right) in anterior view, illustrating: 224[0], proximal portion of lesser tubercle of humerus extends anterolaterally, overlaps head in anterior view; 224[1], lesser tubercle does not extend anterolaterally, remains medial to head in anterior view. **f** Right incus of *Manis crassicaudata* (FMNH 57338, on left) and left incus of *Smutsia temminckii* (FMNH 38144, on right, distal end of crus longum broken) in lateral view, illustrating: 343[1], body of incus stout and rectangular, crura short. **g** Skull of *Manis javanica* (USNM 198852) in ventral view, illustrating: 322[2], broad orbitosphenoid/squamosal contact. Abbreviations: **aas,** anterior articular surface; **as,** alisphenoid; **astf,** astragalar facet; **bo,** basioccipital; **cb,** crus breve; **cc,** costal cartilage; **cl,** crus longum; **cuf,** cuboid facet; **dpc,** deltopectoral crest; **eec,** entepicondyle; **eef,** entepicondylar foramen; **ef,** ectal facet; **f,** frontal; **ff,** fibular facet; **gmtp,** groove for m. tibialis posterior tendon; **gt,** greater tubercle; **h,** head; **lt,** lesser tubercle; **mb,** manubrium; **mlf,** mallear facet; **mma,** medial malleolus of tibia; **mnf,** medial navicular facet; **mx,** maxilla; **mxf,** maxillary foramen; **ns,** neural spine; **os,** orbitosphenoid; **pal,** palatine; **pe,** petrosal; **pm,** premaxilla; **pt,** pterygoid; **sb,** sternebra; **sq,** squamosal; **suf,** sustentacular facet; **tf,** transverse foramen; **tp,** transverse process; **tym,** tympanic (=ectotympanic); **xs,** xiphisternum; **zp,** zygomatic process. **f** modified from Segall (1973). Scale bars=1 cm.

ies to determine if its anatomy was also consistent with a common ancestry between pangolins and palaeanodonts. It should also be noted that our analysis did not include any representatives of the order Xenarthra, the other extant placental group to which the palaeanodonts sometimes have been linked (Simpson 1945; Patterson et al. 1992; Gaudin 1995, 2004). As discussed in the Introduction to this work and by Rose et al. (2005) and others, a definitive resolution of palaeanodont ordinal relationships still awaits a comprehensive phylogenetic study that includes representatives of all known xenarthran and pholidotamorph families, as well as a wide array of basal eutherians and representatives of a variety of placental orders, including all the major supraordinal clades. Only then can the various competing hypotheses be adequately tested.

One of the more intriguing results of the present study is its inclusion of the enigmatic "edentate"

Fig. 10 Synapomorphies of the Smutsiinae. Characters numbered as in Appendix 2. **a** Left calcaneus of *Phataginus tricuspis* (CM 16206) in dorsal view, illustrating the following character: 90[2], fibular facet of calcaneus extends further proximally than astragalar facet. **b** Axis of *Phataginus tricuspis* (CM 16206, on left) and *Patriomanis americana* (USNM P299960, on right, incomplete specimen) in anterior view, illustrating: 183[1], width and depth of anterior articular surface of axis nearly equivalent, ratio <1.25; 184[0], axial anterior articular surface and articular facet of dens contiguous; 184[1], facets separate. **c** Dorsal vertebrae, ribcage, sternum, sacrum and pelvis of *Phataginus tricuspis* (CM 16206) in left lateral view, illustrating: 194[2], posterior elongation of the cartilaginous xiphisternum such that it reaches the pelvis and then curls dorsally toward vertebral column at its distal end. **d** Axis of *Manis javanica* (USNM 198852, on left, cranial articular facets and dens not visible, reconstructed based on other *Manis*) and *Phataginus tricuspis* (CM 16206, on right) in left lateral view, illustrating: 177[0], posterior extension of neural spine of axis absent, posterior surface of neural spine with two oval concavities for attachment of nuchal ligament. **e** Right manus of *Phataginus tricuspis* (CM 16206) in dorsal view, illustrating: 295[1], metacarpal V forms peg-and-socket articulation with hamate, lateral tubercle of metacarpal V lies proximal to proximal articular surface on metacarpal IV. **f** Left malleus of *Smutsia temminckii* (FMNH 38144) in lateral view, illustrating: 342[2], mallear head rotated dorsad 90°, incudal facet facing dorsally, caudally, and medially. **g** Left stapes of *Smutsia temminckii* (FMNH 38144, on left) in dorsal view and right stapes of *Manis crassicaudata* (FMNH 57338, on left) in ventral view, illustrating: 344[0], stapedial columella elongated, height nearly equal to or exceeding greatest width of footplate; 344[1], stapedial columella short, height much less than greatest width of footplate. **h** Skull of *Phataginus tricuspis* (CM 86715) in ventral view, illustrating: 312[1] presence of vomerine exposure on palate; 330[0] presence of ectotympanic inflation. Abbreviations: **aas,** anterior articular surface; **apm,** anterior process of malleus; **as,** alisphenoid; **bo,** basioccipital; **bs,** basisphenoid; **d,** dens; **ef,** ectal facet; **f,** frontal; **ff,** fibular facet; **hm,** hamate; **il,** ilium; **inf,** incudal facet; **isch,** ischium; **lv,** lumbar vertebra; **mbm,** manubrium of malleus; **mc,** metacarpal; **mx,** maxilla; **ns,** neural spine; **occ,** occipital condyle; **pal,** palatine; **perp,** peroneal process; **pm,** premaxilla; **pt,** pterygoid; **pub,** pubis; **pz,** posterior zygapophysis; **sq,** squamosal; **suf,** sustentacular facet; **sv,** sacral vertebra; **tf,** transverse foramen; **tp,** transverse process; **tv,** thoracic vertebra; **tym,** tympanic (= ectotympanic); **v,** vomer; **xs,** xiphisternum. **c** based in part on Kingdon (1974). **f** and **g** modified from Segall (1973).

Eurotamandua joresi within the Pholidota, coupled with its lack of support for the monophyly of the genus *Eomanis*, and, by extension, the family Eomanidae (Fig. 1). The phylogenetic affinities of *Eurotamandua* have been the subject of much controversy, with various authors suggesting affinities with xenarthran anteaters (Storch 1981; Storch and Habersetzer 1991), with xenarthran pilosans (anteaters and sloths) (Gaudin and Branham 1998), palaeanodonts (Rose 1999), or a palaeanodont-pangolin assemblage (Cifelli 1983). Szalay and Schrenk (1998) went so far as to place *Eurotamandua* in its own order, the Afrodentata, albeit with the suggestion that this group may bear some distant relationship to palaeanodonts. In the most recent review of the matter, the authors themselves could not agree on the proper allocation of *Eurotamandua*, with one author advocating vermilinguan affinities, and the other three suggesting a closer relationship to palaeanodonts or *Eomanis* (Rose et al. 2005).

Based on a series of detailed resemblances in the humerus, ulna, and third metacarpal, Rose (1999) hypothesized that *Eurotamandua* was a close relative of palaeanodonts. Rose et al. (2005) pointed out additional resemblances between *Eurotamandua* and palaeanodonts, including a loosely attached, C-shaped premaxilla, an anteriorly situated infraorbital foramen, an ossified auditory bulla, a lacrimal with subequal facial and orbital exposures, enlarged anapophyses and metapophyses in the posterior thoracic and lumbar vertebrae, and short, robust digits. Nevertheless, our results do not support a close relationship between metacheiromyid palaeanodonts and *Eurotamandua*. Among the autapomorphies that were assigned to *Eurotamandua* in the MPT shown in Fig. 1, only four are convergent on the Palaeanodonta (Node 2; see Appendix 4): presence of a posterior distal tibial process (105[1]), styloid process of radius oriented distolaterally (247[1]), length of metacarpal II>IV (273[2]), and articulation between metacarpal II and III formed by convex facet on metacarpal II, concave facet on metacarpal III (282[2]). Of these, only 105[1] and 282[2] are features unique to *Eurotamandua* and the palaeanodonts among the taxa included in this study.

Shoshani et al. (1997) were the first to propose an explicit relationship between *Eurotamandua* and pangolins, and their hypothesis was incorporated into the classification scheme of McKenna and Bell (1997), who placed *Eurotamandua* into the family Manidae (equivalent to our usage of "Pholidota"), but outside the subfamilies Maninae and Smutsiinae, into which they placed all the undoubted fossil and extant pangolins, including *Eomanis*. Our results are closely aligned with the latter arrangement. In our MPT (Fig. 1), *Eurotamandua* is interposed between *"Eomanis"*

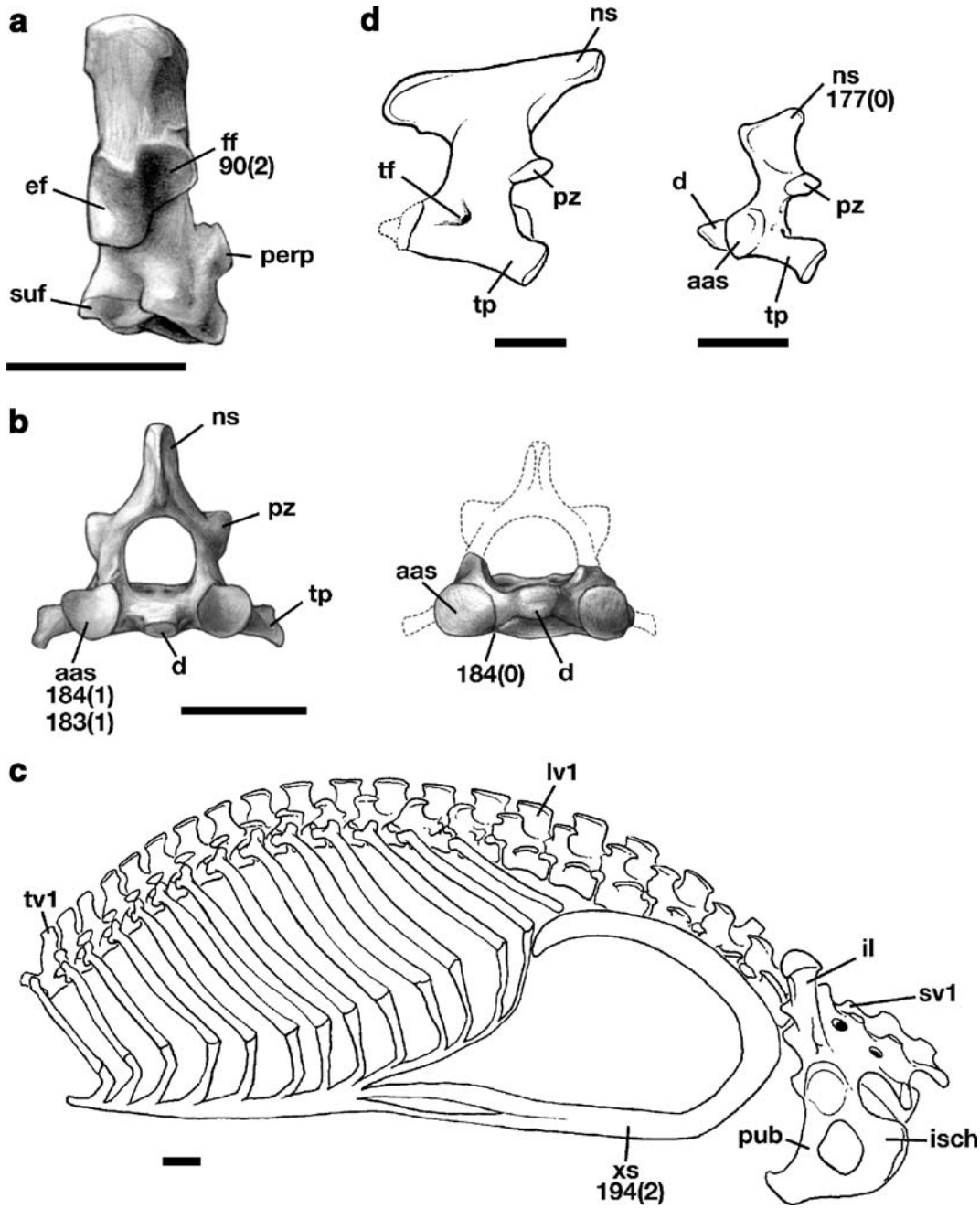

krebsi and a clade including *Eomanis waldi* and all more derived pangolins. Because *Eomanis* (including both *E. waldi* and *"Eomanis" krebsi*) has been widely accepted as the oldest fossil pangolin genus, and *E. waldi* is known to bear the epidermal scales that are the hallmark of this group (Koenigswald et al. 1981), we have chosen to assign the ordinal epithet "Pholidota" to the clade whose common ancestor lies at the base of the three Messel taxa (*Eurotamandua, E. waldi* and *"Eomanis" krebsi*), making *Eurotamandua* a pholidotan by this definition. The basal pholidotan node is not diagnosed by a large number of apomorphies—four

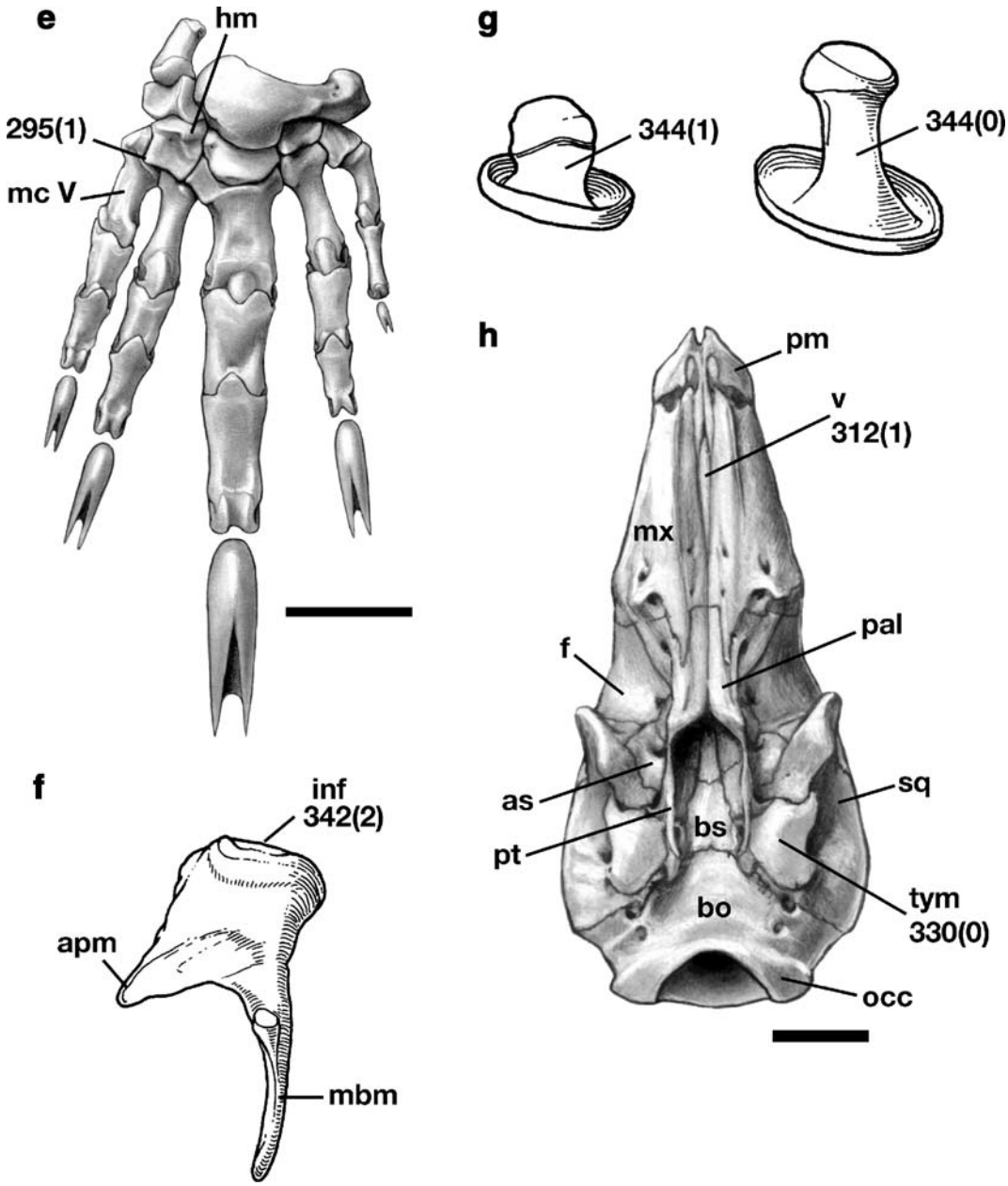

Fig. 10 (continued)

unambiguous synapomorphies, two of which are unique, and eight ambiguous synapomorphies (see "Results" section, Appendix 4, Fig. 3). Moreover, the node receives only modest Bremer and bootstrap support (Fig. 1). However, as noted above, the next node (Node 4; see "Results" section, Appendix 4, Figs. 1 and 3) linking *Eurotamandua* with other pangolins exclusive of *"Eomanis" krebsi*, is supported by an additional three unambiguous synapomorphies and a large number of ambiguous synapomorphies. Most of these are ambiguously assigned to this node because they could not be coded in *"Eomanis" krebsi,* but among these are five features that are unique to Node 4 as the matrix now stands. Thus we believe the

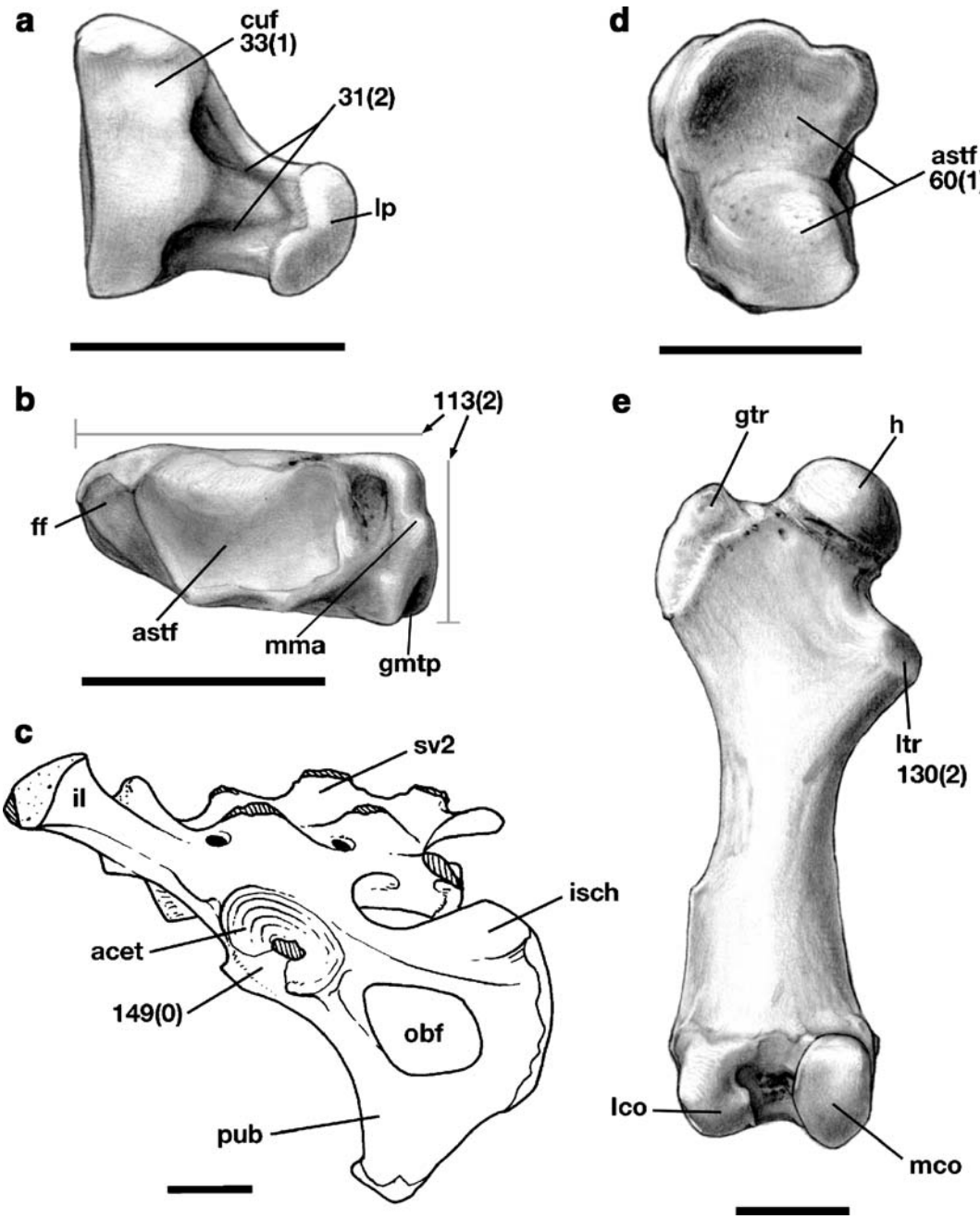

inclusion of *Eurotamandua* in Pholidota is a fairly robust result of this study. Moreover, it highlights the anatomical similarity between the two genera of Messel "edentates," *Eomanis* and *Eurotamandua*, previously noted by Rose and Emry (1993) and Rose et al. (2005). Nevertheless, as was the case with palaeanodonts, this analysis was not designed to provide a definitive resolution of the phylogenetic relationships of *Eurotamandua*. We have assumed at the outset that *Eurotamandua* was closely related to pangolins and palaeanodonts, but a definitive test of this idea would require a more extensive analysis, one that included a large sample of xenarthrans and other placental groups as well as pholidotamorphs.

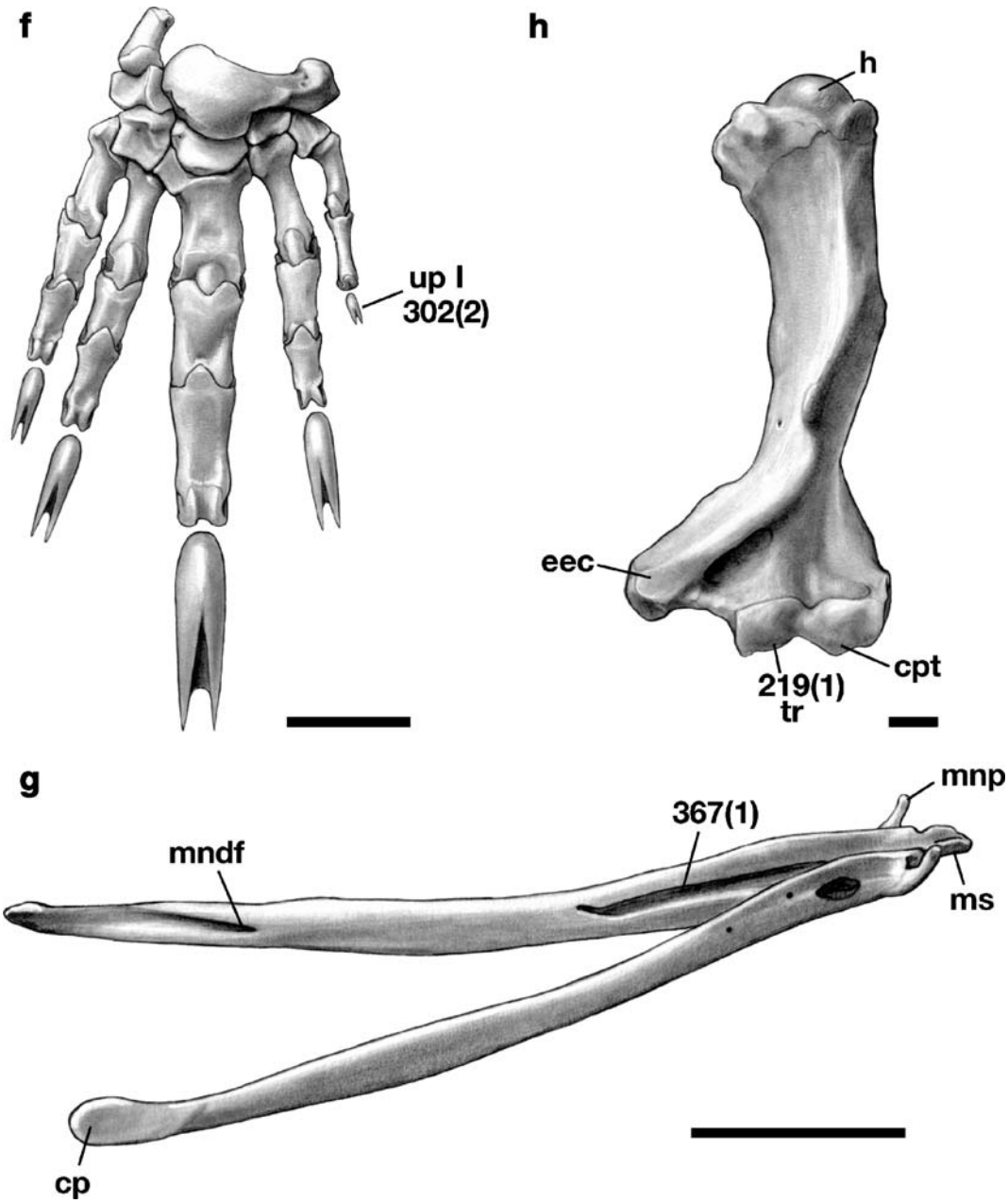

Fig. 11 (continued)

It should also be made clear that although we have chosen to designate Node 3 as the order Pholidota, the term could justifiably have been applied elsewhere. *Eomanis waldi* is the only Messel taxon known to have possessed epidermal scales, perhaps the single most distinctive and recognizable feature of the modern pangolins. We do not know whether the other Messel forms possessed scales or not, but if we were to employ a character-based definition of Pholidota based on our present knowledge of which taxa are "scaly," we would have assigned the term to Node 5, currently designated as the suborder Eupholidota.

The failure of the present analysis to support the monophyly of the genus *Eomanis* and its family, Eomanidae, is quite as surprising as its allocation of *Eurotamandua*. *Eomanis* currently has two species

◀ **Fig. 11** Synapomorphies of *Phataginus*. Characters numbered as in Appendix 2. **a** Left metatarsal V of *Phataginus tricuspis* (CM 16206) in proximal view (dorsal surface at bottom of figure), illustrating the following characters: 31[2], lateral flange of metatarsal V elongate dorsoventrally, separated from cuboid facet by pit enclosed by dorsal and ventral ridges; 33[1], cuboid facet transversely compressed with width<depth, but expanded ventrally. **b** Right tibia of *Phataginus tricuspis* (CM 16206) in distal view (anterior surface at top of figure), illustrating: 113[2], distal tibia compressed, ratio of maximum width to anteroposterior depth ≥2 (gray lines indicate width and depth). **c** Sacrum and pelvis of *Phataginus tricuspis* (CM 16206) in left lateral view, illustrating: 149[0], acetabular fossa opens ventrally. **d** Left navicular of *Phataginus tricuspis* (CM 16206) in proximal view (dorsal surface at bottom of figure), illustrating: 60[1], concavity on astragalar facet of navicular restricted to ventral side of convexity. **e** Left femur of *Phataginus tricuspis* (CM 16206) in posterior view, illustrating: 130[2], lesser trochanter directed medially, largely obscured by head but visible medially in proximal view. **f** Right manus of *Phataginus tricuspis* (CM 16206) in dorsal view, illustrating: 302[2], manual ungual phalanx on digit I greatly reduced,<1/2 the length of ungual phalanx V. **g** Mandible of *Phataginus tricuspis* (CM 86715) in right dorsolateral view, illustrating: 367[1], presence of elongated medial perforation in mandibular canal. **h** Left humerus of *Phataginus tricuspis* (CM 16206) in anterior view, illustrating: 219[1], distal edge of trochlea of humerus convex in anterior view. Abbreviations: **acet,** acetabulum; **astf,** astragalar facet; **cp,** condylar process; **cpt,** capitulum; **cuf,** cuboid facet; **eec,** entepicondyle; **ff,** fibular facet; **gmtp,** groove for m. tibialis posterior tendon; **gtr,** greater trochanter; **h,** head; **il,** ilium; **isch,** ischium; **lco,** lateral condyle; **lp,** lateral process; **ltr,** lesser trochanter; **mco,** medial condyle; **mma,** medial malleolus; **mndf,** mandibular foramen; **mnp,** mandibular prong; **ms,** mandibular spout/symphysis; **pub,** pubis; **obf,** obturator foramen; **sv,** sacral vertebra; **tr,** trochlea; **up,** ungual phalanx. Scale bar in **a** and **d**= 0.5 cm. Scale bars in **b**, **c**, and **e** through **h**=1 cm.

assigned to it, the type species, *Eomanis waldi* Storch, 1978, and *Eomanis krebsi* Storch and Martin, 1994. Whereas multiple complete or nearly complete specimens of the former are known (Appendix 1), the latter is based upon a single skeleton lacking a skull (Storch and Martin 1994). Szalay and Schrenk (1998) claimed that this specimen should not have been designated a new species of *Eomanis.* Rather, they believed the specimen to represent a juvenile individual of *Eurotamandua joresi,* despite a rather lengthy section from the original description where Storch and Martin (1994) discuss the differences between *"Eomanis" krebsi* and *Eurotamandua*. Szalay and Schrenk (1998) observed that, despite the juvenile attributes of the skeleton of *"Eomanis" krebsi*, including unfused epiphyses in the long bones and lack of fusion of the pelvic elements, it is much larger than all the known specimens of *Eomanis waldi*, and is much closer in size to *Eurotamandua*. They also noted similarities in the morphology of the scapula, ulna, astragalus, and third manual ungual phalanx between *"Eomanis" krebsi* and *Eurotamandua*, and implied but do not explicitly state that these features are absent in *Eomanis waldi.* A subsequent study by Horovitz et al. (2005) disputed the findings of Szalay and Schrenk (1998). Based on the morphology of the distal tibia and calcaneus, Horovitz et al. (2005) claimed that *"Eomanis" krebsi* shows distinct differences from *Eurotamandua*, including the absence of a posterior distal tibial process and a different arrangement of the sustentaculum astragali, and that these differences preclude a taxonomic reassignment of *"Eomanis" krebsi* to *Eurotamandua joresi*. Horovitz et al. (2005: 548), however, did not conduct a phylogenetic analysis of the relationships among the three Messel taxa, asserting at the end of their study, "Whether *Eo. krebsi* does indeed belong to the genus *Eomanis*, to Pholidota or to some other group of eutherians (the genus *Eurotamandua* included) remains to be solved with a higher level phylogenetic analysis of Eutheria."

It is unfortunate that neither study included a detailed treatment of the relevant anatomy of *Eomanis waldi,* and that the studies focused on entirely different skeletal elements. Horovitz et al. (2005) might be faulted particularly for not addressing the similarities in the scapula, ulna, manus, and astragalus of *"Eomanis" krebsi* and *Eurotamandua* noted previously by Szalay and Schrenk (1998). The data set employed in the present study contains characters from all the skeletal elements discussed by both Szalay and Schrenk (1998) and Horovitz et al. (2005). As noted above and in Fig. 1, our results place *"Eomanis" krebsi* and *Eurotamandua* at the base of Pholidota, where they form successive sister taxa to the clade we have designated Eupholidota. There are at least 13 unambiguous and 11 ambiguous synapomorphies shared by *Eomanis waldi* and more derived pangolins exclusive of *"Eomanis" krebsi* and *Eurotamandua* (Appendix 4), and the node uniting *Eomanis waldi* to these more derived taxa (Node 5, Eupholidota) receives relatively strong branch support

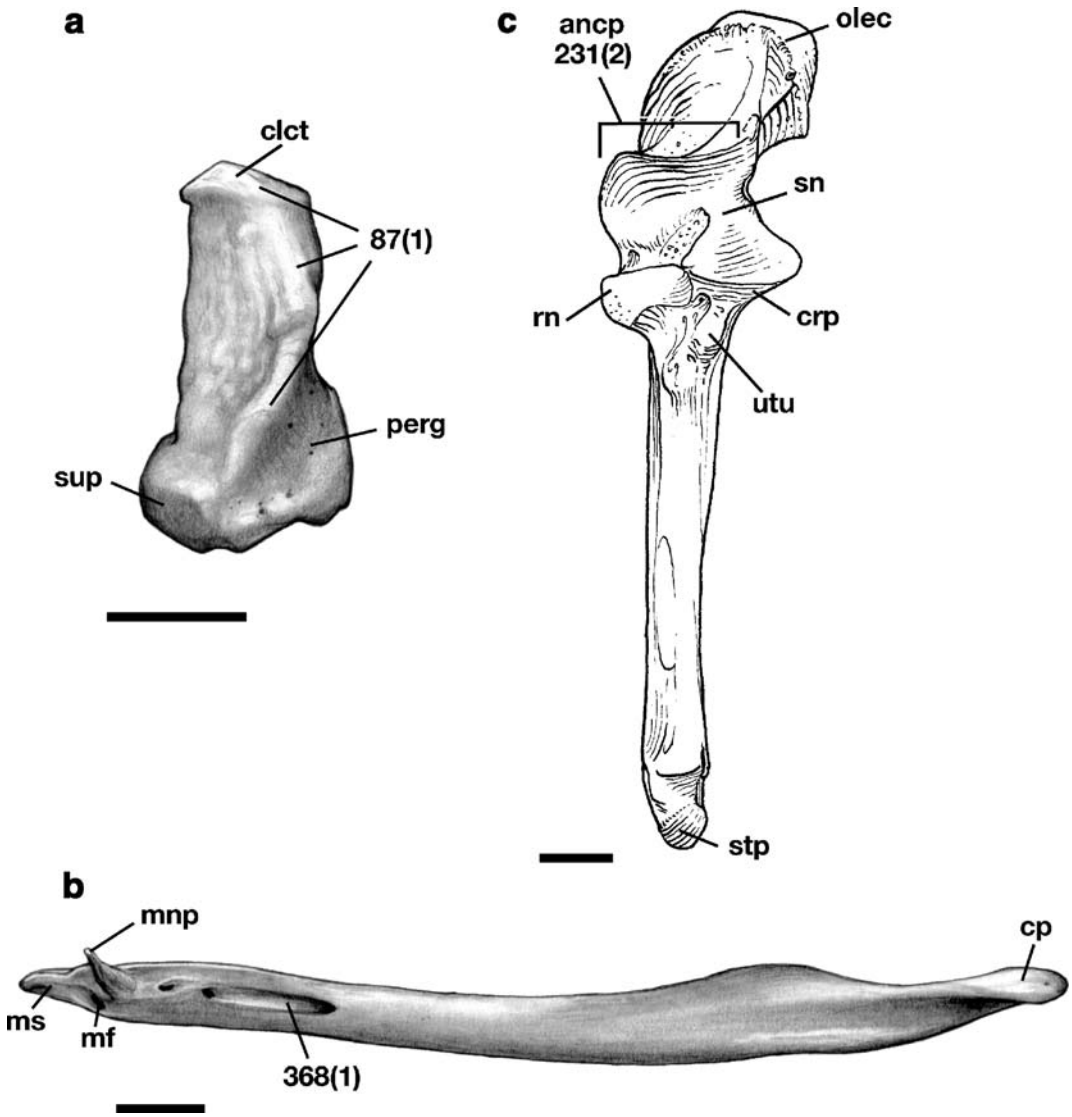

Fig. 12 Synapomorphies of *Smutsia*. Characters numbered as in Appendix 2. **a** Left calcaneus of *Smutsia temminckii* (AMNH 168954) in plantar view, illustrating the following character: 87 [1], enlarged attachment surface for the Achilles' tendon extending forward along plantar surface of calcaneus for more than half its length. **b** Mandible of *Smutsia gigantea* (AMNH 53858) in left lateral view, illustrating: 368[1], presence of an elongated lateral perforation in mandibular canal. **c** Left ulna of *Smutsia gigantea* (AMNH 53858) in anterior view, illustrating: 231[2], wide anconeal process of ulna, maximum width >15% of maximum ulnar length. Abbreviations: **ancp,** anconeal process; **clct,** calcaneal tuber; **cp,** condylar process; **crp,** coronoid process of ulna; **mf,** mental foramen; **mnp,** mandibular prong; **ms,** mandibular spout/symphysis; **olec,** olecranon; **perg,** peroneal groove; **rn,** radial notch; **sn,** sigmoid notch; **stp,** styloid process; **sup,** sustentacular process; **utu,** ulnar tuberosity. Scale bar in **a**=0.5 cm. Scale bars in **b** and **c**=1 cm.

(Fig. 1). Although only seven of the synapomorphies from Node 5 could be coded for *"Eomanis" krebsi* (40, 63, 96, 151, 155, 157, 303; see Appendices 2–4), there are seven other characters (2, 12, 13, 70, 91, 124, 160; see Appendices 2 and 3) in the matrix for which *Eomanis waldi* and *"Eomanis" krebsi* receive different codings. Therefore, we believe there is enough evidence to conclude that *Eomanis waldi* and *"Eomanis" krebsi* do not share a unique common ancestry, and do not belong in the same genus. As noted above, in our MPTs, *"Eomanis" krebsi* and *Eurotamandua* are successive sister taxa to Eupholi-

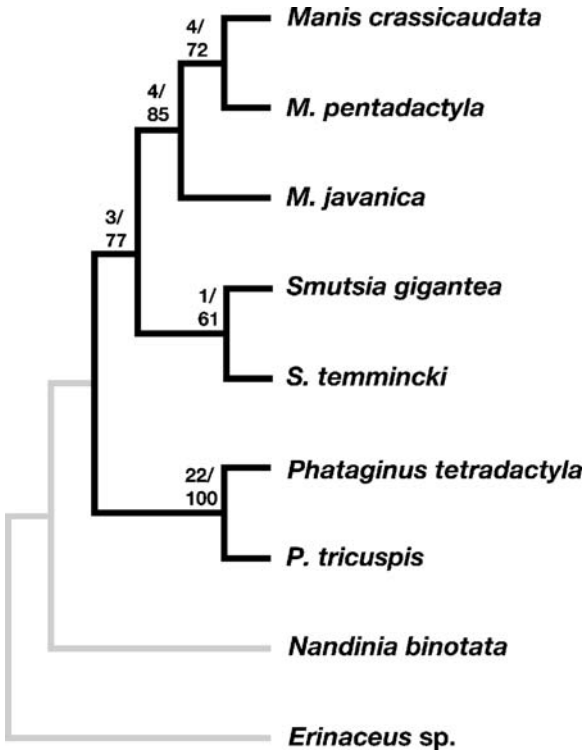

Fig. 13 Phylogeny of Pholidota based on PAUP analysis of 395 osteological characters in nine taxa, including only the seven extant pangolin species examined in the present study, and two successive extant outgroups, the Laurasiatherian placental mammals *Nandinia binotata,* a basal feliform carnivoran, and the eulipotyphlan *Erinaceus* sp. This analysis yields a single MPT (TL=998, CI=0.763, RI=0.661). The numbers in bold type at each node represent Bremer support values (given first) and bootstrap values, calculated as described in Materials and Methods.

dota (see "Results" section; Fig. 1), and the two taxa differ in a significant number of features, including those noted by Horovitz et al. (2005—equivalent to our characters 91 and 105—see also characters 2, 3, 12, 49, 70, 124, 158, 160, and 298, Appendices 2, 3). Therefore, we have chosen to place *"Eomanis" krebsi* in a new genus (see "Systematic Paleontology" section below).

Storch (2003) recently advocated placing the two nominal species of *Eomanis* into their own separate family, Eomanidae, a group defined by the presence of pangolin synapomorphies such as horny scales and an edentulous skull, as well as by the absence of derived features of other recent and fossil pangolins, like a distally situated third trochanter of the femur and the loss of the clavicle and the zygomatic arch. Needless to say, because the results of the present study do not support the monophyly of the genus *Eomanis* as employed by Storch (2003), they also do not support the monophyly of his family Eomanidae. However, we do retain the name, restricting its scope so that it becomes a monotypic taxon that includes only one genus and species, *Eomanis waldi*.

The clade that includes all living and fossil pangolins exclusive of the Messel taxa (Node 6) is one of the best supported in the entire analysis, with the third highest Bremer support value, and a bootstrap value of 100 (Fig. 1). It is diagnosed by a very large number of synapomorphies—27 unambiguous synapomorphies, six of which are unique, and 23 ambiguous synapomorphies, six of which are also unique (Appendix 4, Fig. 5). As noted in the Results section above, this list includes many if not most of the features that have been labeled pangolin synapomorphies in previous studies (Emry 1970; Gaudin and Wible 1999; Rose et al. 2005). We have elected to apply a new superfamilial name to this node, Manoidea. In turn, Manoidea can be divided into two families, Patriomanidae, which includes only extinct pangolins, and Manidae, which includes all the extant pangolins, with one extinct Tertiary taxon, *Necromanis,* of uncertain affinities.

The family Patriomanidae was initially proposed by Szalay and Schrenk (1998) to house all of the then known genera of fossil pangolins, *Eomanis*, *Patriomanis*, and *Necromanis*. This designation allowed them to formally recognize the close "phyletic unity" (Szalay and Schrenk 1998: 172) of the extant pangolins, as well as the generally more primitive anatomies of the extinct forms as compared to those of the living taxa. Although supporting the distinction between extant pangolins in the family Manidae and the fossil forms, Storch (2003) removed *Eomanis* to its own family, Eomanidae. Based implicitly on new, complete but undescribed material of *Necromanis*, he also advocated the removal of *Necromanis* from the Patriomanidae. Gaudin et al. (2006) largely concurred with the conclusions of Storch (2003), suggesting that Patriomanidae as defined by Szalay and Schrenk (1998) was paraphyletic, with *Eomanis* more primitive than *Patriomanis,* and *Necromanis* more derived, sharing several features with modern pangolins not present in other fossil forms, including (Gaudin et al. 2006: 157) "a flat astragalar head, enlarged metapodial keels, and a more distally situated femoral third

trochanter." However, Gaudin et al. (2006) advocated the retention of a revised Patriomanidae to include only *Patriomanis* and their newly described genus *Cryptomanis*, providing a revised diagnosis for the taxonomically more restricted family.

The results of the present study support the recognition of a monophyletic family Patriomanidae with a content mirroring that of Gaudin et al. (2006), i.e., including only *Patriomanis* and *Cryptomanis*. The Patriomanidae is diagnosed by 16 unambiguous synapomorphies, including three unique features, and 13 ambiguous synapomorphies (Appendix 4, Fig. 6). As is evident in the light of prior discussions, these results corroborate assertions by Storch (2003) and Gaudin et al. (2006) that *Eomanis waldi* and *"Eomanis" krebsi* should be excluded from the Patriomanidae, contra Szalay and Schrenk (1998). The results also confirm the very strong anatomical similarities between *Patriomanis* and *Cryptomanis* noted by Gaudin et al. (2006). The weak Bremer and bootstrap support for this node can perhaps be attributed to the fact that, as Gaudin et al. (2006) pointed out, each of these taxa possesses their own suite of derived features shared with extant forms.

The phylogeny in Fig. 1 fails to resolve unambiguously the affinities of *Necromanis.* In one of the MPT, *Necromanis* is allied as the sister taxon to Patriomanidae, recalling the original formulation of the family Patriomanidae by Szalay and Schrenk (1998), who included *Necromanis* in the group. In the other MPT, *Necromanis* is placed as the sister taxon to Manidae, the clade including all extant taxa. This latter arrangement is consistent with statements by Storch (2003) implying that *Necromanis* was more derived than *Patriomanis*, i.e., more similar to living pangolins. Additionally, Gaudin et al. (2006) listed several derived features shared by *Necromanis* and modern pangolins but absent in patriomanids, e.g., ventrally elongated keels on the metapodials and a distally situated third trochanter on the femur. As described in the Results section above, *Necromanis* shares a virtually identical number of unambiguous, ambiguous, and unique synapomorphies with Patriomanidae and Manidae—ten unambiguous, 12 ambiguous, and two unique in the case of the former, ten unambiguous, 13 ambiguous, and three unique in the case of the latter (see Appendix 4). It thus shows significant morphological resemblances to both groups (Fig. 7). Heretofore, *Necromanis* has been known from very incomplete remains (Koenigswald 1969, 1999; Koenigswald and Martin 1990). Therefore, we anticipate that with the description and analysis of the "extremely rich and complete" new specimens of *Necromanis* currently under study (Storch 2003: 56), the phylogenetic affinities of this taxon might be more clearly resolved. Given this taxon's position as the youngest of the extinct Tertiary fossil pangolin genera, a clearer understanding of its systematic position will be vital to understanding the phylogenetic and biogeographic origin of the modern forms.

Although Gaudin and Wible (1999) included only one fossil pangolin in their cladistic analysis of cranial characters, their results strongly indicated the monophyly of the extant pangolins to the exclusion of the Tertiary forms. They identified at least six unambiguous cranial synapomorphies shared by all pangolins that were absent in *Patriomanis*, and the node uniting the extant forms was one of the strongest in their analysis. Gaudin and Wible (1999: 57) asserted that "Tertiary pholidotans probably ought to be placed in a separate family from the living forms," in agreement with Szalay and Schrenk (1998), who formally restricted Manidae to this group of extant taxa. This arrangement is strongly supported by the results of the present study. The node uniting extant pangolins is the second strongest in the entire analysis, with a bootstrap value of 100 and a Bremer support value of 35. The Manidae is diagnosed by more apomorphies than any other node on the tree, including 77 unambiguous synapomorphies, 30 of which are unique, and 24 ambiguous synapomorphies, five of which are unique (Appendix 4, Fig. 8). The living pangolins are considerably more derived in their skeletal anatomy than the Messel taxa, the patriomanids, and *Necromanis*. Cranial specializations include the loss of the coronoid process of the mandible, endocranial venous grooves, and the nuchal crest, and the flattening of the petrosal promontorium (334[1], 352[1], 361[2], 371[2]; see Appendices 2, 4, Fig. 8). Postcranial modifications of the manids include a number of features exemplifying the trend identified by Gaudin et al. (2006), of the digging adapted features becoming more distally situated, with the proximal elements becoming gracile, in the extant taxa relative to patriomanids. For example, Manidae is characterized by (Fig. 8) distal keels on the metatarsals and metacarpals that extend along the

entire dorsoventral length of condyles (8[2]), a shortened third metatarsal (21[1]), a concavity on the head of the astragalus (59[1]), shafts of metacarpals and manual proximal and intermediate phalanges that are deeper than they are wide (275[1], 296 [1]), a reduction in length of the manual proximal phalanges (298[3]), and elongated proximodorsal processes on the manual intermediate phalanges (301[1]), as well as a strong reduction of the cnemial crest of the tibia (103[2]), a loss of the fovea capitis, trochanteric fossa, and intertrochanteric ridge of the femur (131[1], 132[1]), strong reduction of the gluteal fossa on the ilium (146[2]), and reduction of the height of the scapular spine (204[1]). Lastly, it should be noted that the monophyly of the Manidae in the present study stands in stark contrast to the taxonomic arrangement of McKenna and Bell (1997), who allied the Tertiary pangolin genera *Eomanis*, *Necromanis*, and *Patriomanis* with extant Asian pangolins in a subfamily Maninae, exclusive of the extant African pangolins allocated to the subfamily Smutsiinae.

There has been considerable controversy concerning the generic level relationships among the living pangolins. The extant species have been allocated to as many as six different genera (Pocock 1924), whereas other authors have placed all in a single genus (Simpson 1945; Nowak 1999; Schlitter 2005). Patterson (1978) and Corbet and Hill (1991) arranged the living pangolins into two genera, *Manis* for the Asian species and *Phataginus* for the African species. Koenigswald (1999) suggested splitting the African forms into two genera, one for the tree pangolins (*Phataginus*) and one for the ground pangolins (*Smutsia*), an arrangement consistent with the phylogenetic results of Gaudin and Wible (1999), though the latter authors did not formally advocate for recognition of these genera given the limited taxonomic and anatomical scope of their study. McKenna and Bell (1997) offered a further division into four genera, placing the two tree pangolins into separate genera, *Phataginus* and *Uromanis.* The results of the present study are clearly consistent with the three genera arrangement. In our MPT (Fig. 1), the seven living species included in the analysis fall into three distinct clades that are moderately to very strongly supported. The Asian taxa form a clade. Because one of these species, *Manis pentadactyla*, is the type species for the genus *Manis* (Pocock 1924; Schlitter 2005), we assign all the extant Asian taxa to this genus. The African ground pangolins also form a clade assigned to the genus *Smutsia,* as the Cape pangolin *Smutsia temminckii* is the type for this genus (Pocock 1924). The African tree pangolins form the third clade, with the tree pangolin *Phataginus tricuspis* as the type species for the genus *Phataginus* that we assign to this grouping. Lastly, the two genera of African pangolins form a monophyletic group exclusive of the Asian taxa. We will refer to this clade as the subfamily Smutsiinae, following the usage of McKenna and Bell (1997).

That the present analysis yields a monophyletic clustering of the Asian pangolins is not a surprise. The distinctiveness of these animals has been amply recognized by previous workers (Pocock 1924; Grassé 1955; Emry 1970; Segall 1973; Patterson 1978; Heath 1992a), and the monophyly of this clade was well supported in the previous cladistic analysis of Gaudin and Wible (1999). In our results, the basal node for the genus *Manis* (Node 9) receives very strong Bremer support and has a bootstrap value of 97 (Fig. 1). It is diagnosed by 24 unambiguous synapomorphies, seven of which are unique, and 29 ambiguous synapomorphies, one of which is unique (Appendix 4, Fig. 9). Within *Manis*, the two more northerly distributed species, *Manis pentadactyla,* the Chinese pangolin from southern China, northern Indochina and the northeast portion of the Indian subcontinent (Corbet 1978; Heath 1992a), and *M. crassicaudata*, the Indian pangolin, which ranges from Afghanistan throughout India south to Sri Lanka (Corbet 1978; Heath 1995), are allied as sister taxa, to the exclusion of *M. javanica,* the Sunda pangolin, which occurs in southern Indochina and the East Indies. In Gaudin and Wible (1999), the two more easterly species were allied as sister taxa, *M. javanica* and *M. pentadactyla*. However, these authors admitted that the relationship was only weakly supported, with an alliance between *M. crassicaudata* and *M. pentadactyla* being equally parsimonious under different character weighting and ordering regimes. The clade uniting *M. crassicaudata* and *M. pentadactyla* receives modest Bremer support and has a relatively high bootstrap value (76, see Fig. 1). It is diagnosed by 23 unambiguous and 20 ambiguous synapomorphies, six of which are unique. Thus our results not only contradict Gaudin and Wible's (1999) tree; they also offer a more robustly supported resolution of the relationships among Asian pangolins than that provided by Gaudin and Wible (1999). It should also be

pointed out that when we constrained this data set to yield a tree consistent with that of Gaudin and Wible (1999), the resulting tree was 23 steps longer than our MPT.

Many of the same analyses that recognized an Asian grouping of modern pangolins also grouped the African pangolins together (Pocock 1924; Grassé 1955; Emry 1970; Segall 1973; Patterson 1978; Heath 1992a). Patterson (1978) went so far as to suggest this grouping is more derived than the Asian cluster. McKenna and Bell (1997) also recognized this grouping, assigning it the subfamilial epithet Smutsiinae. However, in the cladistic analysis of Gaudin and Wible (1999), the extant African pangolins formed a paraphyletic assemblage, with the African tree pangolins and African ground pangolins representing successive sister clades to the Asian taxa. Gaudin and Wible (1999) noted that a monophyletic African clade was obtained in a tree only one step longer than their most parsimonious tree. Our results provide clearer support for the monophyly of the extant African pangolins. Our Node 11, which we label Smutsiinae following McKenna and Bell (1997), receives rather low bootstrap and Bremer support (Fig. 1), but is diagnosed by 21 unambiguous synapomorphies, five of which are unique to the clade, as well as one unique ambiguous synapomorphy. These unique traits include not only the ossicular characters from the skull first described by Segall (1973) and highlighted by Gaudin and Wible (1999) as diagnosing this clade (Fig. 10f–g), but also features of the calcaneus, axis, metacarpal V, and xiphisternum (see "Results" section, Appendix 4, Fig. 10a–e). Given the longstanding recognition of an African grouping in the systematic literature on pangolins, and the wide range of skeletal similarities that they share, it is curious that the monophyly of this group is not supported when we restrict our analysis to living taxa only. As described in the Results section, when the analysis was repeated with all fossil taxa excluded, the resulting MPT placed the clade including the two species of African ground pangolins in a monophyletic grouping with *Manis*, to the exclusion of the African tree pangolins (Fig. 13). We interpret this result as more indicative of the importance of fossils for polarizing character transformations within Pholidota than as evidence of the inherent weakness of the smutsiinine node. Many of the "derived" features shared by *Manis* and the African ground pangolins, in fact 19 of the 28 unambiguous synapomorphies, are known to occur in *Necromanis,* patriomanids, or the Messel taxa, rendering their support for this relationship questionable, either because they change the nature of the character state polarization, or perhaps more directly because they change the phylogenetic distribution of the features in question. The importance of fossils in reconstructing phylogeny, particularly through their effect upon just these sorts of polarity and character distribution issues, has already been discussed extensively in the literature (e.g., see Carrano et al. 2006 and references therein). This seems to be yet another example where fossils have a significant impact on the resolution of relationships among extant taxa via the information they provide on character polarity and character distributions.

Within Smutsiinae, the results of the present study yield two monophyletic clades, one for the African ground pangolins and one for the African tree pangolins (Fig. 1). The African ground pangolins are assigned to the genus *Smutsia*, following Pocock's (1924) original formulation of this genus, an arrangement also advocated by McKenna and Bell (1997) and Koenigswald (1999). The genus is comprised of the giant pangolin, *Smutsia gigantea,* and the Cape pangolin, *Smutsia temminckii* (Heath 1992b; Kingdon 1997). The monophyly of *Smutsia* is also consistent with the phylogenetic results of Gaudin and Wible (1999), although they noted that the node uniting the two species in their analysis collapsed in trees only one step longer than the most parsimonious. The present study provides slightly better support for this relationship. The support for this node is nearly identical to that for the Smutsiinae as a whole, with similar branch support and bootstrap values (2 and 54, respectively, Fig. 1), and an identical number of synapomorphies. The genus is diagnosed by 21 unambiguous and 20 ambiguous synapomorphies, though only three of the unambiguous synapomorphies are unique (Appendix 4, Fig. 12). The monophyly of *Smutsia* is also supported in the analysis that includes only living taxa, although the branch support and bootstrap values indicate that this is the weakest node on the tree (Fig. 13). It seems clear, based on our results, that this is the most weakly supported of the three extant pangolin genera, a somewhat ironic result considering that these two were the only two pangolin species that Pocock (1924) elected to place in the same genus.

Whereas *Smutsia* is the most weakly supported of the three extant pangolin genera in our analysis, *Phataginus* is the best supported. This genus includes two species of small bodied, arboreal pangolins, the tree pangolin *Phataginus tricuspis*, and the long-tailed pangolin, *P. tetradactyla* (Kingdon 1997). The node uniting the two African tree pangolins is the strongest node on the entire tree, failing to collapse even after the addition of 35 steps to the MPT, and receiving a bootstrap support value of 100. The monophyly of this genus is diagnosed by 49 synapomorphies, ten of which are unique to these two species, along with 20 ambiguous synapomorphies (Appendix 4, Fig. 11). These two species are highly distinctive skeletally relative to the other pangolins, in part because of shared adaptations for life in the trees, including some of the skeletal synapomorphies identified in the present study (e.g., more uniform, slender digits—10[0], 274[0]; more gracile limb elements—83[2], 207[2]; 210[1], 227 [0]; and an elongate tail-159[0]; see Appendix 4), as well as soft tissue features like a naked pad at the end of tail that is used when employing the prehensile tail during climbing (Pocock 1924; Patterson 1978; Kingdon 1997). However, many of the shared features seem unrelated in any obvious way to climbing. The assignment of these two genera to *Phataginus* follows Patterson (1978), Corbet and Hill (1991), and Koenigswald (1999). It is somewhat curious that Patterson (1978) chose to place all the African pangolin species in *Phataginus*, given that both *Smutsia* and *Uromanis* appear to have been used in a more inclusive sense in the prior literature. *Smutsia,* the genus subsuming the two species of African ground pangolins, was the basis for Pocock's (1924) subfamily Smutsiinae (also used in McKenna and Bell 1997, but incorporating all four African species). *Uromanis*, the genus in which Pocock (1924) placed the long-tailed pangolin, served as the basis for his subfamily Uromaninae (changed to tribe Uromanini in McKenna and Bell 1997), the group to which he assigned both species of African tree pangolins. However, as we can find no instance of the two tree pangolin species being placed together under *Uromanis* in the previous systematic literature, and we have at least three instances where both are placed in *Phataginus*, we follow the latter usage. Note that this arrangement, which is very strongly supported in our analysis, differs from the taxonomic treatment of McKenna and Bell (1997), who placed the long-tailed and tree pangolins in separate genera, *Uromanis* and *Phataginus* respectively, following Pocock (1924).

Biogeography

The systematic results of the present study have clear implications for the biogeographic history of the Pholidotamorpha, and in particular the Pholidota, and should help to resolve outstanding questions, such as the site of origin of the Pholidota as a whole and of modern pangolins in particular. As discussed in Gaudin et al. (2006), there are two likely scenarios for the site of origin of the order Pholidota (as defined in the present study). It is possible that the group is an "old African" order, like Hyracoidea and Proboscidea. This would be consistent with the extant distribution of the group, with half of the living species endemic to sub-Saharan Africa. It would also be consistent with morphology-based studies of eutherian interordinal relationship that ally Pholidota with the South American order Xenarthra (e.g., Novacek and Wyss 1986; Novacek 1992) and suggest a Gondwanan origin for this superordinal clade and its members. Finally, there is one Paleogene record of pangolins from Africa, based on several isolated ungual phalanges recovered from early Oligocene deposits in the Fayum of Egypt (Gebo and Rasmussen 1985). However, given the highly fragmentary nature of these fossils, and the absence of any additional pangolin fossils from the fairly well studied Fayum, the importance of this last piece of evidence is questionable. The second likely site of origin for Pholidota is on one of the Laurasian continents (Rose et al. 2005), and more particularly, an origin on the European landmass (Storch 2003). This scenario is consistent with most recent molecular studies of placental interordinal phylogeny, which have placed Pholidota in the Laurasiatheria, a clade that includes northern groups like Artiodactyla, Perissodactyla, Chiroptera, and the Eulipotyphla (e.g., Springer et al. 2004, 2005). These studies hypothesized a particularly close affinity between pangolins and the order Carnivora (Springer et al. 2004, 2005). As Gaudin et al. (2006) explained, this scenario is also consistent with the early fossil history of Pholidota. Not only are the oldest pholidotans, *Eomanis waldi*, *"Eomanis" krebsi*, and *Eurotamandua joresi* from Europe, but all

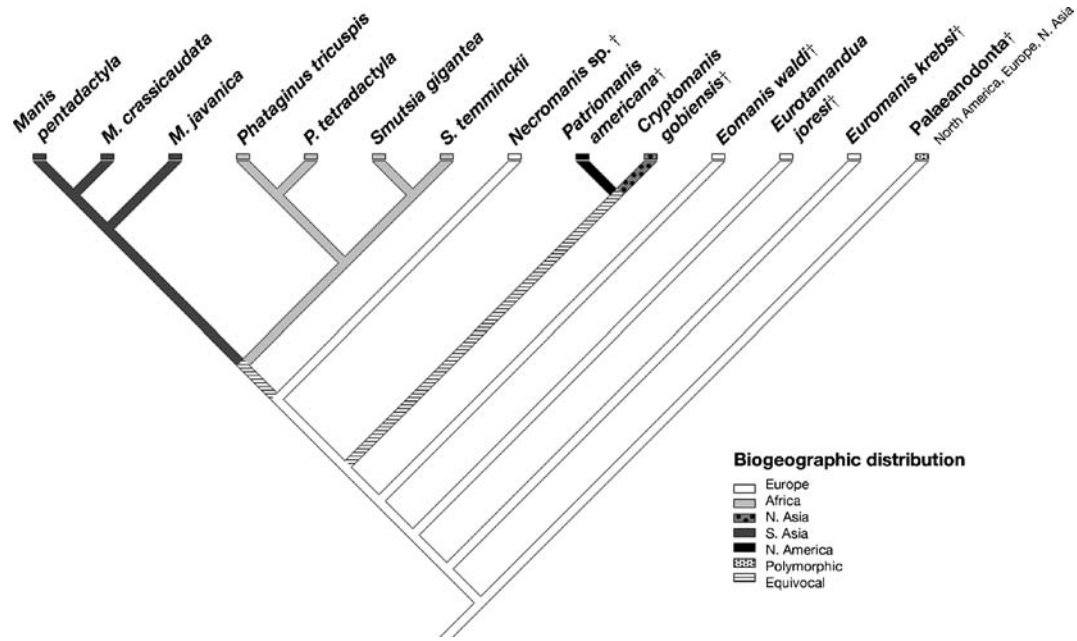

Fig. 14 Biogeographic distributions of Pholidotamorpha mapped onto one of the two MPT used to construct the consensus phylogeny in Fig. 1 (see "Biogeography" section of text). Although only one of two MPTs is illustrated, results are identical using either MPT, i.e., whether *Necromanis* is placed as sister taxon to Manidae (as illustrated) or Patriomanidae. In both instances, the branches leading to the common ancestor of Manidae and Patriomanidae have an equivocal optimization, whereas all the basal nodes, including that for Manoidea, are optimized as having a European origin.

of the Paleogene and early Neogene taxa represented by relatively complete fossil material obtain from Laurasian continents: from Europe, *Eomanis waldi*, *"Eomanis" krebsi*, *Eurotamandua joresi,* and *Necromanis*; *Cryptomanis* from Asia, and *Patriomanis* from North America. Finally, the results of the present study provide additional anatomical synapomorphies that serve to diagnose a sister group relationship between Palaeanodonta and Pholidota, reinforcing the robusticity of this relationship. Palaeanodonta is an extinct group endemic to Laurasia, with its center of diversity (and likely center of origin—see Rose and Lucas 2000) in North America but with representatives known from both Europe and Asia (Rose et al. 2005). Given that the likely sister-taxon to Pholidota is also Laurasian, the preponderance of evidence clearly favors a Laurasian origin for Pholidota, with the fossil record implying an origin in Europe, as indicated by Storch (2003).

This scenario was confirmed by plotting the geographic distributions of the OTU's onto the cladogram from Fig. 1 using MacClade (Maddison and Maddison 2001). The tree illustrated in Fig. 14 represents one of the MPT used to construct the consensus tree in Fig. 1, specifically the tree in which *Necromanis* is sister-taxon to Manidae, but the results of the biogeographic analysis do not change if the other MPT, with *Necromanis* as sister to Patriomanidae, is substituted. Europe is optimized as the continent of origin for the entire Pholidotamorpha, as well as for Pholidota and its basal branches, up to and including *Necromanis*. The site of origin for *Patriomanis* and *Cryptomanis* is equivocal irrespective of the placement of *Necromanis.*

The site of origin for modern pangolins is somewhat harder to establish. The phylogenetic results of the present study (Fig. 1) are consistent with earlier analyses (e.g., Patterson 1978) that identified two clades of modern pangolins—an African clade and an Asian clade. The biogeographic distributions of both these clades lie well to the south of the areas where Paleogene and early Neogene fossil pangolins have been recovered, suggesting modern pangolins may have originated in Laurasian continents, most likely in Europe, which has the only fossil records from the Neogene, including a number of *Necromanis* remains as well as a dubious Pliocene

record (Koenigswald 1999), and subsequently dispersed into southern Asia and sub-Saharan Africa (Gaudin et al. 2006). However, the biogeographic analysis illustrated in Fig. 14 shows the origin of the modern clade to be equivocal, and this result is obtained whether *Necromanis* is placed as the sister taxon to Manidae or to Patriomanidae. The fossil record of pangolins from the areas lying within their extant range does not extend far back into the Cenozoic. The oldest pangolins from Africa are Pliocene in age (Botha and Gaudin 2007—notwithstanding the one doubtful record mentioned above from the early Oligocene of Fayum, well north of the modern range of African pangolins), whereas pangolins do not even extend as far back as the Tertiary in south Asia, the oldest forms being Pleistocene in age (Guth 1958; Emry 1970). The older African record suggests a pathway of dispersal from Europe through Africa and finally into south Asia. This model would also be consistent with Patterson's (1978) assertion that African pangolins are, as a group, more derived than the Asian taxa, because the African forms would have been resident in their current range longer and had greater opportunities for specialization. This model would be better supported, perhaps, by a phylogeny like that of Gaudin and Wible (1999) or the one obtained in our analysis using only extant taxa, in which the African species were paraphyletic sister taxa to the Asian taxa, or a phylogeny in which *Necromanis* was unambiguously allied as a sister taxon to the Manidae, but it is not inconsistent with the preferred phylogeny from this study (Fig. 1). It should also be remembered that the Neogene record of pangolins is, if anything, even poorer than the Paleogene record. This biogeographic scenario could easily be overturned by the discovery of one well-preserved pangolin fossil from the early Neogene of Asia.

Systematic paleontology

Class Mammalia Linnaeus, 1758
Order Pholidota Weber, 1904
Suborder Uncertain

†*Euromanis,* new genus

Type species.—*Eomanis krebsi* Storch and Martin, 1994

Diagnosis and Description.—As for the single included species described below.

Etymology.—'Euro' is a reference to the European provenance of the specimen; 'manis' refers to the modern genus of Asian pangolins.

†*Euromanis krebsi* (Storch and Martin, 1994), new combination

Holotype.—The original (Storch and Martin 1994: figs. 1, 2, 3, 4, 5 and 6, tafel 1) is in the possession of Dr. G. Jores, Darmstadt, Germany; a cast is in the Forschunginstitut Senckenberg, Frankfurt am Main, Germany (SMF 94/1).

Distribution.—Lower middle Eocene (MP 11), Messel Formation, Messel, Germany.

Diagnosis.—Fossil pangolin larger than contemporaneous *Eomanis waldi* from Messel (femoral length of *Euromanis krebsi*=78 mm; femoral length of *Eomanis waldi* (SMF MEA 263)=58 mm). Shares pangolin synapomorphies, including crescentic fibular facet of astragalus; prominent ischiatic spine; triangular manual and pedal subungual processes with grooves along either side leading to subungual foramina; and lack of a distinct lateral process on lateral malleolus of fibula; but lacks features that define manoideans, including fissured unguals; enrolled lumbar zygapophyses; displacement of third trochanter to midshaft of femur. Generally similar to both *Eomanis waldi* and *Eurotamandua joresi*, but differing in numerous traits including: entocuneiform quadrangular in medial view, dorsoventral depth equivalent distally and proximally; anterior plantar tubercle even with or distal to cuboid facet of calcaneus; angle between femoral head and shaft <130°; neural spine of seventh cervical vertebra vertical.

Description.—Storch and Martin (1994: figs. 1, 2, 3, 4, 5 and 6, tafel 1) provided detailed descriptions and illustrations of the only known specimen, a skeleton missing the skull and parts of the shoulders, forelimbs, and tail, in a private collection in Darmstadt, Germany. Szalay and Schrenk (1998: figs. 2, 3, 4, 5, 6 and 7) provided additional illustration of the only known specimen and proposed *"Eomanis krebsi"* as a juvenile *Eurotamandua joresi*. Horovitz et al. (2005: figs. 1 and 2) reanalyzed and reillustrated ankle elements of the only known specimen. They noted differences from *Eurotamandua joresi* and concluded that the only known specimen and *Eurotamandua joresi* are separate taxa. The manual ungual phalanges of *Euromanis krebsi* are illustrated in the present study (Fig. 3c).

Revised classification

The phylogenetic results and conclusions of the present study are at odds in several important respects with existing, widely used taxonomic treatments of the pholidotamorph taxa (e.g., McKenna and Bell 1997; Nowak 1999; Schlitter 2005; Rose et al. 2005). Because the present study is the most detailed cladistic examination of the phylogenetic relationships among these taxa currently available (or likely to be available in the near future), we felt it important to perform a formal revision of the taxonomy of Pholidotamorpha, with particular attention paid to the Pholidota (Table 1). In this taxonomic treatment, we recognize several new higher categories and modify the content of various other families, subfamilies, genera, and subgenera. We have chosen to assign taxonomic rank to these new monophyletic groupings, but it should be noted that we do not believe these rankings to be the most significant part of the revision. The family ranks, and those below the family level, have somewhat greater significance, because these latter fall under stricter ICZN rules for priority and related matters. It does not matter greatly to us whether Pholidota is viewed as an order, a suborder, or given yet some other rank. It is the phylogenetic content of these higher-level groupings that we view as particularly significant. Note that several aspects of this classification are based on the work of other authors, and do not derive directly from our phylogenetic results. For the taxonomy of the extinct genus *Necromanis,* we follow Koenigswald (1999), who recognized three discrete species. As noted in the Introduction to this work, the recognition of pangolins from the Palawan and Culion Islands in the Philippines as a discrete species, *Manis culionensis*, postdates the research conducted for this study (Gaubert and Antunes 2005). However, *Manis culionensis* is very similar anatomically to *Manis javanica*, and was widely considered a subspecies of the latter prior to the work of Gaubert and Antunes (2005). Therefore, we are placing it in the same subgenus as *Manis javanica*. Finally, there are three Plio-Pleistocene species of extinct pangolin that were not included in the present study: *Manis hungarica* from the Pliocene of Hungary (Kormos 1934), *Manis lydekkeri* from the Pleistocene of India (Dubois 1908), and *Manis palaeojavanica* from the Pleistocene of Java (Dubois 1926). The former two species are based on isolated phalanges, and are therefore of questionable validity. The last is based on nearly complete skeletal material, but was not included in the present study for logistical reasons. Of the two extinct Asian taxa, Emry (1970:461) stated that "these differ so little from the living species that they shed little light on the history of the group," and Patterson (1978:270) made similar assertions, claiming that these forms are "almost certainly referable to *Manis*." Given their similarity to modern taxa (though both are larger, *M. palaeojavanica* much more so, than any living pangolin species—see Dubois 1926), and their Asian provenance, we have few qualms in assigning them to the genus *Manis*, although their relationship to the extant species in this genus is left unresolved. The retention of the Pliocene European species in *Manis* is more questionable, but given the fragmentary nature of the available material, there is little evidence for moving it elsewhere, so we leave it in *Manis* with some discomfort. Koenigswald (1999) suggested that *M. hungarica* is a nomen nudum.

Synapomorphies for the new higher taxa Pholidotamorpha, Eupholidota, Eomanoidea, and Manoidea can be found in Appendix 4. Definitions for the ranks of genera and above are included in the Results.

Conclusions

The goal of the present study was to conduct a comprehensive phylogenetic analysis of the order Pholidota, examining a wide range of osteological characters from the entire skeleton in all extant species and all the well-known fossil taxa, in order to improve understanding of the systematics, and biogeographic and evolutionary history of the pangolins. In addition, the relationship of pangolins to several putative relatives, including the palaeanodonts and the enigmatic "edentate" *Eurotamandua*, were investigated. Data were collected from all extant species except for one recently recognized form from a small group of islands in the Philippines, and from all well-known fossil species except for a giant Pleistocene taxon from Java, *Manis palaeojavanica*, and one recently described specimen from South Africa. The phylogeny resulting from this study (Fig. 1) is largely well resolved and well supported. It includes only one unresolved polytomy, an internal node (Node 6, Manoidea) that joins the extant family Manidae, the extinct Tertiary family Patriomanidae, and the extinct Tertiary European pangolin genus *Necromanis*. Most of the nodes on the

Table 1 Revised classification proposed here

Abbreviations: Afr = Africa, E = Early, Eoc = Eocene, Eur = Europe, L = Late, M = Middle, Mioc = Miocene, NA = North America, Olig = Oligocene, Paleoc = Paleocene, Pleist = Pleistocene, Plioc = Pliocene, Rec = Recent.

Superorder PHOLIDOTAMORPHA **new taxon**

Order PALAEANODONTA Matthew, 1918 **new rank**

Order PHOLIDOTA Weber, 1904

Suborder uncertain

Genus *†Eurotamandua joresi* Storch, 1981

Species *†Eurotamandua joresi* Storch, 1981: M Eoc, Eur

Suborder uncertain

Genus *†Euromanis*, **new genus**

Species *†Euromanis krebsi* (Storch and Martin, 1994), **new combination**: M Eoc, Eur

Suborder Eupholidota **new taxon**

Superfamily †Eomanoidea **new taxon**

Family †Eomanidae Storch, 2003

Genus *†Eomanis* Storch, 1978

Species *†Eomanis waldi* Storch, 1978: M Eoc, Eur

Superfamily Manoidea **new taxon**

Family uncertain

Genus *†Necromanis* Filhol, 1893

Type Species *†Necromanis franconica* (Quenstedt, 1886)

Synonyms *†Leptomanis* Filhol, 1893; *†Necrodasypus* Filhol, 1893; *†Teutomanis* Ameghino, 1905; *†Galliaetatus* Ameghino, 1905

Species *†Necromanis franconica* (Quenstedt, 1886): M Olig – M Mioc, Eur

Species *†Necromanis quercyi* Filhol, 1893: M Olig, Eur

Species *†Necromanis parva* Koenigswald, 1969: L Mioc, Eur

Family †Patriomanidae Szalay and Schrenk, 1998

Genus *†Patriomanis* Emry, 1970

Species *†Patriomanis americana* Emry, 1970: L Eoc, NA

Genus *†Cryptomanis* Gaudin, Emry, and Pogue, 2006

Species *†Cryptomanis gobiensis* Gaudin, Emry, and Pogue, 2006: L Eoc, Asia

Family Manidae Gray, 1821

Subfamily Maninae Gray, 1821

Genus *Manis* Linnaeus, 1758

Table 1 (continued)

Type Species: *Manis pentadacyla* Linnaeus, 1758

Synonyms: *Pholidotus* Brisson, 1762; *Pangolinus* Rafinesque, 1821; *Paramanis* Pocock, 1824; *Phatages* Sundevall, 1843

†Species *Manis hungarica* Kormos, 1934: Plioc, Eur

†Species *Manis lydekkeri* Dubois, 1908: Pleist, India

†Species *Manis palaeojavanica* Dubois, 1907: Pleist, Java

Subgenus *Manis* Linnaeus, 1758

Species *Manis pentadactyla* Linnaeus, 1758: Rec, Taiwan, S. China west to Nepal

Synonyms: *Manis brachyura* Erxleben, 1777; *Manis auritus* Hodgson, 1836; *Manis* (*Pholidotus*) *dalmanni* Sundevall, 1843; *Pholidotus assamensis* Fitzinger, 1872; *Phatages bengalensis* Fitzinger, 1872; *Manis pusilla* J. Allen, 1906; *Pholidotus kreyenbergi* Matschie, 1907

Species *Manis crassicaudata* E. Geoffroy, 1803: Rec, Afghanistan, Pakistan, India, Sri Lanka

Synonyms: *Pholidotus indicus* Gray, 1865

Subgenus *Paramanis* Pocock, 1924

Species *Manis javanica* Desmarest, 1822: Rec, southeast Asia, Indonesia

Synonyms: *Manis leptura* Blyth, 1842; *Manis aspera* Sundevall, 1843; *Manis leucura* Blyth, 1846; *Manis guy* Focillon, 1850; *Manis sumatrensis* Ludeking, 1862; *Pholidotus malaccensis* Fitzinger, 1872; *Pholidotus labuanensis* Fitzinger, 1872

Species *Manis culionensis* (de Elera, 1915): Rec, Culion & Palawan Islands, Philippines

Synonyms: *Manis culionensis* (de Elera, 1895) [*nomen nudum*]

Subfamily Smutsiinae Gray, 1873

Genus *Smutsia* Gray, 1865

Type Species: *Smutsia temminckii* (Smuts, 1832)

Species *Smutsia gigantea* (Illinger, 1815): E Plioc – Rec, modern species in western & central Afr, fossils from eastern & southern Afr

Synonyms: *Pholidotus africanus* Gray, 1865; *Manis wagneri* Fitzinger, 1872

Species *Smutsia temminckii* (Smuts, 1832): Rec, eastern & southern Afr

Synonyms: *Phatages hedenborgii* Fitzinger, 1872

Genus *Phataginus* Rafinesque, 1821

Type Species: *Phataginus tricuspis* Rafinesque, 1821

Synonyms: *Phatagin* Gray, 1865; *Triglochinopolis* Fitzinger, 1872; *Uromanis* Pocock, 1924

Table 1 (continued)

Species *Phataginus tricuspis* Rafinesque, 1821: Rec, western & central Afr

Synonyms: *Manis multiscutata* Gray, 1843; *Manis tridentata* Focillon, 1850

Species *Phataginus tetradactyla* (Linnaeus, 1766): Rec, western & central Afr

Synonyms: *Pholidotus longicaudatus* Brisson, 1762; *Manis macroura* Erxleben, 1777; *Manis ceonyx* Rafinesque, 1820; *Manis africana* Desmarest, 1822; *Manis guineensis* Fitzinger, 1872; *Manis senegalensis* Fitzinger, 1872

MPT receive modest to high bootstrap and branch support values (Fig. 1) and are diagnosed by a large number of unambiguous and unique synapomorphies (Appendix 4). Although a close relationship between Palaeanodonta and Pholidota is assumed based on the work of previous authors (Emry 1970; Storch 2003; Rose et al. 2005), the analysis provides support for the monophyly of Palaeanodonta and Pholidota and a large number of anatomical synapomorphies that would support a relationship between the two groups. In addition, the clade including Palaeanodonta and Pholidota is given a new name, the superorder Pholidotamorpha, as a means to resolve longstanding nomenclatural problems regarding this grouping.

The results provide robust support for the monophyly of the extant pangolins in the family Manidae relative to all the extinct taxa, and for the recognition of three distinct genera within Manidae: *Manis* for the Asian pangolins, *Smutsia* for the African ground pangolins, and *Phataginus* for the African tree pangolins (with the last the best supported, and the middle genus least well supported). The results also support monophyly of the two African genera in a subfamily Smutsiinae. Although the consensus tree fails to resolve the relationships of the important extinct European taxon *Necromanis,* the youngest of the extinct pangolin genera, it does support an alliance between the late Eocene Asian taxon *Cryptomanis* and the latest Eocene North American taxon *Patriomanis* into a single family Patriomanidae. Furthermore, it provides strong support for the monophyly of a clade including *Necromanis,* Patriomanidae, and Manidae exclusive of the middle Eocene pangolins from the Messel deposit in Germany. Perhaps the most surprising results of the analysis are its lack of support for the monophyly of the genus *Eomanis* and its inclusion of *Eurotamandua* within Pholidota. The monophyly of Pholidota itself receives modest bootstrap and branch support, but the clade is diagnosed by surprisingly few synapomorphies, although this may be largely an artifact of the incomplete nature of the basal taxa, particularly *Euromanis krebsi*.

Because the preferred phylogeny differs from previous taxonomic arrangements of Pholidota, a systematic revision of the group is offered. This revision recognizes a superorder Pholidotamorpha containing two orders, Pholidota and Palaeanodonta. Within Pholidota, a suborder Eupholidota containing two superfamilies is recognized: Eomanoidea, a group made monotypic by restricting its contents to the species *Eomanis waldi*; and Manoidea, which contains two families: Patriomanidae, a group whose content has varied in previous treatments but includes two genera in our revision, *Patriomanis*, and *Cryptomanis*; and Manidae, which includes all extant taxa as well as three Plio-Pleistocene fossil species. The European Tertiary form *Necromanis* is also included in Manoidea, though its family level affinities are unresolved. *Eurotamandua* is formally included in Pholidota, and a third Messel "edentate," "*Eomanis*" *krebsi*, is moved to its own newly diagnosed genus, *Euromanis.*

The biogeographic implications of the preferred phylogeny are discussed. The present study strongly corroborates previous suggestions that the Pholidota has its origin on the Laurasian continents, most likely in Europe. This is consistent with both the fossil record for pangolins, their likely sister-group relationship to the Laurasian Palaeanodonta, and with molecular studies of eutherian phylogeny that link Pholidota to Carnivora and other Laurasian clades. The recognition of distinct African and Asian clades of modern pangolins would be consistent with several biogeographic hypotheses of origin. However, the fossil record seems to imply a Laurasian origin of the modern taxa, with dispersal first into Africa, and subsequently into Asia. However, the depauperate nature of the fossil record for pangolins makes such a conclusion tentative at present.

Comparison of the phylogenetic results of this analysis with and without fossil taxa (Fig. 1 vs. Fig. 13) shows the importance of extinct taxa for resolving systematic relationships within the order. Thus, although the results of the present study provide a much clearer resolution for the systematic and biogeographic problems associated with this order than previous work, we cannot help but feel that there is much more to learn about the evolutionary history of this group. The discovery of more, and more complete, fossil taxa, would be invaluable in improving our understanding of pangolin phylogenetic and biogeographic history. Additionally, a comprehensive molecular phylogenetic study on modern pangolins has yet to be conducted. Pangolins are not well represented in zoos and museum collections worldwide, and tend to live at low population densities predominantly in remote forested regions of tropical Africa and Asia. Therefore, obtaining fresh tissue samples for sequence analysis presents particular difficulties. However, such an analysis could provide a critical test for the phylogenetic hypotheses offered in the present study. We hope that ultimately, this study may provide impetus for others to join the search for new fossils or for new molecular data on this group, and that we can improve our understanding of this fascinating, bizarre, highly specialized branch of the mammalian evolutionary tree.

Acknowledgments We wish to thank the following institutions and individuals for providing access to the specimens that formed the basis of this study: Ross MacPhee, Richard Monk, Nancy Simmons, and Eileen Westwig, Department of Mammalogy, American Museum of Natural History, New York, NY; John Flynn and Meng Jin, Department of Vertebrate Paleontology, American Museum of Natural History, New York, NY; Bruce Patterson, Larry Heaney, and Bill Stanley, Division of Mammals, Field Museum of Natural History, Chicago, IL; Prof. Gerhard Storch, Forschungs-Institut Senckenberg, Frankfurt am Main, Germany; Norbert Micklich and Connie Kurz, Hessisches Landesmuseum Darmstadt, Darmstadt, Germany; Ken Rose, Johns Hopkins University, Baltimore, MD; Richard, Thorington, Linda Gordon, and Helen Kafka, Department of Mammalogy, National Museum of Natural History, Washington, D.C.; and Eberhard "Dino" Frey, Staatliches Museum für Naturkunde, Karlsruhe, Germany. For help with the preparation and casting of fossil specimens connected with this study, we thank Fred Grady, Pete Kroehler, and Steve Jabo of the Department of Paleobiology at the National Museum of Natural History. We gratefully acknowledge Jeremy Jacobs of the Department of Mammalogy, National Museum of Natural History, who prepared radiographs from alcohol specimens of extant pangolins that were useful for coding portions of the matrix. Special thanks go to Prof. Gerhard Storch, who provided access to new, undescribed material of *Necromanis* for the purposes of coding this taxon, and who also provided us casts of several specimens of *Eomanis waldi* and the type of *Euromanis krebsi,* and showed us his three-dimensional x-ray photographs of *Eurotamandua joresi*. His material help and insightful comments were critical to the success of this project. We thank Ken Rose (Johns Hopkins University); Jeremy Bramblett, Stylianos Chatzimanolis, Charles Nelson, and Joey Shaw (University of Tennessee at Chattanooga); and John Rawlins (Carnegie Museum of Natural History) for useful discussions concerning this study; and, Michelle Spaulding (American Museum of Natural History) for providing information on *Nandinia*. In addition, this manuscript was greatly improved by the comments of three anonymous reviewers. We thank Julia Morgan Scott for her skillful work in the preparation of illustrations. For housing T. Gaudin during his 2002 period of sabbatical study, and once again during the summer of 2004, special thanks goes to the Department of Paleobiology at the National Museum of Natural History. T. Gaudin's work on this project was supported by a sabbatical grant from the University of Chattanooga Foundation, and by NSF RUI Grant DEB 0107922 and NSF AToL Grant 0629959; J.R. Wible was supported by NSF AToL Grant 0629959.

Appendix 1

Specimens examined in connection with the present study

OTU	Specimen nos.
Outgroups:	
Erinaceus sp.	USNM 25164, 25167, 271142 (*Erinaceus europaeus*)
	UTCM 1001 (*Erinaceus* sp.)
	Petrosal characters from UTCM 727 (*Atelerix algirus*)
Nandinia binotata	AMNH 134969
	CM 42282
	FMNH 149360
	UTCM 1249

Extant pangolins:	
Manis crassicaudata	FMNH 53788 (juv.), 57404*, 82823*, 98232, 98264*, 104032*
	USNM 13065 (alcohol spec.)
Manis javanica	CM 40597
	FMNH 33550*, 37989*, 62919*, 62921*, 68742-3*
	USNM 49875, 49936, 144418, 153975, 198852, 236633, 257682*, 300025*, 321551, 358009 (juv.)
Manis pentadactyla	FMNH 39384-8*, 75874-9*, 94945*, 98909*
	USNM 238735*, 294178, 307385, 308733, 308865, 332899*, 355454, 356431 (juv.)
Phataginus tetradactyla	AMNH 53861
	FMNH 54447*, 54682*, 62209-10*
	USNM 481805-6, exhibit specimen (no catalog no.)
Phataginus tricuspis	CM 16206, 86715, 41123
	FMNH 42679-83*, 62205-8*, 62768*
	USNM 220403, 435022 (juv.), 450073*, 465921, 465927, 481808 (juv.), 537785
Smutsia gigantea	AMNH 53847-9, 53850*, 53851, 53854-5*, 53858
	CM 5764
	USNM 269706 (juv.), 314972
Smutsia temminckii	AMNH 83609 (juv.), 83772, 168954, 244696 (juv.)
	FMNH 34610*, 35682*, 38144*
	USNM 268914, 314972*, 368617 (skull & alcohol spec.), 502722 (alcohol spec.)
Fossil pangolins:	
Cryptomanis gobiensis	AMNH 26140 (holotype)
Euromanis krebsi	SMF 94/1 (cast)—also examined holotype material from private collection of Dr. G. Jores
Eomanis waldi	SMF ME 84 (holotype, cast), MEA 263 (cast), ME 1573a-e, ME 1978/7, ME 15643A & B
	LNK Me 718
	Pohl specimen
Necromanis sp.	SMF M3379a, b, c,
	SMF Qu Hdb2/19, 2/20, 2/18
	SMF uncatalogued specimens
Patriomanis americana	AMNH F:AM 78999 (holotype)
	USNM P299960, P460256, P494439, P531556, P531557
Fossil “edentates”:	
Eurotamandua joresi	HLMD-Me 17.000 (holotype)
	SMF cast of GMH XIV-3912, XIV-4318
Metacheiromys sp.	USNM 26132, 452349
	YPM-PU 18107
Palaeanodon sp.	USGS 4726, 6000, 16471, 21876, 38070, 38498
	USNM 491829

* Specimens marked by an asterisk were used to code skull characters in the Gaudin and Wible (1999) study, but were not used to code additional skull or postcranial characters utilized in the present study.

Appendix 2

Listing of characters and character states [beginning with hind limb from distal to proximal, then axial skeleton (except skull) from caudal to cranial, forelimb from proximal to distal, and skull and mandibular characters]. * denotes multistate characters; ** denotes multistate and ordered characters. Abbreviations: UP=ungual phalanges.

1. Fissured unguals: absent (0), or present (1).

*2. Ratio of maximum width vs. maximum height of proximal articular surface on manual and pedal unguals (UP): width and height roughly equivalent, ratio ≥1 (0), manual but not pedal UP compressed mediolaterally, ratio <1 (1), or manual and pedal UP compressed mediolaterally, ratio <1 (2).

*3. Manual and pedal unguals in dorsal view: waisted, with distinct constriction distal to base (0), manual UP nearly uniform width, constriction rudimentary or absent (1), or manual and pedal UP nearly uniform width, constriction rudimentary or absent (2).

*4. Shape of manual and pedal subungual process in ventral view: rounded triangular platform, perforated by subungual foramina (0), triangular platform but lacking perforations for subungual foramina, with grooves along either side of subungual process leading to subungual foramina instead (1), narrow subungual process, with grooves on either side leading to subungual foramina (2), or triangular or ovate process, unconstricted by grooves, subungual foramina dorsal to subungual process (3).

*5. Surface of proximal articulation, manual and pedal intermediate phalanges: unpaired, transversely wide fossae (0), paired, shallow, ovate fossae only slightly longer dorsoventrally than wide, bordered by well-developed lateral ridges (1), or paired fossae deep, elongate dorsoventrally with poorly marked lateral ridges (2).

6. Width of distal condyles of manual and pedal intermediate phalanges: narrows dorsally, lateral fossae for tendinous insertion visible in dorsal view (0), or nearly uniform, lateral fossae obscured dorsally by lateral ridges of distal condyles (1).

7. Distal condyles of manual and pedal proximal phalanges: with single, transversely elongate, cylindrical condyles (0), or condyles divided into medial and lateral pulleys (1).

**8. Distal keel on metatarsals and metacarpals: present only as a moderate ridge on ventral half of articulation, distinct fossa on dorsal surface of metacarpal above the condyle (0), ventral ridge on ventral half of articulation hypertrophied, distinct fossa on dorsal surface of metacarpal above the condyle still present (1), or keel extends along entire dorsoventral length of condyle, dorsal fossa above condyle absent (2).

9. Width of distal condyles of metatarsals/metacarpals vs. epicondyles: condyles narrower than epicondyles (0), or condyles as wide or wider than epicondyles (1).

**10. Size of pedal ungual phalanx III (UP III) relative to next largest ungual (UP II or IV): next largest ungual larger than, equal to or only slightly smaller than UP III, greatest length ≥95% of III (0), greatest length of next largest ungual ≥80%, <95% of UP III (1), or UP III enlarged, greatest length of next largest <80% of III (2).

**11. Size of pedal ungual I: not greatly reduced, ≥70% length of UP III (0), intermediate, ≥40%, <70% length of UP III (1), or greatly reduced, <40% length of UP III (2).

**12. Shape of proximal phalanges (PP) II-V of pes: elongate, with cylindrical shaft and narrow distal condyles, ratio of maximum width of condyles to maximum length of PP <0.5 (0), intermediate length, ratio of width of condyles to length of PP ≥0.5, <0.9 (1), or wide and short, without cylindrical shaft and with wide distal condyles, ratio of width of condyles to length of PP ≥0.9 (2).

**13. Relative lengths of proximal (PP) and intermediate (IP) phalanges of pes: proximal phalanges elongate, ratio of length of IP IV to PP IV <1.0 (0), proximal and intermediate phalanges approximately equal in length, ratio of length of IP IV to PP IV≥1.0, <1.2 (1), or proximal phalanges greatly shortened, ratio of length of IP IV to PP IV>1.2 (2).

14. Shape of proximal phalanx I of pes: elongate and slender, ratio of maximum length to

maximum proximal depth ≥2.2 (0), or short and deep, ratio of maximum length to maximum proximal depth ≤2.0 (1).

15. Shape of proximal margin, proximal phalanx I of pes, in lateral view: convex (0), or concave (1).

*16. Relative lengths of pedal proximal phalanges: proximal phalanges I–III subequal (0), proximal phalanx I is the longest (1), proximal phalanx II is the longest (2), or proximal phalanx III is the longest (3).

17. Relative lengths of metatarsals I and V: I is shorter (0), or V is shorter (1).

*18. Relative lengths of metatarsals III and IV: III measurably longer, i.e., longer by more than 0.5 mm (0), III and IV subequal (1), or IV measurably longer (2).

**19. Shape of metatarsals III and IV in dorsal view: ratio of width at midshaft to maximum length ≥20% (0), ratio of width to length <20%, >15% (1), or slender, ratio of width to length ≤15% (2).

*20. Midshaft width versus depth of metatarsals: all cylindrical or wide and flat, width ≥ depth (0), all but first wide and flat (1), only first and fifth wide and flat, others with depth > width (2), only fifth wide and flat, others with depth > width (3), or all but third wide and flat (4).

21. Length of metatarsal III vs. tibia: metatarsal III elongate, ≥30% of tibial length (0), or metatarsal III short, <28% tibial length (1).

22. Shape of metatarsal I: straight (0), or curved laterally at its distal end (1).

23. Medial depression on ventromedial surface of proximal metatarsal II: present (0), or absent (1).

24. Proximal end of metatarsal II: unexpanded transversely (0), or expanded transversely (1).

*25. Number of contacts between metatarsals II and III, III and IV: one, dorsal only (0), only dorsal contact between II and III, two separate dorsal and ventral contacts between III and IV (1), or two separate contacts present (2).

26. Orientation of proximal articular surface of metatarsal III: facet vertical, forms flat contact with lateral cuneiform (0), or articular facet overlaps the dorsal surface of metatarsal III (1).

*27. Shape of proximal articular surface of metatarsal III in proximal view: roughly dumbbell shape, expanded dorsally and ventrally and constricted in between (0), roughly triangular, narrowing ventrally (1), or quadrangular, without constriction (2).

28. Proximal contacts of metatarsal IV: contacts cuboid only (0), or overlapped by lateral cuneiform, contacts both lateral cuneiform and cuboid (1).

*29. Dorsal surface, proximal end of metatarsal IV: flat (0), with narrow proximodistal groove (1), or markedly concave (2).

*30. Shape of proximal articular surface, metatarsal IV: quadrangular or triangular (0), triangular or quadrangular with distinct indentation along dorsal margin (1), or irregularly shaped, extended dorsomedially with strongly indented ventromedial margin (2).

*31. Shape of lateral flange of metatarsal V: elongated distally, straight or curved ventrally at distal end, separated from cuboid facet by groove (0), elongated distally, curved dorsally at distal end, separated from cuboid facet by groove (1), or elongate dorsoventrally, separated from cuboid facet by pit enclosed by dorsal and ventral ridges (2).

32. Position of lateral process on metatarsal V: proximal to or at the same level as cuboid articular surface (0), or distal to cuboid articulation (1).

*33. Shape of cuboid facet of metatarsal V: ovate, transversely compressed, width < depth (0), transversely compressed with width < depth, but expanded ventrally (1), or triangular or quadrangular, width ≅ depth (2).

34. Orientation of cuboid facet of metatarsal V: horizontal (0), or tilted proximally and medially (1).

35. Articular facets on metatarsal V for cuboid and metatarsal IV: surfaces contiguous but distinct, oriented at different angles and separated by distinct ridge (0), or surfaces continuous, poorly demarcated (1).

36. Prehallux: absent (0), or present (1).

37. Well-defined articular surface on medial cuneiform for prehallux: absent (0), or present (1).

38. Well-defined articular surface on navicular for prehallux: absent (0), or present (1).

39. Prehallux shape: strongly concave laterally, convex medially (0), or nearly straight (1).

*40. Shape of medial cuneiform in medial view: irregular, elongated proximodistally, com-

pressed dorsoventrally (0), triangular, tapered dorsoventrally at its proximal end (1), or quadrangular, dorsoventral depth equivalent distally and proximally (2).

*41. Shape of distal facet for metatarsal I on medial cuneiform: oval (0), triangular (1), or sigmoid or boomerang-shaped (2).

**42. Shape and size of navicular and middle cuneiform facets on medial cuneiform: middle cuneiform facet elongated dorsoventrally, larger than navicular facet (0), facets circular, nearly equal in size (1), or navicular facet elongate dorsoventrally, larger than middle cuneiform facet (2).

43. Position of middle cuneiform facet and facet for metatarsal II on medial cuneiform: contiguous (0), or separate (1).

44. Number of facets for middle cuneiform on the lateral surface of medial cuneiform: one (0), or two (1).

**45. Dorsal surface of middle cuneiform: elongated dorsoventrally [ratio of width/height <0.9] (0), nearly square, width ≅ proximodistal height [ratio of width/height ≥0.9, ≤1.1] (1), or elongated mediolaterally [ratio of width/height ≥1.2] (2).

*46. Shape of navicular facet on middle cuneiform: ovate (0), quadrangular (1), elongated dorsoventrally with distinct indentation along the middle of medial edge (2), or L-shaped with ventrolateral indentation and elongate dorsoventrally (ratio of maximum dorsoventral depth to greatest width ≥1.8) (3).

47. Shape of articulation between middle and lateral cuneiform: short, occupies less than half of dorsoventral extent of lateral face of middle cuneiform (0), or elongated dorsoventrally, occupies ≥75 % of dorsoventral extent of lateral face of middle cuneiform (1).

48. Distinct foramen on dorsal surface of tarsus formed between lateral cuneiform and cuboid: absent (0), or present (1).

**49. Shape of dorsal surface of lateral cuneiform: elongated proximodistally, ratio of width to height ≤0.8 (0), transverse width ≅ proximodistal height, ratio of width to height ≥1.0, <1.3 (1), or widened transversely, ratio of width to height ≥1.4 (2).

*50. Shape of navicular facet of lateral cuneiform: triangular or quadrangular (0), butterfly-shaped, expanded transversely on dorsal and ventral ends with concave medial and lateral margins (1), or extended ventrally onto plantar tubercle (2).

*51. Shape of metatarsal III facet on lateral cuneiform: quadrangular or trapezoidal, with relatively straight medial and lateral edges (0), expanded dorsally and ventrally with sharp medial and lateral indentations (1), or T-shaped (2).

52. Plantar process of lateral cuneiform: distinctly separate from distal edge of bone in lateral view (0), or contiguous with distal edge (1).

53. Shape of plantar process of cuboid in plantar view: elongated transversely (0), or round (1).

**54. Orientation of plantar process of cuboid in plantar view: tilts proximomedially (0), horizontal (1), or tilts proximolaterally (2).

55. Distal facet of cuboid: deepest point lies at or near medial edge (0), or portion of distal facet that articulates with metatarsal IV with shallow medial extension, deepest part of distal cuboid facet near midline of facet (1).

56. Size of calcaneal facet of cuboid: large, maximum length >80% maximum height of cuboid (0), or small, maximum length ≤70% maximum height of cuboid (1).

*57. Shape of navicular facet of cuboid: facet absent (0), facet elongated dorsoventrally (1), facet elongated proximodistally (2), or facet round or triangular (3).

58. Relative size of astragalar and calcaneal facets of cuboid: calcaneal facet clearly larger (0), or astragalar facet as large or larger than calcaneal facet (1).

59. Astragalar facet of navicular: facet evenly concave, astragalar head evenly convex (0), or facet concave ventromedially, convex dorsolaterally, astragalar head with large corresponding concavity (1).

60. Extent of concavity and convexity on astragalar facet of navicular: concavity extends medial to convexity (0), or concavity restricted to ventral side of convexity (1).

*61. Distal articular facets of navicular for cuneiforms: medial, middle, and lateral cuneiform facets contiguous, separated by low ridge (0), facets for middle and lateral cuneiform continuous, medial cuneiform facet contiguous, separated by low ridge (1), facets for medial, middle, and lateral cuneiforms continuous,

medial/middle cuneiform facet partly separated from lateral cuneiform facet by narrow depression (2), or facets for medial, middle, and lateral cuneiforms continuous, forming a y-shaped surface with facets partly separated by narrow depressions (3).

**62. Astragalar canal: present (0), rudimentary (1), or absent (2).

**63. Astragalar trochlea shape in dorsal view: symmetrical, proximodistal depth of medial and lateral trochlea roughly equivalent [ratio of lateral to medial depth <1.2] (0), moderately asymmetrical [ratio of lateral to medial depth ≥1.2, <1.4] (1), or strongly asymmetrical [ratio of lateral to medial depth ≥1.4] (2).

64. Proximal edge (=posterior edge) of astragalar trochlea in dorsal view: concave (0), or straight or convex (1).

65. Extension of astragalar trochlea onto ventral surface of astragalus: present (0), or absent (1).

66. Distinct facet for tendon of m. flexor digitorum fibularis: present (0), or absent (1).

**67. Proximal extent of ectal facet versus astragalar trochlea: ectal facet distal to or even with proximal edge of trochlea (0), only slightly extended past proximal edge of trochlea [extension beyond trochlea <10% of overall proximodistal length of astragalus] (1), ectal facet extended proximally [extension beyond trochlea ≥10%, <20% length of astragalus] (2), or greatly extended proximally [extension beyond trochlea ≥20% length of astragalus] (3).

68. Ratio of maximum dorsoventral depth of astragalus to maximum transverse width: ≤60% (0), or >65% (1).

69. Width of astragalar neck vs. maximum width of astragalus: <60% (0), or ≥60% (1).

**70. Position of astragalar head: medially situated, distance from lateral edge of head to lateral edge of body >40% of overall width of body (0), distance >35%, ≤40% (1), distance >30%, ≤35% (2), distance >25%, ≤30% (3), or displaced laterally, distance from lateral edge of head to lateral edge of body ≤25% of overall width of body (4).

71. Shape of astragalar head in distal view: head wide, ratio of maximum transverse width to maximum dorsoventral depth >1.25 (0), or head almost circular, ratio of width to depth <1.25 (1).

72. Deep groove for calcaneal-navicular "spring" ligament on ventral margin of astragalar head: absent (0), or present (1).

73. Dorsal margin of astragalar head: concave (0), or convex (1).

**74. Shape of ectal facet of astragalus: very narrow, maximum length more than twice width measured perpendicular to long axis (0), intermediate shape, length less than twice but more than one-and-a half times width (1), or broader, maximum length less than one-and-a-half times width measured perpendicular to long axis (2).

75. Orientation of long axis on astragalar ectal facet: proximodistal (0), or proximomedial to distolateral (1).

*76. Sustentacular facet of astragalus: separate facet centrally located (0), separate facet, displaced distally (1), contiguous with medial navicular and cuboid facet distally (2), or absent (3).

*77. Shape of sustentacular facet of astragalus: quadrangular, width≈length (0), ovate, elongated proximodistally (1), triangular, elongated proximodistally (2), or elongated mediolaterally (3).

**78. Position of sustentacular facet of astragalus: near lateral edge of astragalar neck (0), in midline of astragalar neck (1), or near medial edge of astragalar neck (2).

*79. Shape of medial navicular facet on astragalar neck in medial view: narrow dorsally, extended proximally along ventral edge (0), depressed proximodistally along entire length (1), or irregular shape, not markedly depressed (2).

80. Astragalus/cuboid contact: absent (0), or present (1).

81. Shape of fibular facet of astragalus: oblique, irregularly triangular or teardrop-shaped, without strong vertical moiety distally (0), or crescentic or boomerang-shaped, with concavity facing proximoplantarly or plantarly, or horseshoe-shaped, with concavity facing proximally (1).

82. Shape of fibular facet of astragalus and position of central concavity: facet crescentic or boomerang-shaped, with concavity facing proximoplantarly or plantarly (0), or facet

horseshoe-shaped, with concavity facing proximally (1).

**83. Length of calcaneus vs. tibia: calcaneus elongate, ≥45% of tibial length (0), calcaneus of intermediate length, ≥30%, <40% tibial length (1), or calcaneus short, <30% of tibial length (2).

*84. Tuber calcis shape: nearly cylindrical, dorsoventral depth ≥ transverse width (0), expanded transversely (1), expanded obliquely, greatest depth lies along dorsomedial to ventrolateral axis (2), or expanded obliquely, greatest depth lies along dorsolateral to ventromedial axis (3).

85. Dorsal surface of tuber calcis: smoothly rounded (0), or with sharp dorsal ridge (1).

86. Length of tuber calcis: ≥50% length of calcaneus (0), or <50% length of calcaneus (1).

87. Roughened distal surface of tuber calcis (attachment surface for Achilles' tendon): vertical or slanted somewhat anteriorly toward plantar surface of calcaneus (0), or enlarged along plantar surface of calcaneus, extends forward more than half calcaneal length (1).

88. Orientation of calcaneal cuboid facet: distal and medial (0), or directly distal (1).

**89. Position of sustentacular facet on calcaneus: situated directly medial to ectal and fibular facets (0), elongated distally, distal portion extends distal to ectal and fibular facets, reaching distal edge of sustentacular flange (1), or situated well distal to ectal and fibular facets, contacting distal margin of calcaneus (2).

**90. Proximal extent of astragalar and fibular facets of calcaneus: astragalar facet extends further proximally (0), proximal extent of two facets nearly equal (1), or fibular facet extends further proximally (2).

91. Position of anterior plantar tubercle vs. cuboid facet of calcaneus: proximal to cuboid facet (0), or even with or distal to cuboid facet (1).

92. Shape of cuboid facet of calcaneus: transverse width≈dorsoventral depth (0), or elongated transversely (1).

*93. Peroneal process of calcaneus: absent (0), present as small knob (1), present as low, proximodistally elongated ridge (2), or present as laterally or proximally and laterally elongated flange (3).

*94. Shape of fibular shaft: compressed anteroposteriorly (0), cylindrical (1), cylindrical distally, compressed mediolaterally in its proximal portion (2), or compressed mediolaterally (3).

95. Distinct lateral process on lateral malleolus of fibula: absent (0), or present (1).

96. Orientation of tibial facet of distal fibula: medial (0), or anteromedial (1).

97. Shape of tibial facet of distal fibula: triangular (0), or elongated anteroposteriorly (1).

98. Proximal extent of astragalar and calcaneal facets of fibula in posterior view: nearly equal (0), or astragalar facet extends further proximally (1).

99. Proximal half of astragalar facet of fibula: extended ventrally (0), or ventral extension absent (1).

*100. Development of processes on posterior surface of proximal fibula: small, simple posterior process immediately distal to proximal tibial facet (0), posterior process immediately distal to proximal tibial facet, process marked by elongated posterior groove(s) bounded by lateral ridges (1), posterior process immediately distal to proximal tibial facet, marked by short groove bounded by lateral ridges (2), posterior process well separated from proximal tibial facet, process marked by short groove bounded by lateral ridges (3), posterior process well separated from proximal tibial facet, unmarked by posterior grooves (4), or posterior process absent (5).

101. Shape of posterior process on proximal fibula: narrow proximodistally (0), or elongate longitudinally (1).

*102. Anterolateral eminence on proximal fibula: absent (0), present, extends anterior to tibial facet (1), or present, coincident with tibial facet (2).

**103. Cnemial crest of tibia: sharp, raised, deeply excavated laterally (0), moderately developed with weak proximal lateral excavation (1), or weak, rounded, lacking lateral excavation (2).

*104. Development of anterior distal and anterior lateral distal processes of tibia: anterior distal process elongated, narrow, anterior lateral distal process absent (0), anterior distal process present but shallow, wide, anterior lateral process absent or rudimentary (1), strongly reduced anterior distal process,

anterior lateral distal process well developed (2), or both processes absent (3).

105. Posterior distal tibial process: absent (0), or present (1).

*106. Grooves for tendons of m. tibialis posterior and m. flexor tibialis on medial malleolus of distal tibia: groove on posterior tibial surface lateral to medial malleolus (0), single groove on posterior edge of medial malleolus (1), or two grooves, with separate posterior groove for m. tibialis posterior on posterior edge of medial malleolus, and anterior groove delimited by distinct anterior and posterior ridges for m. flexor tibialis on medial surface of medial malleolus (2).

107. Distal extent of anterior and posterior projections of medial malleolus of distal tibia: distal extent of two processes nearly equal (0), or posterior process extends further distally (1).

108. Depth of groove for m. tibialis posterior tendon: shallow (0), or deep, closed over by soft tissue to form tunnel (1).

**109. Tibial torsion: distal tibial facets rotated clockwise (on L tibia, counterclockwise on R) approximately 45° relative to proximal articulation (0), moderate tibial torsion, distal facets rotated 15–30° (1), or little tibial torsion, distal facets rotated 0–5° (2).

**110. Dorsoventral depth of distal tibial articulations for medial and lateral trochleae of astragalus: medial facet depth > lateral facet (0), facets of approximately equal depth (1), or lateral facet depth > medial facet (2).

111. Distal tibial articulation for medial trochlea of astragalus overlaps anterior face of medial malleolus' posterior extension: absent (0), or present (1).

112. Distal tibial articulation for fibula: not visible in distal view (0), or visible (1).

**113. Maximum width vs. anteroposterior depth of distal tibia: ratio of width to depth <1.5 (0), ratio of width to depth ≥1.5, <2 (1) or distal tibia compressed, ratio of width to depth ≥2 (2).

**114. Relative size of lateral and medial condyles of tibia in proximal view: medial condyle larger than lateral condyle (0), subequal (1), or lateral condyle larger than medial condyle (2).

**115. Shape of tibial lateral condyle in proximal view: elongated transversely (0), transverse width and anteroposterior depth roughly equivalent (1), or elongated anteroposteriorly (2).

*116. Surface contour of tibial lateral condyle: concavo-convex (0), concave (1), convex (2), or flat (3).

117. Pit for attachment of meniscal ligament anterior to medial condyle of tibia: absent (0), or present (1).

118. Proximal fibular facet of tibia: not visible in anterior view (0), or visible (1).

119. Facet for tibial sesamoid (cyamelle) on proximal fibula: absent (0), or present (1).

120. Anterior surface of patella: rugose (0), or with fine longitudinal striations (1).

121. Articulations on posterior surface of patella: distinct medial and lateral facets separated by a sharp ridge (0), or medial and lateral facets confluent (1).

122. Surface of confluent medial and lateral patellar articulations: convex transversely (0), or nearly flat (1).

123. Shape of femoral shaft: slender, minimum width <11% of maximum length (0), or broadened transversely, minimum width >13% maximum length (1).

**124. Angle between femoral head and shaft: <130° (0), 130–135° (1), or >135° (2).

**125. Shape of greater trochanter of femur in proximal view: anteroposterior depth > transverse width (0), L-shaped, elongated both anteroposteriorly and transversely (1), or anteroposterior depth ≤ transverse width (2).

126. Orientation of patellar groove of femur in anterior view: directed toward greater trochanter, medial edge inclined proximally and laterally (0), or directed toward head, medial edge inclined proximally and medially (1).

127. Surface contour of patellar groove of femur in distal view: concave (0), or flat (1).

**128. Distance between proximal end of femur and third trochanter: <50% of maximum length of femur (0), ≥50, <60% of maximum length (1), ≥60, <70 % of maximum length (2), or ≥70 % of maximum length (3).

129. Distance between femoral head (measured from proximal-most point) and tip of lesser trochanter: lesser trochanter close to head,

distance <25% maximum length of femur (0), or lesser trochanter further separated from head, distance ≥25% maximum length (1).

**130. Orientation of lesser trochanter: directed posteriorly, visible posterior to head in proximal view (0), directed posteromedially, partially obscured by head but visible posteriorly in proximal view (1), or directed medially, largely obscured by head but visible medially in proximal view (2).

131. Fovea capitis: present (0), or absent (1).

*132. Trochanteric fossa and intertrochanteric ridge: well developed (0), rudimentary or absent (1), or trochanteric fossa large but intertrochanteric ridge rudimentary or absent (2).

**133. Maximum depth vs. transverse width of distal femur in distal view: width almost equal to depth, ratio=1 (0), width greater than depth, ratio 1.20–1.29 (1), or width greatly exceeds depth, ratio ≥1.30 (2).

134. Maximum depth of medial vs. lateral condyle of femur in distal view: almost equal, ratio of medial depth to lateral <1.20 (0), or medial condyle deeper, ratio ≥1.20 (1).

135. Maximum width of medial vs. lateral condyle of femur in distal view: medial condyle wider, ratio of medial width to lateral ≥1.20 (0), or almost equal, ratio >0.9, <1.20 (1).

136. Sacroiliac attachment: unfused (0), or fused (1)

**137. Extent of sacroiliac junction: ends anterior to acetabulum (0), extends to midpoint of acetabulum (1), or extends past midpoint of acetabulum, sacral vertebrae contact anterior ischium (2).

*138. Number of sacral vertebrae: 2, both attached to ilium (0), 3, 2 attached to ilium (1), 3, all attached to ilium (2), 4, 3 attached to ilium (3), or 4, 2 attached to ilium (4).

*139. Metapophyses and neural spines of sacral vertebrae: unfused (0), neural spines of two or more sacral vertebrae fused, but metapophyses unfused (1), metapophyses of two or more sacral vertebrae fused, but neural spines unfused (2), or metapophyses and neural spines fused (3).

140. Dorsal spinal nerve foramina of sacral vertebrae: face dorsally, well separated laterally from base of metapophyses (0), or face dorsolaterally, situated immediately underneath metapophyses (1)

141. Process for sacrospinous ligament at posteroventral base of transverse process of last sacral vertebra: absent (0), or present (1).

*142. Shape of transverse process of last sacral vertebra: wing-like, expanded anteroposteriorly but thin dorsoventrally (0), unexpanded, rod-like (1), or expanded anteroposteriorly and thick dorsoventrally (2).

143. Lateral extent of transverse process of last sacral vertebra in dorsal view: does not extend lateral to body of ischium or acetabulum (0), or extends lateral to ischium (1).

144. Metapophyses of sacral vertebrae: short, less than half neural spine height (0), or elongated, >2/3 neural spine height (1).

**145. Angle between sacral vertebrae and ilium: ≤10° (0), >20°, ≤30° (1), or >35° (2).

*146. Gluteal fossa on ilium: large, with prominent lateral iliac crest, medial dorsal flange of ilium and caudal dorsal iliac spine (0), weak, iliac crest rounded but still well developed, small dorsal flange and free caudal dorsal iliac spine (1), poorly demarcated, iliac crest rounded, weak, dorsal flange absent, caudal dorsal iliac spine incorporated in sacroiliac junction (2), or poorly demarcated, iliac crest rudimentary but small dorsal flange and caudal dorsal iliac spine present (3).

*147. Position of femoral spine (= tuberosity for m. rectus femoris): on acetabular eminence, directly dorsal to iliopubic eminence (0), on lateral iliac crest, anterior to acetabular and iliopubic eminence (1), or absent (2).

148. Shape of lunate surface of acetabulum: U-shaped, broadly open (0), or C-shaped, nearly a closed loop (1).

**149. Orientation of acetabular fossa: fossa opens ventrally (0), posteroventrally (1), or posteriorly (2).

150. Size of obturator foramen: large, maximum diameter of acetabulum <75 % that of obturator foramen (0), or small, maximum diameter of acetabulum ≥75 % that of obturator foramen (1).

151. Orientation of ischial tuberosities: not flared laterally, or only weakly so (0), or flared laterally (1).
152. Development of ischial spine: small (0), or prominent (1).
153. Position of ischial spine: separated anteriorly from ischial tuberosity, dorsal to anterior portion of obturator foramen (0), or close to ischial tuberosity, dorsal to posterior portion of obturator foramen (1).
154. Position of dorsal edge of ischium: at same level as transverse processes of sacral and anterior caudal vertebrae (0), or ventral to transverse processes of sacral and anterior caudal vertebrae (1).
*155. Shape of pubis and position of attachment to ilium: rod-like, elongated, attached to ilium under anterior edge of acetabulum (0), slightly compressed mediolaterally, attached to ilium beneath midpoint of acetabulum (1), short, flat, attached to ilium under posterior edge of acetabulum (2), or elongated, flat, attached to ilium under anterior edge of acetabulum (3).
156. Anterior edge of pubic symphysis in ventral view: forms narrow V (0), or forms broad U (1).
**157. Number of thoracic vertebrae: 11 (0), 12 (1), 13 (2), 14 (3), 15 (4), or 16 (5).
**158. Number of lumbar vertebrae: 7 (0), 6 (1), or 5 (2).
**159. Number of caudal vertebrae: more than 30 (0), 20–30 (1), or less than 15 (2).
**160. Position of diaphragmatic vertebra: T9 (0), T10 (1), T11 and T12 (1), T12 (2), T12 and T13 (3), or T13 (4).
*161. Transverse process of last lumbar vertebra: rodlike, reduced in lateral and anteroposterior extent (0), reduced in anteroposterior extent versus that of penultimate lumbar (1), reduced in lateral extent versus that of penultimate lumbar (2), or unreduced (3).
162. Transverse processes of anterior lumbar vertebrae: directed anterolaterally (0), directed laterally (1), or directed posterolaterally (2).
163. Attachment of pedicel to lumbar centra: ventrolateral to dorsal edge of centrum, spinal nerves form grooves on posterodorsolateral surface of centrum (0), or pedicels attach to dorsal edge of centrum, spinal nerve foramina dorsal to centrum (1).
164. Shape of centrum of third lumbar vertebra: short anteroposteriorly, length ≤1.5 times maximum depth (0), or elongated anteroposteriorly, length >1.5 times maximum depth (1).
**165. Neural spine of third lumbar vertebra: elongated dorsoventrally, height >1.5 times anteroposterior length (0), low, height 1.0–1.5 times anteroposterior length (1), or elongated anteroposteriorly, height <0.7 times anteroposterior length (2).
166. Surface contour of zygapophyses of lumbar vertebrae: flat or slightly concave (0), or embracing (1).
167. Relative heights of neural spines of anterior thoracic vertebrae: elongated, much longer than in more posterior thoracics (0), or not dramatically elongated (1).
**168. Anteriormost thoracic vertebra in which the diapophysis is completely separated posteroventrally from the metapophysis: T10 (0), T11 (1), T12 (2), T13 (3), or T14 (4).
**169. Anteriormost thoracic vertebra in which the capitular facet is entirely confined to a single centrum: T10 (0), T11 (1), T12 (2), T13 (3), T14 (4), or T15 (5).
170. Surface contour of anterior and posterior zygapophyses of cervical vertebrae: flat (0), or anterior concave, posterior convex (1).
171. Cervical anterior and posterior zygapophyses extend far anterior and posterior to centrum: absent (0), or present (1).
172. Heights of neural spines in cervical vertebrae 3-7: C3>C4>C5<C6<C7 (0), or C3≤C4≤C5<C6<C7 (1).
**173. Inclination of neural spine of C3: vertical (0), weakly inclined posteriorly (1), or strongly inclined posteriorly (2).
174. Neural spine of C7: vertical (0), or inclined posteriorly (1).
175. Transverse process of C7: rectangular (0), or flared distally (1).
*176. Posterior edge of lamina of C4-6 in dorsal view: straight (0), concave (1), or irregular (2).
**177. Posterior extension of neural spine of axis: absent, posterior surface of neural spine with two oval concavities for attachment of nuchal ligament (0), deep, blunt extension over anterior portion of C3 (1), or elongated, narrow extension to midpoint of C3 or beyond (2).

**178. Anterior extension of neural spine of axis: absent (0), present but small, little overlap of posterior edge of atlas (1), present, strongly overlaps posterior portion of atlas with surface for ligamentous attachment to arch of atlas (2), or present, elongated and narrow with diamond-shaped anterior expansion for ligamentous attachment to arch of atlas (3).

179. Ventral surface of transverse process of axis: flat or convex (0), or with longitudinal concavity (1).

180. Ventral surface of axial centrum: with midline crest or eminence and lateral excavations (0), or surface relatively smooth, eminence and crest rudimentary or absent (1).

181. Ratio of axial centrum maximum anteroposterior length (including dens) to width (measured immediately behind anterior articular surface): ≥1.0 (0), or <0.85 (1).

*182. Surface contour of anterior articular surface of axis: flat or convex transversely (0), convex medially, concave laterally (1), or concave transversely (2).

183. Shape of anterior articular surface of axis: elongated transversely, ratio of width to maximum dorsoventral depth >1.30 (0), or ratio of width to depth <1.25 (1).

184. Axial anterior articular surface and articular facet of dens: contiguous (0), or separate (1).

185. Transverse foramen of axis in anterior view: not visible, obscured by anterior articular surface (0), or visible (1).

186. Transverse process of atlas: broad dorsoventrally (0), or shallow dorsoventrally (1).

187. Anterodorsomedial groove connecting transverse canal of atlas with lateral vertebral foramen: open (0), or enclosed by contact between anteromedial edge of transverse process and arch of atlas (1).

188. Distinct depressions for origin of mm. rectus capitis anterior and lateral to neural spine of atlas: absent (0), or present (1).

**189. Maximum width vs. maximum anteroposterior length of atlas (excluding transverse processes): narrow transversely, ratio <1.0 (0), ratio 1.5–2.0 (1), or widened transversely, ratio >2.0 (2).

190. Separation of anterior zygapophyses of atlas: widely separate, distance between medial edge of two facets ≥40% of maximum width of atlas (0), or narrowly separated, distance between medial edge of two facets <40% of maximum width of atlas (1).

191. Relationship of sternal ribs and sternum: ventral surface of sternum flat, sternal ribs articulate with lateral surface of sternebrae (0), or ventral surface of sternebrae with large, anteroventral processes, sternal ribs overlap posteroventral surface of sternebrae, contact or nearly contact one another in midline (1).

192. Shape of manubrium in cross-section: cylindrical (0), or flattened dorsoventrally (1).

*193. Xiphisternum: short (0), elongated (1), or elongated and bifurcate (2).

*194. Cartilaginous extension of xiphisternum: short, length much less than ossified portion of xiphisternum, shovel shaped at distal end (0), elongated, length much greater than ossified portion of xiphisternum, shovel shaped at distal end with central perforation (1), or greatly elongated, extending posteriorly to pelvis, then curling dorsally toward vertebral column at its distal end (2). (see Grassé 1955; Kingdon 1971.)

**195. Number of true ribs: 6 (0), 7 (1), 8 (2), or 9 (3).

196. Shape of first rib: shaft expanded mediolaterally (0), or unexpanded, or only slightly expanded at distal end (1).

197. Clavicle: present (0), or absent (1).

198. Shape of ventral end of scapular spine: elongated acromion process present (0), or acromion rudimentary (1).

**199. Shape of acromion: blunt, without any indication of bifurcation (0), weakly bifurcated (1), or strongly bifurcated with well-developed metacromion process (2).

**200. Coracoid process of scapula: present, robust (0), rudimentary (1), or absent (2).

**201. Distance from ventral corner of anterior scapular edge to anterior edge of glenoid: close, distance <15% of maximum length of scapula [measured from ventral edge of glenoid to dorsal edge of scapula] (0), distance ≥15%, <20% (1), distance ≥25%, <35% (2), or widely separated, distance ≥55 % of maximum length of scapula (3).

**202. Secondary scapular spine: sharp crest (0), rounded crest (1), or absent or rudimentary (2).

203. Teres minor fossa on posteroventral edge of scapula: present (0), or absent (1).
204. Height of scapular spine in distal view: elongated, height roughly equivalent to mediolateral width of glenoid (0), or reduced in height, <85% of mediolateral width of glenoid (1).
205. Orientation of long axis of humeral head in posterior view: oriented proximodistally, or somewhat distolateral (0), or oriented distomedially (1).
**206. Orientation of deltopectoral crest of humerus: canted medially at its distal end (0), extends straight down shaft (1), or canted laterally at its distal end (2).
**207. Length of deltopectoral crest: extends >75% of the length of the humerus (0), extends >65, ≤75% of the length of the humerus (1), extends >55, ≤65% of the length of the humerus (2), or extends ≤55% of the length of the humerus (3).
208. Pulley for m. biceps brachii at distal termination of deltopectoral crest: present (0), or absent (1).
209. Deep anterior groove between greater tubercle and lesser tubercle of humerus for head of m. biceps brachii: present (0), or groove shallow or absent altogether (1).
210. Large distinct deltoid crest extends across lateral surface of humerus: present (0), or absent (1).
211. Distinct fossa for mm. infraspinatus and teres minor on lateral surface of humerus: absent (0), or present (1).
**212. Width across humeral epicondyles: relatively narrow, <40% of length of humerus (0), intermediate width, 40–50% of length of humerus (1), or wide, >50% of length of humerus (2).
**213. Length of entepicondyle: short, <30% of epicondylar width of humerus (0), intermediate length, 30–40% of epicondylar width of humerus (1), or elongated, >40% of epicondylar width of humerus (2).
214. Position of proximal entepicondylar foramen: visible in anterior view (0), or visible in posterior view (1).
*215. Entepicondylar notch: absent (0), weak (1), or present (2).
**216. Size and proximal extent of supinator crest: greatly enlarged, with free-standing proximal extension reaching to middle region of humeral shaft (0), well developed but lacking free-standing proximal extension, extends proximal to proximal opening of entepicondylar foramen and extends far lateral to humeral shaft (1), moderately developed, extends proximal to proximal opening of entepicondylar foramen but weakly flared laterally (2), or reduced, ends at level of proximal opening of entepicondylar foramen (3).
217. Form of supinator crest: flared laterally at its distal end, with well-developed anterior concavity (0), or extends nearly straight distally, anterior concavity poorly marked or absent (1).
218. Posterior surface of distal humerus between supinator crest and posterior edge of entepicondyle/entepicondylar foramen, proximal to olecranon fossa: flat (0), or concave (1).
219. Distal edge of trochlea of humerus in anterior view: straight or slightly concave (0), or convex (1).
220. Medial lappet of trochlea of humerus extending underneath entepicondyle in distal view: present (0), or absent (1).
221. Medial extent of radial fossa of humerus: extends over lateral half of trochlea (0), or situated directly above capitulum, does not extend medially over trochlea (1).
222. Size of olecranon fossa of humerus: large, wider transversely than trochlea in posterior view (0), or small, narrower transversely than trochlea (1).
223. Relative proximal extent of greater and lesser tubercle of humerus: greater tubercle extends proximal to lesser (0), or proximal extent of greater and lesser tubercle roughly equivalent (1).
224. Position of proximal portion of lesser tubercle of humerus: extends anterolaterally, overlaps head in anterior view (0), or does not extend anterolaterally, remains medial to head in anterior view (1).
225. Bicipital groove of humerus continuous with well-developed fossa anteromedial to greater tubercle: present (0), or absent (1).
226. Orientation of greater tubercle of humerus relative to head in proximal view: divergent from head posterolaterally (0), or approximately parallel to lateral surface of head (1).

**227. Length of olecranon process of ulna: short, <20% of maximum ulnar length (0), intermediate length, 20–30% of maximum ulnar length (1), or elongated, >30% of overall ulnar length (2).

228. Olecranon process of ulna inflected medially in anterior view: absent (0), or present (1).

229. Olecranon process of ulna inflected ventrally in medial view: absent (0), or present (1).

**230. Maximum width of radiohumeral articular surface of ulna: wide, ≥20% of maximum ulnar length (0), intermediate, ≥15%, <20% of maximum ulnar length (1), or narrow, ≤10% of maximum ulnar length (2).

**231. Width of anconeal process of ulna: narrow, <10% of maximum ulnar length (0), 10–15% of maximum ulnar length (1), or wide, >15% of maximum ulnar length (2).

232. Distance between coronoid process and ulnar tubercle of ulna: close, ≤10% of maximum ulnar length (0), or biceps tubercle displaced distally, distance >10 % of maximum ulnar length (1).

*233. Relative anterior extent of anconeal and coronoid processes of ulna: anconeal process extends further anteriorly (0), coronoid process extends further anteriorly (1), or equal in anterior extent (2).

234. Shape of interosseous border of ulna: sharp (0), or rounded, poorly marked (1).

**235. Medial concavity on distal ulnar shaft: well marked (0), weakly present (1), or absent (2).

236. Depth of distal ulnar shaft: deep, ≥10% of maximum ulnar length (0), or narrow, <10% of maximum ulnar length (1).

237. Shape of styloid articulation of ulna in distal view: maximum transverse width ≥ anteroposterior depth (0), or compressed mediolaterally, width < depth (1).

**238. Ratio of ulnar length to humeral length: ≤90% (0), >90, ≤100% (1), >100, ≤120% (2), or >120% (3).

**239. Ratio of radial length to humeral length: <75% (0), >75, ≤85% (1), or >95% (2).

**240. Maximum depth of radial shaft: <15% of maximum radial length (0), ≥15, <20% of maximum radial length (1), ≥20, <25% of maximum radial length (2), or ≥25% of maximum radial length (3).

*241. Radial (=bicipital) tuberosity: absent (0), present, weakly developed (1), strong, angular process (2), or present as a well-developed tubercle (3).

242. Size of trochlear facet on radial head: large, ≥1/3 the overall width of the head (0), or small, <1/3 the overall width of the head (1).

243. Ulnar facet and sesamoid facet on radial head: contiguous (0), or separate (1).

**244. Sesamoid facet on radial head: absent (0), small, not visible in proximal view (1), or large, visible in proximal view (2).

245. Condylar facet of radial head: concave medially with flat lateral portion (0), or evenly concave (1).

*246. Styloid and pseudostyloid processes and dorsal tuberosity of distal radius: styloid process rudimentary, pseudostyloid process prominent, dorsal tuberosity weak (0), styloid process, pseudostyloid process and dorsal tuberosity all prominent (1), styloid process and dorsal tuberosity prominent, pseudostyloid process rudimentary or absent (2), dorsal tuberosity prominent, much larger than styloid process, pseudostyloid process weakly developed (3), dorsal tuberosity prominent, styloid process and pseudostyloid process weakly developed (4), or styloid process prominent, pseudostyloid process and dorsal tuberosity weakly developed or absent (5).

247. Orientation of radial styloid process: distal (0), or distolateral (1).

**248. Orientation of distal radial articular surface: long axis transverse (0), long axis runs dorsomedial to ventrolateral (1), or long axis runs dorsoventral, or nearly so (2).

249. Fused scaphoid and lunate bone: absent (0), or present (1).

250. Contact between scapholunar and hamate: present (0), or absent (1).

251. Proximodistal depth of palmar tuberosity on scapholunar: palmar tuberosity narrow, depth <30% of maximum width of scapholunar (0), or palmar tuberosity deep, depth >35% of maximum width of scapholunar (1).

252. Shape of palmar margin of radial articular surface of scapholunar: nearly straight (0), or strongly indented, concave in palmar direction (1).

253. Triquetral articular surface on scapholunar: absent (0), or present (1).
254. Connection between trapezoid and capitular articular surfaces on scapholunar: capitular divided from trapezoid facet by sharp ridge (0), or trapezoid and capitular facets continuous (1).
255. Shape of ulnar articular facet of triquetrum: compressed dorsoventrally, transverse width much greater than dorsoventral depth (0), or width ≤ depth (1).
256. Ulnar/pisiform articular facets vs. scapholunar facet on triquetrum: facets separate (0), or facets contiguous (1).
*257. Surface contour of scapholunar facet on trapezium: convex (0), concave (1), or complex, concavo-convex (2).
258. Extent of scapholunar facet on trapezium: restricted to medial portion of proximal surface (0), or covers entire proximal surface of bone (1).
259. Surface contour of scapholunar facet on trapezoid: concave (0), or convex (1).
**260. Orientation of scapholunar facet on trapezoid in dorsal view: facet tilted to face proximally and laterally (0), facet horizontal (1), or tilted to face proximally and medially (2).
**261. Orientation of facet for trapezium on trapezoid: distally and medially (0), medially (1), or proximally and medially (2).
**262. Width of proximal articulation on capitate: narrow, width <50% of maximum dorsoventral depth of capitate (0), ≥50%, <60% (1), ≥60%, <70% (2), ≥70%, <80% (3), or very wide, ≥85% (4).
*263. Shape of proximal articulation on capitate: ovate or rectangular, without lateral indentation (0), roughly triangular, with slight lateral indentation (1), or L-shaped, with abrupt, step-like lateral indentation between dorsal portion of facet and its palmar extension (2).
*264. Relationship of capitate and trapezoid: trapezoid overlaps capitate proximally, trapezoid facet of capitate faces proximally and medially (0), capitate overlaps trapezoid proximally, trapezoid facet of capitate faces distally and medially (1), or capitate and trapezoid abut along a vertical surface (2).
*265. Shape of distal articulation of capitate: dumbbell shape, with indentations along the medial and lateral margins (0), roughly triangular, narrower ventrally than dorsally (1), bilobate, with an indentation along the medial margin only (2), or rectangular (3).
266. Position of hamate facet of capitate: near dorsal edge of bone, dorsal to dorsoventral midline (0), or displaced ventrally, lies at or ventral to dorsoventral midline (1).
*267. Unciform process of hamate: absent (0), directed distally and ventrally (1), or directed distally and ventrally at its base, with a distinct proximal and ventral extension (2).
268. Dorsal surface of hamate: narrow proximodistally, proximodistal length < transverse width (0), or narrow transversely, length ≥ width (1).
269. Facet for metacarpal IV on hamate: narrow transversely (width < dorsoventral depth) (0), or wide transversely (1).
270. Metacarpal III length vs. humerus: III elongated,≈30% of humerus length (0), or short, <25% of humerus length (1).
271. Shortest metacarpal: V (0), or I (1).
272. Longest metacarpal: IV (0), or III (1).
**273. Relative length of metacarpal II and IV: II < IV (0), II=IV (1), or II>IV (2).
**274. Width vs. length of metacarpal IV: narrow transversely, minimum width <20% of maximum length (0), minimum width ≥20, <30% of maximum length (1), minimum width ≥30, <45% of maximum length (2), or expanded transversely, minimum width ≥45% of maximum length (3).
*275. Cross-sectional shape of shaft of metacarpals I-V: roughly cylindrical, width ≥ depth (0), dorsoventrally elliptical, depth > width (1), or depth > width on all but metacarpal III, in which width ≥ depth (2).
*276. Articulation between distal metacarpals and proximal phalanges: distal condyles and keels of metacarpals convex, joint mobile (0), all but metacarpal III with mobile joints, metacarpal III with nearly vertical keel and ventral stop, joint immobile (1), or joint surface flat or concavoconvex on metacarpals I-IV, joints immobile (2).
*277. Shape of metacarpal I in medial view: with elongated cylindrical shaft, may be slightly

expanded proximally and distally (0), dumbbell shaped, with broadly expanded proximal and distal ends joined by short shaft (1), or expanded distally only, with shaft narrowing towards proximal end (2).

278. Shape of proximal articular surface of metacarpal I in proximal view: triangular, transverse width≈dorsoventral depth (0), or compressed transversely (1).

279. Distal keel on condyle of metacarpal I: present (0), or absent (1).

280. Concavity on dorsal surface of metacarpal II, proximal end: absent (0), or present (1).

281. Facet for trapezium on metacarpal II: restricted to dorsal half of medial surface (0), or extends almost to ventral extremity of medial surface (1).

*282. Articulation between metacarpal II and III: articular surfaces curved, concave on metacarpal II, convex on metacarpal III (0), articular surfaces flat (1) or facet convex on metacarpal II, concave on metacarpal III (2).

283. Palmar extent of capitular facet on metacarpal III: palmar tuberosity well developed, little overlap of capitular facet on shaft (0), or facet overlaps shaft proximally, palmar tuberosity weakly developed (1).

284. Shape of capitular facet of metacarpal III in medial view: evenly convex (0), or sigmoid, extended to form dorsal shelf (1).

285. Dorsal surface of metacarpal III, proximal end: smoothly convex (0), or with sharp midline crest terminating in prominent tubercle proximally (1).

286. Proximal and lateral extension of shaft of metacarpal III overlapping metacarpal IV proximally, lateral to capitate facet: present (0), or absent (1).

287. Hamate facet of metacarpal III: elongated dorsoventrally (0), or restricted to dorsal half of proximomedial surface (1).

*288. Extensor tubercle on dorsal surface of metacarpals: present on metacarpals III and IV (0), present on metacarpals II and III (1), or absent (2).

*289. Dorsal surface of metacarpal IV extended laterally and medially for articulations with metacarpals III and V: absent (0), T-shaped proximal end, extensions present medially and laterally (1), or extension present laterally but not medially (2).

*290. Surface contour of proximal articulation of metacarpal IV: evenly convex transversely and anteroposteriorly (0), mostly convex but with strong concave pit (1), or concave transversely, convex anteroposteriorly (2).

*291. Shape of proximal articulation of metacarpal IV: rectangular, long axis oriented dorsoventrally (0), triangular with base facing dorsally (1), or semicircular with flat edge facing dorsally (2).

292. Contour of articular surface for metacarpal III on metacarpal IV: flat dorsoventrally (0), or convex dorsoventrally (1).

293. Contour of articular surface for metacarpal V on metacarpal IV: concave dorsoventrally (0), or convex dorsoventrally (1).

*294. Shape of articular surface for metacarpal V on metacarpal IV: ovate, proximodistal depth ≥ dorsoventral depth (0), ovate, compressed proximodistally (1), or triangular, tapers ventrally (2).

295. Lateral tubercle and proximal articulation on metacarpal V: lateral tubercle of metacarpal V at or below the level of proximal articular surface on metacarpal IV, articulation on metacarpal V for hamate fairly level (0), or metacarpal V forms peg-and-socket articulation with hamate, lateral tubercle of metacarpal V lies proximal to articular surface on metacarpal IV (1).

296. Cross-sectional shape of shaft of proximal and intermediate manual phalanges: width ≥ depth, shaft cylindrical or even slightly compressed dorsoventrally (0), or compressed mediolaterally, width < depth (1).

297. Lateral fossae for insertion of tendons on distal end of proximal manual phalanges: present (0), or absent (1).

*298. Relative lengths of manual proximal (PP) and intermediate (IP) phalanges: nearly equivalent, ratio of IP/PP length <1.2 on all digits (0), proximal phalanx shorter on digits II and III (1), proximal phalanges shortened on digits III-V (2), or all proximal phalanges shortened (3).

**299. Relative widths of proximal phalanges on digits II and IV: II>IV (0), II=IV (1), or II<IV (2).

300. Distal articulation of proximal phalanx on digit III: with paired distal condyles separate (0), or with paired distal condyles joined at their dorsoventral midpoint by a transverse eminence (1).

*301. Proximal articulations of manual intermediate phalanges: visible in dorsal view, dorsal midline process does not extend as far proximally as basal tubera (0), not visible dorsally, dorsal midline process elongated proximally (1), or not visible dorsally, but dorsal midline process relatively short (2).

**302. Size of manual ungual phalanx (UP) on digit I: roughly equal to UP V (0), reduced, smaller than UP V (1), or greatly reduced, <1/2 the length of UP V (2).

303. Size of ungual phalanx on digit III: not enlarged at all or only slightly enlarged relative to next largest ungual (0), or greatly enlarged, length >1.3 times that of next longest ungual (1).

**304. Length of metatarsal III+proximal phalanx III+intermediate phalanx III+ungual phalanx III vs. tibial length: toes short, <70% tibial length (0), toes intermediate length, 70–85% of tibial length (1), or toes elongate, >90% tibial length (2).

**305. Length of metacarpal III+proximal phalanx III+intermediate phalanx III+ungual phalanx III vs. humeral length: toes short, <60% humeral length (0), toes intermediate length, 70–80% of humeral length (1), or toes elongate, >80% humeral length (2).

*306. Anterior border of nasal: with shallow notch (0), with deep notch forming elongated medial and lateral processes, with deep fossa on lateral process (1), or deeply concave, with elongated lateral process but medial process rudimentary or absent (2).

307. Nasal length: less than or equal to (0), or greater than one-third skull length (1).

308. Maxillonasal suture: subparallel (0), or convergent anterior to maxillofrontal junction (1).

309. Dorsal (facial) process of premaxilla: C-shaped, broad anteroposteriorly with distinct anteroventral and anterodorsal processes (0), or inclined posterodorsally (1).

310. Incisive foramen: within premaxilla (0), or between premaxilla and maxilla (1).

311. Size of palatal process of premaxilla: small or absent, if present, extending posteriorly between maxillae for a distance less than or equal to the maximum diameter of the incisive foramen (0), or elongate, extends posteriorly for a distance clearly greater than the maximum diameter of the incisive foramen (1).

312. Vomerine exposure on palate: absent (0), or present (1).

313. Maxilla with deep median longitudinal palatal concavity: absent (0), or present (1).

314. Alveolar sulcus on maxilla: absent (0), or present (1).

315. Maxilla with narrow posterior palatal process extending lateral to palatine: absent (0), or present (1).

*316. Palatine foramina: multiple within palatine and maxilla (0), double within palatine (or posterior within palatine, anterior between palatine and maxilla) (1), single within maxilla (2), double within maxilla (3), or single large foramen within palatine, at times with smaller accessory foramina in palatine (4).

*317. Anterolateral shelf of palatine: absent (0), lies posterior to (1), or medial to zygomatic process of maxilla (2).

318. Palatines within choanae: subparallel, widely separated by presphenoid and/or vomer (0), or converging anteriorly, nearly contacting (1).

**319. Lacrimal bone and lacrimal foramen: both present (0), bone present, foramen absent (1), or both absent (2).

320. Lacrimal fenestra: absent (0), or present (1).

321. Ethmoidal foramen: within frontal (0), or between frontal and orbitosphenoid (1).

**322. Orbitosphenoid/squamosal contact: absent (0), narrow, alisphenoid approximates frontal (1), or broad (2).

323. Small foramen posterior to optic foramen in orbitosphenoid: absent (0), or present (1).

324. Foramen rotundum and sphenorbital fissure: separate (0), or confluent, opening into same fossa (1).

325. Foramen subovale: absent (0), or present (1).

326. Foramen ovale: within alisphenoid (0), or between alisphenoid and squamosal (1).

327. Flange on pterygoid process behind foramen ovale: absent (0), or present (1).

*328. Pterygoid hamulus: distal tip anterior to auditory tube (0), distal tip extends to level of fenestra vestibuli (1), distal tip extends to level of anterior rim of jugular foramen (2), or absent (3).

329. Pterygoid/ectotympanic contact: widely separated (0), or closely approximated or in contact (1).

330. Ectotympanic inflation: present (0), or absent (1).

331. Entotympanic or facet for entotympanic on basioccipital: present (0), or absent (1).

**332. Course of internal carotid artery: transpromontorial (0), on the ventromedial edge of petrosal, lateral to entotympanic if present (1), or within or medial to entotympanic (2).

333. Auditory tube orientation: anteromedial (0), or medial (1).

334. Promontorium of petrosal: prominent, globose (0), or weakly developed, flat (1).

**335. Course of facial nerve: open sulcus, crista parotica weak (0), open sulcus, crista parotica prominent (1), or closed canal (2).

336. Fusion between distal tip of tympanohyal and lateral surface of promontorium: absent (0), or present (1).

337. Position of fenestra cochleae: well separated from fenestra vestibuli, facing posteriorly and slightly laterally (0), or immediately next to fenestra vestibuli, facing laterally and slightly posteriorly (1).

338. Shielding of fenestra cochleae: open posteroventrally (0), or shielded posteroventrally by flange on petrosal (1).

*339. Position of fossa incudis within epitympanic recess: in lateral wall, facing medially (0), in posterior wall, facing anteriorly (1), or in medial wall, facing laterally (2).

340. Squamosal participation in roof of epitympanic recess: absent or forming small part of lateral wall (0), or extensive, forming much of roof (1).

341. Surface contour of incudal facet of malleus: concave (0), or convex (1).

**342. Orientation of mallear head/incudal facet: mallear head unrotated, incudal facet facing caudally and laterally (0), mallear head unrotated, incudal facet facing caudally and medially (1), or head rotated dorsad 90°, incudal facet facing dorsally, caudally and medially (2).

*343. Incus: body gracile, may or may not be rectangular, crura elongated (0), body stout and rectangular, crura short (1), or body gracile with extreme elongation of crus longum, reduction of crus breve (2).

344. Stapedial columella: elongated, height nearly equal to or exceeding greatest width of footplate (0), or short, height much less than greatest width of footplate (1).

345. Mastoid/exoccipital contact: broad, squamosal well separated from lateral rim of jugular foramen (0), or narrow, squamosal approximates lateral rim of jugular foramen (1).

346. Vomer: underlies presphenoid in posterior nasopharynx, visible through choanae (0), or restricted to anterior nasal cavity, not visible from choanae (1).

347. Tympanic process of pterygoid: absent (0), or present (1). [Note: This feature was termed the "lateral wing of basisphenoid" in Gaudin and Wible (1999). In adult pangolins, the basisphenoid, alisphenoid, and pterygoid are fused. However, a juvenile *Phataginus tricuspis (CM 41123)* clearly shows this feature to be part of the pterygoid and not the basisphenoid.]

**348. Tympanic process of basioccipital: absent or weak, does not reach level of promontorium (0), moderate, even with promontorium (1), or prominent, ventral to promontorium (2). [Note: This feature is termed the "basioccipital wing" in Gaudin and Wible (1999).]

349. Exoccipital constriction anterior to occipital condyle: present (0), or absent (1).

350. Foramen magnum shape: circular (0), or oval transversely (1).

351. Supraoccipital/parietals suture shape: subtends an angle greater than 90° (0), or less than or equal to 90° (1).

352. Nuchal crest: strongly developed (0), or rudimentary to absent (1).

**353. Squamosal inflation posterior to external auditory meatus/porus acousticus: absent (0), weak, not clearly demarcated on external surface (1), or strong, with distinct lateral bulge on external surface (2).

354. Position of alisphenoid/squamosal suture: widely separated from (0), or approximating base of zygomatic process (1).

*355. Orientation (and size) of zygomatic process of squamosal: laterally directed (0), ventrally directed, elongated (1), or ventrally directed, short (2).
*356. Glenoid fossa: concave anteroposteriorly (0), convex anteroposteriorly (1), or flat anteroposteriorly (2).
*357. Postglenoid foramen: on posterior aspect of zygomatic process (0), on lateral aspect of zygomatic process (1), posterior to zygomatic process (2), or absent (3).
358. Temporal lines: present (0), or absent (1).
359. Postorbital process: present (0), or absent (1).
360. Postorbital constriction: present (0), or rudimentary to absent (1).
**361. Tentorial ossification: absent (0), present but weak, developed only inferiorly on petrosal (1), or present, strongly developed, extends to roof of cranial cavity (2).
362. Endocranial venous grooves: present (0), or absent (1).
363. Floor of middle cranial fossa: formed by sphenoid (0), or formed by squamosal (1).
364. Mandibular symphysis length: long, extends well posterior to level of anterior mental foramen (0), or short, ends at or near level of anterior mental foramen (1).
**365. Mandibular symphysis shape in lateral view: with anterior convexity (0), straight profile (1), or with anterior concavity (2).
**366. Anterodorsolaterally directed prongs on outer surface of mandibular symphyseal region: absent (0), incipiently developed as dorsolaterally extended folds of dorsal symphyseal margin (1), or well-developed, tooth-like conical prongs (2).
367. Elongated medial perforation in mandibular canal: absent (0), or present (1).
368. Elongated lateral perforation in mandibular canal: absent (0), or present (1).
*369. Mandibular condyle: mediolaterally elongate (0), circular (1), or anteroposteriorly elongated (2).
370. Position of mandibular condyle: dorsal to (0), or at the level of the mandibular symphysis (1).
**371. Coronoid process of mandible: present, well developed (0), present but strongly reduced in size (1), or absent (2).
372. Angular process of mandible: present (0), or absent (1).
373. Length of nasal/premaxillary vs. nasal maxillary suture: maxillonasal suture longer (0), or premaxillonasal suture longer (1).
**374. Position of infraorbital foramen in lateral view: foramen situated toward back of maxilla, distance from maxillopalatine suture to infraorbital foramen <20% of the distance from maxillopalatine suture to maxillary/premaxillary suture (0), foramen displaced anteriorly, distance from maxillopalatine suture to infraorbital foramen ≥20%, <30% of the distance from maxillopalatine suture to maxillary/premaxillary suture (1), or foramen near midpoint of maxilla, distance from maxillopalatine suture to infraorbital foramen ≥30% of the distance from maxillopalatine suture to maxillary/premaxillary suture (2).
**375. Position of maxillopalatine suture in ventral midline: posterior to maxillary foramen (0), at or slightly anterior to maxillary foramen (1), or well anterior to maxillary foramen (2).
376. Extension of orbital wing of palatine posterior to sphenorbital fissure: absent (0), or present (1).
377. Optic foramen size: small, diameter <2% greatest skull length (0), or large, diameter >3% (1).
**378. Position of optic foramen relative to frontal/squamosal suture [or if absent lateral portion of frontal/parietal suture]: posterior to (0), approximately level with (1), or anterior to suture (2).
379. Position of foramen ovale: anterior to anterior edge of ectotympanic (0), or at level of anterior edge of ectotympanic (1).
380. Jugal: present (0), or absent (1).
381. Zygomatic arch: complete (0), or incomplete (1).
382. Frontal/parietal suture position: well anterior to glenoid, at or near postorbital constriction (0), at or posterior to glenoid, well posterior to postorbital constriction (1).
383. Alisphenoid/parietal contact: present (0), or absent (1).
**384. Temporal fossa on braincase: large (0), slightly reduced in size (1), or strongly reduced (2).
385. Length of parietal/squamosal suture: <25% greatest skull length (0), or ≥25% (1).

386. Shape of zygomatic process of squamosal: elongated, uninflated, with blunt tip or elongated anterior sutural contact with jugal (0), or short, inflated at base, and pointed at tip (1).
*387. Lateral exposure of mastoid and posttympanic process of squamosal: present (0), absent (1), or mastoid lateral exposure present, posttympanic process of squamosal absent (2).
388. Foramen for inferior petrosal sinus separate from jugular foramen: absent (0), or present (1).
389. Position of superior petrosal sinus: in groove between petrosal and tentorium (0), or perforates ventral portion of tentorium (1).
*390. Position of jugular foramen and hypoglossal foramen: jugular foramen lateral to hypoglossal foramen, foramina well separated (0), jugular foramen lateral to hypoglossal foramen, foramina close, may even share a common fossa (1), jugular foramen anterior to or more medial than hypoglossal foramen, foramina well separated (2), or jugular and hypoglossal foramina confluent (3).
391. Epitympanic sinus between squamosal and petrosal: absent (0), or present (1).
392. Basicranial/basifacial axis: linear (0), or reflexed (1).
*393. Teeth: normal mammalian dentition present (0), teeth present but reduced with large triangular canine but no incisors and only a few peg-like postcanine teeth (1), or teeth absent (2).
394. Depth of horizontal ramus of mandible: deep, >10% maximum mandibular length (0), or shallow, ≤10% (1).
395. Medial buttress on posterior portion of mandibular ramus: absent (0), or present (1).

Appendix 3

Data matrix.

The symbol '?' represents either missing data or a case where a character is not applicable to a given taxon. The following symbols are used to represent character states in polymorphic taxa: a=(0, 1); b=(1, 2); c=(0, 1, 2); d=(1, 3); e=(0, 2); f=(3, 4); g=(2, 3); h=(0, 3); i=(1, 2, 3); j=(1, 4); k=(4, 5); m=(1, 5); n=(0, 1, 3). This data matrix has been deposited in MorphoBank and can be obtained at http://www.morphobank.org.

Appendix 4

Distribution of apomorphies on the single MPT illustrated in Fig. 1. Characters shown in bold type are unambiguous synapomorphies; those in regular type are ambiguous synapomorphies. Those characters marked with a "U" are unique apomorphies, as defined in the Results section.

Erinaceus <=> *Nandinia* + Pholidotamorpha:

4(3) <=> **4(0), 5(0) <=> 5(1), 7(0) <=> 7(1)[U], 21(1) <=> 21(0), 25(1) <=> 25(2), 63(2) <=> 63(0), 74(2) <=> 74(1), 75(0) <=> 75(1), 76(1) <=> 76(0), 77(1) <=> 77(0), 93(1) <=> 93(2), 102(0) <=> 102(1), 107(1) <=> 107(0), 109(0) <=> 109(1), 110(2) <=> 110(0), 124(2) <=> 124(1), 135(0) <=> 135(1), 138(0) <=> 138(1), 142(2) <=> 142(0), 157(3) <=> 157(2), 158(2) <=> 158(1), 159(2) <=> 159(1), 161(2) <=> 161(3), 162(2) <=> 162(0), 165(2) <=> 165(1), 169(4) <=> 169(2), 175(1) <=> 175(0), 181(1) <=> 181(0), 186(0) <=> 186(1), 189(2) <=> 189(1), 201(3) <=> 201(2), 203(1) <=> 203(0), 207(3) <=> 207(2), 209(1) <=> 209(0), 221(0) <=> 221(1), 233(2) <=> 233(0), 237(0) <=> 237(1), 238(3) <=> 238(2), 239(2) <=> 239(1), 246(5) <=> 246(1), 251(1) <=> 251(0), 258(1) <=> 258(0), 264(2) <=> 264(0), 265(3) <=> 265(0), 272(0) <=> 272(1), 279(1) <=> 279(0), 293(2) <=> 293(0), 304(0) <=> 304(1), 305(0) <=> 305(1), 329(1) <=> 329(0), 332(0) <=> 332(1), 335(0) <=> 335(1), 342(0) <=> 342(1), 343(2)** <=> **343(0), 350(2) <=> 350(1), 351(1) <=> 351(0), 354(0) <=> 354(1), 361(0) <=> 361(2), 376(1) <=> 376(0), 378(2) <=> 378(1), 385(1)** <=> **385(0), 387(2)** <=> **387(0).**

Node 1. Pholidotamorpha:

10(1), 15(1), 19(1), 20(1), 45(1), 54(1), 79(0), 83(1), 86(0), 98(1), **106(0), 113(1), 145(0), 157(1), 165(0), 170(1), 176(1), 180(1), 196(0), 201(1), 206(0), 207(1), 212(1), 216(0), 217(0), 227(1), 230(1), 231(1), 240(1), 241(0), 260(1), 262(1), 269 (1), 273(1), 274(2), 306(0), 307(1), 309(0), 340(1)[U], 373(0), 386(1),** 390(0), **391(1).**

		10		20		30		40	
Nandinia	02201	01000	00000	30220	01002	00000	00010	000?0	0a010
Erinaceus	00230	00000	?1010	30120	10001	00000	00010	000?0	02100
Palaeanodon	01201	0100?	?0???	???0?	0??0?	?????	?????	?????	?????
Metacheiromys	01201	01002	?1011	30111	00?0?	1?02?	0???0	0????	????1
Eurotamandua	0b011	01001	020??	??00a	0??0?	0?00?	?0?0?	?????	????2
Eomanis waldi	01111	a1002	12111	3100a	000??	02???	0????	????1	?11??
Euromanis krebsi	00111	0100?	?10??	????c	?????	?????	?????	?1??2	?????
Patriomanis	10001	01001	01000	00010	01002	00000	00100	10001	01101
Cryptomanis	10001	01010	01000	1?001	00002	00000	???01	11012	01002
Necromanis	120a1	011?1	1????	??00b	?110b	00?00	???0?	11??1	2210?
Manis javanica	12202	11212	?1a11	302ad	1111b	11022	10100	10101	2201b
M. crassicaudata	1?2?2	1121?	?2211	11013	11112	11122	01100	101?1	12012
M. pentadactyla	10002	11211	12211	11113	11110	11022	10100	100?1	22??2
Smutsia gigantea	122e2	11211	12211	10b0f	11110	11122	0111[a]	1101b	be?12
S. temminckii	122?2	11212	221?1	?0202	11110	11111	01110	11012	12012
Phataginus tricuspis	12222	11210	21201	10122	11110	12111	20200	11111	00001
P. tetradactyla	12222	11210	20111	g0122	11110	12111	21200	11111	00001

	50		60		70		80		90
Nandinia	10100	20020	13?0?	01000	10100	00011	00120	0?231	1001?
Erinaceus	00100	1?020	13?0?	00200	10100	10120	11120	0?200	10010
Palaeanodon	??10?	?????	0??0?	0a000	10100	00111	01100	0?130	a0000
Metacheiromys	??11?	??00?	1??0?	?2000	12100	00110	00100	0?130	0?00?
Eurotamandua	??01?	?????	0??0?	??000	10001	101??	?0?00	??100	000??
Eomanis waldi	1???0	?????	0??0?	0?b0?	????1	101??	0010?	??a??	10010
Euromanis krebsi	???0?	0?0??	???0?	??00?	??000	??1??	?????	10???	??0??
Patriomanis	00110	a0010	0100?	00001	0100b	00101	00101	10100	00000
Cryptomanis	10010	20000	0100?	00101	02103	00001	11001	10010	00010
Necromanis	??1??	??010	010??	?0101	02100	00101	00101	10100	00010
Manis javanica	g0122	201ba	1b010	31201	1211f	01121	11221	10121	a0121
M. crassicaudata	30122	21001	11110	32201	11104	11121	g3221	10120	0?121
M. pentadactyla	30120	00020	11110	12101	11014	1a121	3??21	101e1	001?0
Smutsia gigantea	2a020	00ab1	13110	21201	1g113	10111	23111	1a120	1102?
S. temminckii	21020	01020	11110	11201	02111	10111	g3011	11120	11022
Phataginus tricuspis	01021	01020	12011	12211	1i01g	00021	2bbb1	11200	a0122
P. tetradactyla	01121	01110	10111	12b11	1301b	00021	22111	11200	1?122

		100		110		120		130	
Nandinia	10211	11?12	01100	20010	01020	20001	10000	10000	02101
Erinaceus	00111	??014	?0110	21002	1?011	30??1	??020	00001	00100
Palaeanodon	002?1	?????	??011	0???0	11112	000??	??0a0	00000	00001
Metacheiromys	0?321	001?0	01111	0???0	11122	001??	??110	00000	00200
Eurotamandua	00210	????3	0?0?1	0????	?????	??0??	1?120	00001	?0201
Eomanis waldi	0??10	10??3	00010	0??b?	????0	3??0?	??11?	10011	00??1
Euromanis krebsi	10?10	00??3	0???0	0????	?????	?00?1	??100	?00??	0????
Patriomanis	00111	00001	01010	10000	00a01	01000	0?110	00110	00010
Cryptomanis	00201	10101	01000	10002	00110	31010	10110	00010	00200
Necromanis	012?1	1010?	??010	10000	01111	01???	??1a1	00211	00001
Manis javanica	11321	1a103	12210	11101	01b11	g1011	11112	1ag11	11201
M. crassicaudata	11h21	11102	02220	21122	11101	31001	10112	00311	11111

M. pentadactyla	11321	1a103	12120	21112	11a01	310a1	111b2	a1311	11aa1
Smutsia gigantea	aa2g1	1a?02	a2210	110a2	11b01	11111	101a2	00311	11110
S. temminckii	?1221	11103	02210	11022	11101	21110	10102	11311	11011
Phataginus tricuspis	10031	10013	02210	20011	01211	h1101	10122	11312	11b01
P. tetradactyla	10111	10013	02210	1001b	01211	31101	10122	11312	11201

	140		150		160		170		180
Nandinia	00101	00001	31010	00013	12001	30a11	00100	01000	21110
Erinaceus	00000	02001	12010	10003	13220	22112	00?30	01?11	22110
Palaeanodon	004a0	?0?00	20010	10000	???1?	?011?	0????	????0	?2??1
Metacheiromys	00j10	?1000	12010	10000	?0110	31110	00?01	0?010	121?1
Eurotamandua	0?b00	1000?	?0011	1???1	?1012	?1??0	00??1	1????	?21?1
Eomanis waldi	00100	?0000	10011	01002	02111	30??0	001?1	?10??	023??
Euromanis krebsi	00100	?000?	1001?	010?1	011?0	????a	00??1	???0?	?????
Patriomanis	00100	00000	00011	01002	0?00?	20000	11??0	0????	??2?0
Cryptomanis	00100	???0?	00???	?10??	??0??	??00?	11??1	1????	????0
Necromanis	00???	?????	10111	010?2	?????	??00?	1???0	0????	???11
Manis javanica	122a1	11a11	21121	a1112	1k11m	ga111	11df1	102aa	1231a
M. crassicaudata	12331	11112	20121	11112	13114	01101	11221	10210	12311
M. pentadactyla	12331	1111b	2a121	11112	15115	00101	113f1	1111a	1b201
Smutsia gigantea	123g1	11112	21121	11112	13213	nb100	11bb1	11ba0	10201
S. temminckii	12201	11112	21121	11112	10111	11110	11001	11010	10201
Phataginus tricuspis	11101	a1011	21101	01112	1310g	b1112	111b1	a10a0	20001
P. tetradactyla	11101	11a11	21101	01112	1gb0g	11112	11111	11010	20g01

	190		200		210		220	
Nandinia	00100	11011	00103	11020	20000	12100	00110	21001	10110
Erinaceus	10100	01021	0a0??	10020	32100	13110	000?0	21001	00001
Palaeanodon	?????	???1?	00???	?????	????0	01000	11011	00001	1?001
Metacheiromys	?0?0?	1111?	00??1	00020	02000	01010	11111	00001	10001
Eurotamandua	?????	1?00?	?????	?00??	?0???	01100	02a10	000?1	1?0??
Eomanis waldi	?????	1a???	01???	000??	100?1	131?0	02010	0010?	10???
Euromanis krebsi	?????	?????	?????	000??	?000?	?????	??0??	???0?	?0???
Patriomanis	00000	00010	0????	01112	10001	00000	00110	20100	00000
Cryptomanis	0000?	?????	?1b??	01??1	????1	0?0??	01??2	1?101	01???
Necromanis	01000	?????	?????	?1112	??101	00000	02102	20100	00000
Manis javanica	02001	01111	11212	01112	1b111	01010	01102	21100	11110
M. crassicaudata	11001	01111	1?112	01112	21111	01010	11102	20100	11110
M. pentadactyla	120a1	01a10	11212	011a2	1a111	01010	11b02	2010a	11110
Smutsia gigantea	10110	1a111	a112b	01102	21111	0b01a	ab112	2aa0a	11101
S. temminckii	10110	1a011	1112a	01102	22111	01110	011?2	31101	?1101
Phataginus tricuspis	12110	a0020	01b2e	11102	2b111	0g111	01212	31111	11101
P. tetradactyla	12a10	00020	01222	11102	22111	0g111	01212	31111	a1101

	230		240		250		260		270
Nandinia	00102	00012	11210	3??01	10010	01100	12000	00000	01101
Erinaceus	00102	0?212	10420	31?00	50100	10100	12110	10023	00001
Palaeanodon	1a00?	1??02	11212	01??0	3100?	?????	?????	?????	????0
Metacheiromys	01101	1?102	01311	01??0	31001	??1?1	1??11	01?0?	10011
Eurotamandua	12101	1?012	0?202	?????	4120?	??100	?0011	1???2	0?011
Eomanis waldi	?110?	11011	01203	?1?01	10100	????0	???11	?2100	01100
Euromanis krebsi	??10?	?????	?1???	?????	?????	?????	?????	?????	?????

Patriomanis	11000	10000	0000b	00010	00110	01000	00001	01100	01000
Cryptomanis	0?01?	?0001	01???	00???	??110	001??	???11	02100	0???0
Necromanis	a2111	10100	01202	00110	10210	00?0?	?????	?????	?101?
Manis javanica	111a1	10102	11101	11a20	21211	11111	01112	141a1	12111
M. crassicaudata	12110	10002	01103	11120	21210	11111	00112	14211	12010
M. pentadactyla	12110	10002	0010g	b1120	21210	11111	01112	14211	10a11
Smutsia gigantea	11110	20011	0110g	11120	21211	11110	01012	23211	1b101
S. temminckii	11110	21002	11103	01120	21211	11111	01112	23211	12101
Phataginus tricuspis	10101	1111b	1a211	20121	20211	a1110	11112	23212	12111
P. tetradactyla	101a1	1a11e	11111	2a121	20211	11110	11112	23212	12111

	280		290		300		310	
Nandinia	11000	00001	00000	1?200	010?0	00010	20011	20011	00001
Erinaceus	10000	00011	10000	11200	01210	0102?	00000	20?11	00001
Palaeanodon	?1230	0???0	02000	?1102	0????	01???	0????	?????	??001
Metacheiromys	?1220	0??00	02000	00122	1????	01000	0?011	01001	00011
Eurotamandua	11230	00??1	12?00	1?000	?1???	011??	0?012	0110?	???11
Eomanis waldi	?1020	?????	????0	0?200	?1???	0102?	0?112	01101	00111
Euromanis krebsi	?????	?????	?????	?????	?????	0?0??	0?0??	?????	?????
Patriomanis	01110	00000	00000	00000	00000	000a0	00011	1?111	0?11?
Cryptomanis	?0010	00001	?0000	00000	0?00?	00b10	0??21	?????	?????
Necromanis	?????	?????	?????	?????	?????	00??0	0?1??	?????	?????
Manis javanica	11b1b	11011	11010	10211	11120	11de0	1a112	1101a	10011
M. crassicaudata	01211	22111	11111	10211	21100	11221	1?1??	11011	11110
M. pentadactyla	012b1	22111	11111	10211	21120	11221	11102	10010	00010
Smutsia gigantea	11221	01101	01110	0a211	1a011	11321	11002	11a10	1a111
S. temminckii	10011	01101	11110	00211	10111	11311	110??	1a110	11111
Phataginus tricuspis	11102	01101	01010	01211	10111	11211	12112	01011	11101
P. tetradactyla	11102	01011	11010	01211	10111	11d21	121a2	01111	111a1

	320		330		340		350		360
Nandinia	00100	10101	00001	01012	10010	01000	00011	00010	00000
Erinaceus	40000	a0000	00011	10000	00010	00200	00?12	10000	20010
Palaeanodon	20???	?0?00	0???1	00?01	0???1	????0	?0?11	00000	00??0
Metacheiromys	10100	10?00	01000	02001	0000?	??000	?0?10	00010	03001
Eurotamandua	?a?0?	10???	????0	?????	?????	????0	?????	000?0	23110
Eomanis waldi	???0?	11???	????1	??00?	?0???	????0	???0?	000?0	?1110
Euromanis krebsi	?????	?????	?????	?????	?????	?????	?????	?????	?????
Patriomanis	ja?01	01010	00???	11?01	00a11	????0	?1011	0001b	?2111
Cryptomanis	?????	?????	?????	?????	?????	?????	?????	?????	?????
Necromanis	?????	?????	?????	?????	?????	?????	?????	?????	??110
Manis javanica	22021	12010	a0201	11112	11121	11101	1120a	01111	10111
M. crassicaudata	2202a	a2a1a	00101	11112	11121	11100	11000	01111	1a???
M. pentadactyla	21a21	12010	10101	1111b	11121	11100	11000	01111	11111
Smutsia gigantea	g1a2a	01011	a1100	01110	11021	1?0?0	11201	a111b	1111a
S. temminckii	21021	aba10	10100	01110	11a21	12010	11a1a	a1211	11111
Phataginus tricuspis	32110	a1111	01110	a1111	11121	12011	11110	11212	10111
P. tetradactyla	32110	0111a	01210	1111b	11121	1201a	11110	11212	12111

		370		380		390	
Nandinia	20010	00000	00102	00000	01000	00002	00000
Erinaceus	00011	00000	00121	10200	00001	020?1	00000
Palaeanodon	?00??	?00??	00??2	???0?	??00?	10??2	101?1
Metacheiromys	???11	00000	00002	00100	01000	10??0	?0101
Eurotamandua	???11	1?0?0	0002?	?02?0	00?10	10???	?121?
Eomanis waldi	???10	100?1	00021	?10?0	00020	10???	11211
Euromanis krebsi	?????	?????	?????	?????	?????	?????	?????
Patriomanis	10001	200?1	1010?	01100	?1121	00000	01210
Cryptomanis	?????	?????	?????	?????	?????	?????	?????
Necromanis	2????	?0???	11???	?????	?112?	?????	??210
Manis javanica	21102	20011	21102	1010a	a1120	01112	11210
M. crassicaudata	21101	20011	21102	10110	11120	01112	11210
M. pentadactyla	21102	20011	21001	0001a	a1120	01111	11210
Smutsia gigantea	211ab	2a121	b1aa0	a0b01	11120	0111d	11210
S. temminckii	211a1	20121	b1011	a1aa1	1112a	01a11	11210
Phataginus tricuspis	21101	21011	21001	012a1	11121	01010	11210
P. tetradactyla	21111	21021	21001	01201	11121	01010	11210

Node 2. Palaeanodonta:

2(1), 71(0), 84(3), **89(0), 105(1), 109(2), 115 (2)^{U}, 116(0),** 130(0), 155(0)^{U}, **208(0), 211(1), 215(1)^{U}, 234(0), 246(3)^{U},** 247(1), 248(0), 273 (2), **280(0),** 281(0), 282(2), **288(1)^{U}, 290(2)^{U},** 331(0), 356(0), 375(2), 393(1)^{U}, 395(1).

Node 3. Pholidota:

4(1), 37(1), 51(0), **81(1)^{U}, 95(0),** 100(4), 123(1), 147(0), **152(1)^{U},** 155(1), 156(0), 202(0).

Node 4:

2(1), 3(0), 18(0), 19(0), 34(0), 45(2), **49(1),** 56 (0), **70(1),** 103(0), 150(1)*^{U}, **160(1),** 226(1), 236(0), 239(0), 240(2), 257(0), 305(2), 308(1), 314(1), 358(1)*^{U}, 366(1), 384(1), 392(1)*^{U}, 393 (2)*^{U}, 394(1)*^{U}.

Node 5. Eupholidota:

11(1), 40(1), **63(1),** 96(1), **129(1)^{U},** 151(0), **155 (2)^{U}, 157(2),** 168(2), **178(2),** 192(1), 205(1)^{U}, **218(1), 235(1),** 262(2), 263(1), 267(1), 286(0), **303(1),** 313(1), **322(1), 370(1)^{U}, 377(1), 384 (2)^{U}.**

Convergences between *Euromanis krebsi* and *Eomanis waldi*: 3(1)^{U}.

Convergences between *Euromanis krebsi* and Node 5: 151(0).

Convergences between *Euromanis krebsi* and *Eurotamandua*: 68(0), 155(1)^{U}.

Convergences between *Eurotamandua* and Node 2, Palaeanodonta: **105(1) ^{U},** 247(1), 273(2), 282(2) ^{U}

Node 6. Manoidea:

1(1)^{U}, 2(2), **4(0), 22(1),** 33(2), 36(1)^{U}, 57(1), 65 (1)^{U}, 67(2), 71(0), 80(1)^{U}, **95(1),** 99(0), **106(1),** 111(0), 117(1)^{U}, **128(1), 166(1)^{U}, 167(1)^{U},** 183 (0), **186(0),** 193(2), **197(1), 198(1)^{U},** 199(1), 200(2), **208(0), 213(1), 215(2), 216(2),** 225(0), **229(1), 234(0), 244(1), 249(1),** 256(0), **274(1),** 287(0), **306(1), 309(1),** 320(1), 324(1)^{U}, 347 (1)^{U}, **355(1), 366(2)^{U}, 371(1),** 374(0), 382(1), **383(1)^{U}, 386(0).**

Node 7. Patriomanidae:

2(0), 11(0), 14(0), 15(0), 42(1), 66(0), 74(0), **100(1)^{U},** 109(0), **112(0)^{U},** 118(1), **120(0), 130 (0), 135(0), 146(0)^{U}, 158(0),** 163(0), 164(0), **180(0),** 221(0), **228(0),** 242(0), 261(0), 270(0), **288(0), 294(0),** 297(0), 299(1), **305(1)**.

Synapomorphies between *Necromanis* and Patriomanidae (Node 7) on MPT #1:

3(0), **62(0), 66(0),** 71(0), **74(0)^{U},** 107(0), **109(0),** 111(0), 151(0), **163(0), 164(0),** 181(0), 183(0), **207(0)^{U},** 208(0), **221(0),** 225(0), 234(0), 235(1), **242(0),** 251(0), **297(0).**

Synapomorphies between *Necromanis* and Manidae (Node 8) on MPT #2:

2(2), **8(1),** 11(1), 20(2), 22(1), **23(1)^{U}, 42(2),** 67 (2), **92(1), 125(1), 128(2), 148(1)^{U},** 200(2), **203 (1),** 215(2), 216(2), 229(1), 243(1), **248(2),** 269 (1), 303(1), 361(2), **372(1)^{U}**.

Node 8. Manidae:

3(2), 5(2)^{U}, 6(1), 8(2)^{U}, 9(1), 13(1), **21(1),** 23 (1), **24(1)^{U}, 26(1), 27(1), 43(0), 49(2)^{U}, 56(1), 59(1)^{U},** 62(1), **63(2), 69(1),** 70(2), **77(3), 89 (2)^{U}, 90(1), 91(1), 102(2)^{U}, 103(2), 110(1), 125 (2)^{U}, 128(3), 131(1)^{U}, 132(1)^{U}, 136(1)^{U}, 137(1), 140(1),** 141(1), **142(1), 144(1)^{U}, 145(1), 146(2),** 148(1), **153(1)^{U}, 154(1), 156(1),** 157(3), 160(2), 171(1), **202(1),** 203(1), **204(1)^{U}, 209(1), 222(1), 223(1),** 238(1), **244(2)^{U}, 246(2)^{U},** 248(2), **251 (1),** 252(1), **254(1)^{U}, 257(1), 258(1), 260(2)^{U}, 262(3), 264(1), 265(1), 266(1), 267(2), 275(1), 277(1),** 282(1)^{U}, **284(1)^{U}, 289(1)^{U}, 290(1)^{U}, 291(1), 293(1), 296(1)^{U}, 298(3), 301(1)^{U}, 302 (1), 311(1),** 316(2), **317(2), 319(1),** 328(1), 333 (1)^{U}, **334(1), 336(1), 337(1)^{U}, 339(2)^{U},** 341(1)^{U}, 346(1)^{U}, **352(1)^{U}, 353(1),** 356(1)^{U}, 360(1), **362 (1)^{U}, 363(1)^{U}, 371(2),** 372(1), 381(1), **387(1)^{U}, 389(1)^{U}.**

Node 9. Maninae (genus *Manis*):

29(2), 30(2), **37(0), 41(2),** 44(1), 46(3), 61(3), **70(3), 72(1)^{U},** 74(2), **78(2),** 79(2), 84(2), 88(1), 92(1), **93(3),** 94(2), 107(1), **108(1)^{U},** 118(1), 137(2), 149(2), 165(1), **169(3), 173(1),** 182(2), **185(1)^{U}, 188(1),** 191(1), 194(1)^{U}, **214(0),** 220 (0), **224(1),** 235(2), 241(1), 247(1), **255(1), 262 (4)^{U}, 279(1), 286(1), 294(2), 308(0),** 319(2), **322(2)^{U}, 335(2)^{U},** 338(1), **343(1)^{U}, 349(0),** 364 (0), 369(1), **377(0),** 388(1), 390(2).

Node 10. *M. crassicaudata* + *M. pentadactyla* (Subgenus *Manis*):

12(2), **13(2),** 16(1), **17(1),** 19(1), 20(3), 58(1), **62 (2), 67(1),** 70(4**), 71(1),** 76(3), **104(2)^{U}, 106(2), 110(2), 111(1), 114(0),** 138(3), **139(3),** 143(1), 151(1), 160(4), **161(0),** 164(0), 168(3), 181(1), **211(1), 227(2), 230(0),** 263(2), **271(0),** 273(2), 276(2)^{U}, **277(2)^{U},** 278(1), **283(1), 285(1)^{U}, 291 (2)^{U}, 298(2),** 300(1), **315(0)^{U},** 350(0), **379(1).**

Node 11. Smutsiinae (African manids):

20(2), **25(0), 28(1),** 29(1), 30(1), 39(1), **47(1),** 61(1), 76(2), 79(1), **82(1), 86(1), 90(2)^{U},** 147(1), **161(1),** 162(1), **177(0)^{U}, 179(0),** 181(1), **183(1), 184(1),** 194(2)^{U}, **199(0), 201(2),** 217(1), **225(1),** 250(1), **261(2),** 263(2), 268(1), 292(0), **295(1)^{U},** 300(1), **312(1),** 321(0), **330(0), 342(2)^{U}, 344 (1)^{U},** 348(1), 369(2), **380(1).**

Node 12. *Phataginus*:

4(2), **10(0),** 11(2), 18(1), 19(1), **27(2), 31(2)^{U}, 33(1)^{U},** 38(1), **42(0), 45(1), 50(1)^{U},** 52(1), **60 (1)^{U}, 62(2), 64(1)^{U}, 68(0), 73(0),** 74(2), **77(2), 83(2), 93(1), 98(0), 99(1), 113(2)^{U}, 124(2),** 126 (1), **130(2)^{U}, 149(0)^{U}, 159(0), 165(2),** 182(2), 187(0), **189(2), 190(0), 196(1), 207(2),** 208(1), **210(1), 213(2),** 216(3), **219(1)^{U}, 227(0), 233(1),** 234(1), 236(1), **239(1), 240(1), 241(2), 245(1), 256(1), 274(0), 275(2), 287(1), 302(2)^{U}, 306(0), 316(3),** 318(1), **323(1),** 327(1), **329(1),** 338(1), 350(0), 351(1), 353(2), **355(2), 367(1), 378(2), 385(1)**.

Node 13. *Smutsia*:

12(2), 18(2), 32(1), **34(1), 41(1),** 44(1), 46(2), 48(0), 58(1), **71(1),** 84(2), **87(1)^{U},** 94(2), 107(1), **110(2), 111(1), 114(0), 119(1), 134(1),** 137(2), 143(1), **145(3),** 149(2), 151(1), **186(1),** 193(1), **230(0), 231(2)^{U},** 247(1), **269(0),** 278(1), **283(1), 303(0), 310(0), 317(1),** 319(2), **331(0), 335(0),** 357(1), **368(1)^{U},** 390 (1).

References

Botha J, Gaudin TJ (2007) A new pangolin (Mammalia: Pholidota) from the Pliocene of Langebaanweg, South Africa. J Vertebr Paleontol 27:484–491

Bremer K (1994) Branch support and tree stability. Cladistics 10:295–304

Carrano MT, Gaudin TJ, Blob RW, Wible JR (2006) Amniote Paleobiology: Perspectives on the Evolution of Mammals, Birds, and Reptiles. University of Chicago Press, Chicago

Chan L-K (1995) Extrinsic lingual musculature of two pangolins (Pholidota: Manidae). J Mammal 76:472–480

Cifelli RL (1983) Eutherian tarsals from the late Paleocene of Brazil. Am Mus Novitates 2761:1–31

Corbet GB (1978) The Mammals of the Palaearctic Region: A Taxonomic Review. British Museum (Natural History), London

Corbet GB, Hill JE (1991) A World List of Mammalian Species. Natural History Museum Publ and Oxford Univ Press, London

Dubois E (1907) Eenige von Nederlandschen kant verkregen uitkomsten met betrekking tot de kennis der Kendeng-Fauna (Fauna van Trinil). Tijdschr K Nederlandsche Aardr Genootsch Ser 2(24):449–458

Dubois E (1908) Das geologische Alter der Kendeng oder Trinil-Fauna. Tijdschr K Nederlandsche Aardr Genootsch Ser 2(25):553–555

Dubois E (1926) *Manis palaeojavanica*, the giant pangolin of the Kendeng fauna. Proc K Nederlandsche Akad Wetensch Amsterdam 29:1233–1243

Emry RJ (1970) A North American Oligocene pangolin and other additions to the Pholidota. Bull Am Mus Nat Hist 142:459–510

Emry RJ (1973) Stratigraphy and preliminary biostratigraphy of the Flagstaff Rim area, Natrona County, Wyoming. Smithsonian Contrib Paleobiol 18:1–43

Emry RJ (2004) The edentulous skull of the North American pangolin, *Patriomanis americanus*. Bull Am Mus Nat Hist 285:130–138

Feiler A (1998) Das Philippinen-Schuppentier, *Manis culionensis* Elera, 1915, eine fast vergessene Art (Mammalia: Pholidota: Manidae). Zool Abh Staatliches Mus Tierkunde Dresden 50:161–164

Feldhamer GA, Drickamer LC, Vessey SH, Merritt JF, Krajewski C (2007) Mammalogy: Adaptation, Diversity and Ecology, 3rd edn. Johns Hopkins University Press, Baltimore

Flynn JJ, Wesley-Hunt GD (2005) Carnivora. In: Rose KD, Archibald JD (eds) The Rise of Placental Mammals. Origins and Relationships of the Major Extant Clades. Johns Hopkins University Press, Baltimore, pp 175–198

Gaubert P, Antunes A (2005) Assessing the taxonomic status of the Palawan pangolin *Manis culionensis* (Pholidota) using discrete morphological characters. J Mammal 86:1068–1074

Gaudin TJ (1995) The ear region of edentates and the phylogeny of the Tardigrada (Mammalia, Xenarthra). J Vertebr Paleontol 15:672–705

Gaudin TJ (1999a) Palaeanodonta. In: Singer RS (ed) Encyclopedia of Paleontology, vol 2. Fitzroy Dearborn Publishers, Chicago, pp 821–823

Gaudin TJ (1999b) Pholidota. In: Singer RS (ed) Encyclopedia of Paleontology, vol 2. Fitzroy Dearborn Publishers, Chicago, pp 855–857

Gaudin TJ (2004) Phylogenetic relationships among sloths (Mammalia, Xenarthra, Tardigrada): the craniodental evidence. Zool J Linn Soc 140:255–305

Gaudin TJ, Branham DG (1998) The phylogeny of the Myrmecophagidae (Mammalia, Xenarthra, Vermilingua) and relationship of *Eurotamandua* to the Vermilingua. J Mammal Evol 5:237–265

Gaudin TJ, Emry RJ, Pogue B (2006) A new genus and species of pangolin (Mammalia, Pholidota) from the late Eocene of Inner Mongolia, China. J Vertebr Paleontol 26:146–159

Gaudin TJ, Wible JR (1999) The entotympanic of pangolins and the phylogeny of the Pholidota. J Mammal Evol 6:39–65

Gaudin TJ, Wible JR (2006) Chapter 6. The phylogeny of living and extinct armadillos (Mammalia, Xenarthra, Cingulata): a craniodental analysis. In: Carrano MT, Gaudin TJ, Blob RW, Wible JR (eds) Amniote Paleobiology: Perspectives on the Evolution of Mammals, Birds, and Reptiles. University of Chicago Press, Chicago, pp 153–198

Gebo DL, Rasmussen DT (1985) The earliest fossil pangolin (Pholidota: Manidae) from Africa. J Mammal 66:538–540

Grassé PP (1955) Ordre de Pholidotes. In: Grassé PP (ed) Traité de Zoologie, vol. 17, Mammifères. Masson et Cie, Paris, pp 1267–1282

Guth C (1958) Pholidota. In: Piveteau J (ed) Traité de Paléontologie, Tome VI, vol. 2, Mammifères Évolution. Masson et Cie, Paris, pp 641–647

Heath ME (1992a) *Manis pentadactyla*. Mammal Species 414:1–6

Heath ME (1992b) *Manis temminckii*. Mammal Species 415:1–5

Heath ME (1995) *Manis crassicaudata*. Mammal Species 513:1–4

Hillis DM, Bull JJ (1993) An empirical test of bootstrapping as a method for assessing confidence in phylogenetic analysis. Syst Biol 42:182–192

Hooijer DA (1947) A femur of *Manis palaeojavanica* Dubois from western Java. Proc K Nederlandsche Akad Wetensch 50:413–418

Horovitz I, Storch G, Martin T (2005) Ankle structure in Eocene pholidotan mammal *Eomanis krebsi* and its taxonomic implications. Acta Palaeontol Pol 50:545–548

Kingdon J (1974) East African Mammals, Volume 1. University of Chicago Press, Chicago

Kingdon J (1997) The Kingdon Field Guide to African Mammals. Princeton University Press, Princeton

Koenigswald W von (1969) Die Maniden (Pholidota, Mamm.) des europäischen Tertiärs. Mitt Bayer Staatssammlg Paläont hist Geol 9:61–71

Koenigswald W von (1999) Order Pholidota. In: Rössner GE, Heissig K (eds) The Miocene Land Mammals of Europe. Verlag Dr. Friedrich Pfeil, Munich, pp 75–80

Koenigswald W von, Martin T (1990) Ein Skelett von *Necromanis franconica*, einem Schuppentier (Pholidota, Mammalia) aus dem Aquitan von Saulcet im Allier-Becken (Frankreich). Eclogae Geol Helvetiae 83: 845–864

Koenigswald W von, Richter G, Storch G (1981) Nachweis von Hornschuppen bei *Eomanis waldi* aus der "Grube Messel" bei Darmstadt (Mammalia, Pholidota). Senckenberg lethaea 61:291–298

Kormos T (1934) *Manis hungarica* n. s., das erste Schuppentier aus dem europäischen Oberpliozän. Folia zool hydrobiol 6:87–94

Maddison DR, Maddison WP (2001) MacClade, version 4.03. Sinauer Associates, Inc., Sunderland, MA

Maddison WP, Donoghue MJ, Maddison DR (1984) Outgroup analysis and parsimony. Syst Zool 33:83–103

Martin RE, Pine RH, DeBlase AF (2001) A Manual of Mammalogy, with Keys to the Families of the World, 3rd edn. McGraw-Hill Co, New York

Matthew WD (1918) Edentata. In: A revision of the Lower Eocene Wasatch and Wind River Faunas. Part V-Insectivora (continued), Glires, Edentata. Bull Am Mus Nat Hist 38:565–657

McKenna MC, Bell SK (1997) Classification of Mammals Above the Species Level. Columbia University Press, New York

Novacek MJ (1992) Mammalian phylogeny: shaking the tree. Nature 356:121–125

Novacek MJ, Wyss AR (1986) Higher-level relationships of the recent eutherian orders: morphological evidence. Cladistics 2:257–287

Nowak RM (1999) Walker's Mammals of the World, 6th edn. Johns Hopkins University Press, Baltimore

Patterson B (1978) Pholidota and Tubulidentata. In: Maglio VJ, Cooke HBS (eds) Evolution of African Mammals. Harvard University Press, Cambridge, pp 268–278

Patterson B, Segall W, Turnbull WD, Gaudin TJ (1992) The ear region in xenarthrans (=Edentata, Mammalia). Part II. Sloths, anteaters, palaeanodonts, and a miscellany. Fieldiana Geol new ser 24:1–79

Pocock RI (1924) The external characters of the pangolins (Manidae). Proc Zool Soc London 707–723

Rose KD (1999) *Eurotamandua* and Palaeanodonta: Convergent or related? Paläontol Zeitschrift 73:395–401

Rose KD, Emry RJ (1983) Extraordinary fossorial adaptations in the Oligocene palaeanodonts *Epoicotherium* and *Xenocranium*. J Morph 175:33–56

Rose KD, Emry RJ (1993) Relationships of Xenarthra, Pholidota, and fossil "edentates". In: Szalay FS, Novacek MJ, McKenna MC (eds) Mammal Phylogeny: Placentals. Springer-Verlag, New York, pp 81–102

Rose KD, Emry RJ, Gaudin TJ, Storch G (2005) Xenarthra and Pholidota. In: Rose KD, Archibald JD (eds) The Rise of Placental Mammals. Origins and Relationships of the Major Extant Clades. Johns Hopkins University Press, Baltimore, pp 106–126

Rose KD, Lucas SG (2000) An early Paleocene palaeanodont (Mammalia, ?Pholidota) from New Mexico, and the origin of the Palaeanodonta. J Vertebr Paleontol 20: 139–156

Schlitter DA (2005) Order Pholidota. In: Wilson DE, Reeder DM (eds) Mammal Species of the World, 3rd edn. Johns Hopkins University Press, Baltimore, pp 530–531

Schoch RM (1984) Revision of *Metacheiromys* Wortman, 1903 and a review of the Palaeanodonta. Postilla 192:1–28

Segall W (1973) Characteristics of the ear, especially the middle ear in fossorial mammals, compared with those in the Manidae. Acta Anat 86:96–110

Shoshani J, McKenna MC, Rose KD, Emry RJ (1997) *Eurotamandua* is a pholidotan not a xenarthran. J Vert Paleont 17:76A

Simpson GG (1931) *Metacheiromys* and the relationships of the Edentata. Bull Am Mus Nat Hist 59:295–381

Simpson GG (1945) The principles of classification and a classification of mammals. Bull Am Mus Nat Hist 85:1–350

Springer MS, Murphy WJ, Eizirik E, O'Brien SJ (2005) Molecular evidence for major placental clades. In: Rose KD, Archibald JD (eds) The Rise of Placental Mammals. Origins and Relationships of the Major Extant Clades. Johns Hopkins University Press, Baltimore, pp 37–49

Springer MS, Stanhope MJ, Madsen O, deJong WW (2004) Molecules consolidate the placental mammal tree. Trends Ecol Evol 19:430–438

Storch G (1978) *Eomanis waldi*, ein Schuppentier aus dem Mittel-Eozän der "Grube Messel" bei Darmstadt (Mammalia: Pholidota). Senckenberg lethaea 59:503–529

Storch G (1981) *Eurotamandua joresi*, ein Myrmecophagide aus dem Eozän der "Grube Messel" bei Darmstadt (Mammalia, Xenarthra). Senckenberg lethaea 61:247–289

Storch G (2003) Fossil Old World "edentates". In: Fariña RA, Vizcaíno SF, Storch G (eds) Morphological Studies in Fossil and Extant Xenarthra (Mammalia). Senckenberg biol 83:51–60

Storch G, Habersetzer J (1991) Rückverlagerte Choanen und akzessorische Bulla tympanica bei rezenten Vermilingua und *Eurotamandua* aus dem Eozän von Messel (Mammalia: Xenarthra). Z Säugetierkunde 56:257–271

Storch G, Martin T (1994) *Eomanis krebsi*, ein neues Schuppentier aus dem Mittel-Eozän der Grube Messel bei Darmstadt (Mammalia: Pholidota). Berliner geowiss Abh E13:83–97

Swart JM, Richardson PRK, Ferguson JWH (1999) Ecological factors affecting the feeding behavior of pangolins (*Manis temminckii*). J Zool Lond 247:281–292

Swofford DL (2002) PAUP: Phylogenetic Analysis Using Parsimony, Version 4.0b10. Sinauer Associates, Inc., Sunderland, MA

Szalay FS, Schrenk F (1998) The middle Eocene *Eurotamandua* and a Darwinian phylogenetic analysis of "edentates". Kaupia Darmstädter Beit Naturgeschich 7:97–186

Vaughan TA, Ryan JM, Czaplewski NJ (2000) Mammalogy, 4th edn. Saunders College Publishing, New York

Wible JR, Gaudin TJ (2004) On the cranial osteology of the yellow armadillo *Euphractus sexcinctus* (Dasypodidae, Xenarthra, Placentalia). Ann Carnegie Mus 73:117–196